Navy Experimental Diving Unit
321 Bullfinch Rd.
Panama City, FL 32407-7015

TA 01-11
NEDU TR 07-13
OCTOBER 2007

PERFORMANCE OF VARIOUS MODELS IN PREDICTING VITAL CAPACITY CHANGES CAUSED BY BREATHING HIGH OXYGEN PARTIAL PRESSURES

Author: B. Shykoff, Ph.D.

REPORT DOCUMENTATION PAGE

1a. REPORT SECURITY CLASSIFICATION Unclassified	1b. RESTRICTIVE MARKINGS
2a. SECURITY CLASSIFICATION AUTHORITY	3. DISTRIBUTION/AVAILABILITY OF REPORT DISTRIBUTION STATEMENT A: Approved for public release; distribution is unlimited.
2b. DECLASSIFICATION/DOWNGRADING AUTHORITY	
4. PERFORMING ORGANIZATION REPORT NUMBER(S) NEDU TR 07-13	5. MONITORING ORGANIZATION REPORT NUMBER(S)
6a. NAME OF PERFORMING ORGANIZATION Navy Experimental Diving Unit 6b. OFFICE SYMBOL (If Applicable)	7a. NAME OF MONITORING ORGANIZATION
6c. ADDRESS (City, State, and ZIP Code) 321 Bullfinch Road, Panama City, FL 32407-7015	7b. ADDRESS (City, State, and Zip Code)
8a. NAME OF FUNDING SPONSORING ORGANIZATION Naval Sea Systems Command 8b. OFFICE SYMBOL (If Applicable) 00C	9. PROCUREMENT INSTRUMENT IDENTIFICATION NUMBER
8c. ADDRESS (City, State, and ZIP Code) 2531 Jefferson Davis Highway, Arlington, VA 22242-5160	10. SOURCE OF FUNDING NUMBERS PROGRAM ELEMENT NO. / PROJECT NO. / TASK NO. 01-11 / WORK UNIT ACCESSION NO.
11. TITLE (Include Security Classification) (U) PERFORMANCE OF VARIOUS MODELS IN PREDICTING VITAL CAPACITY CHANGES CAUSED BY BREATHING HIGH OXYGEN PARTIAL PRESSURES	
12. PERSONAL AUTHOR(S) B. Shykoff, Ph.D.	
13a. TYPE OF REPORT Technical Report 13b. TIME COVERED FROM Jan 2002 TO Dec 2003	14. DATE OF REPORT (Year, Month, Day) October 2007 15. PAGE COUNT 156
16. SUPPLEMENTARY NOTATION	

17. COSATI CODES			18. SUBJECT TERMS (Continue on reverse if necessary and identify by block number)
FIELD	GROUP	SUB-GROUP	Vital capacity models, predictive models, hyperoxia, pulmonary oxygen toxicity

19. ABSTRACT (Continue on reverse if necessary and identify by block number):
Vital capacity changes caused by breathing high oxygen partial pressures (Po_2) were modeled as functions of partial pressure and duration of exposure and recovery. Nine basic model formulations with variations were fitted to a data set of all known vital capacity measurements during oxygen exposures and during recovery from them. Vital capacity changes varied greatly among subjects. Data included constant elevated Po_2 followed by recovery; a saturation dive with compression, decompression, and recovery; and intermittent exposures with air breaks. Marquardt's algorithm was used to find parameters, and fits were assessed for the data subsets. Several models were proposed to explain slow recovery from some experiments and fast recovery from others. None of the tested models explained the results of all exposures to high Po_2, but the autocatalytic and exponential models in which curvature with time is a function of Po_2 showed the most promise.

20. DISTRIBUTION/AVAILABILITY OF ABSTRACT [ ] UNCLASSIFIED/UNLIMITED [X] SAME AS RPT. [ ] DTIC USERS	21. ABSTRACT SECURITY CLASSIFICATION Unclassified

22a. NAME OF RESPONSIBLE INDIVIDUAL NEDU Librarian	22b. TELEPHONE (Include Area Code) 850-230-3100	22c. OFFICE SYMBOL

DD Form 1473

CONTENTS

Figures

Tables

EXECUTIVE SUMMARY

Studies of pulmonary effects of oxygen in dry hyperbaric chambers have been conducted for more than 50 years. Data now available about injury development were obtained during steady oxygen partial pressure (P_{O_2}) values from 0.21 atmospheres (atm) to 2.5 atm, and at intermittent P_{O_2} values fluctuating between 0.21 atm and 2 atm. Recovery data were obtained after some of the exposures to steady P_{O_2} and after intermittent exposures stepping down from 2.8 atm. We follow other authors[1–10] in seeking a model of the changes in vital capacity (ΔVC) that occur during or after exposure to elevated P_{O_2}, but with more data available to us than were to the other authors.

We have fitted five categories of models from the literature in both their published and modified formulations, and four new categories of model. The goal of the work was to find a universally applicable model of ΔVC as a function of P_{O_2}. Although this goal has not been realized, both the limitations and the occasional strengths of the various models are presented here. Even piecewise models can be useful within the regions that they approximate.

Models using Marquardt's algorithm were fitted for nonlinear regression implemented in Pascal (Borland Delphi Professional, ver 4.0). An option to use the Simplex method was included, and Simplex fits were used sometimes as starting values for Marquardt fits. Marquardt's lambda was set initially to 10^{-2} and constrained to a maximum of 10.[3] One parameter was perturbed at a time in the numerical differentiation, and iterations were deemed to have converged when either the absolute or the fractional difference between iterations was less than 10^{-7} for all parameters; this value is adjustable. To confirm that no other local minima of the fitting surfaces were located near the fits obtained, initial estimates of parameters were varied by an order of magnitude in each direction from the first fit obtained with the entire data set, and the fits were repeated with the combinations of starting values.

Model fits were compared to the intersubject average ΔVC expressed as functions of time for each P_{O_2} profile. Data collected during or after 19 experiments with a total of 408 subjects were used in the fits. For recovery fits, time was reset to zero at the end of the exposures. Fits were conducted for all of the data from all experiments, for subgroupings of the experiments, and, whenever appropriate, for data truncated to omit recovery, truncated to include only early (8-hour) recovery, and not truncated.

The intersubject average ΔVC, the quantity to be modeled, varies with P_{O_2} and with time. When $P_{O_2} < 0.5$, there is little to no ΔVC; when P_{O_2} is near 1 atm, ΔVC decreases with time, either slightly concave upwards or almost linearly; and when P_{O_2} is greater than 1.5 atm, ΔVC is curvilinear and increasingly concave downward with time as P_{O_2} increases. Within this general pattern, the intersubject variability in response is large. Recovery rates are clearly different across exposures and are not a function only of exposure P_{O_2}.

All ΔVC values were normalized by baseline VC. However, the problem of serial correlation cannot be avoided for variables expressed as change from baseline. Differences among the experiments also introduce possible bias: some experiments have few subjects with frequent measurements, and others have more subjects and longer time intervals between measurements. Fits were computed with weighting "by datum" — that is, with each measurement weighted equally. Some models were also fitted with weighting "by subject," where the sums of the weights for all measurements for each subject were equal. The weightings had little influence either on the goodness of fit or on the parameter values.

Seven types of models of acute injury were fitted to the data set:

1. Unit Pulmonary Oxygen Toxicity (UPTD) models, previously published;[1–3]
2. proportional models, previously published;[4–6]
3. proportional rate of healing models, previously published;[6]
4. autocatalytic models, adapted here for pulmonary application;[7]
5. exponential models, both previously published and modified;[8–10]
6. sigmoidal dose response models, proposed here; and
7. models with two kinetic components, proposed here.

Two types of model in which inflammatory injury was considered also were proposed here:

8. injury memory models, and
9. delayed inflammation models.

Model Descriptions and Assessments

1. The UPTD model, first presented by Clark and Lambertsen for elevated P_{O_2} only, was based on the data available at that time.[1–3]

$$\begin{aligned} \text{UPTD} &= t \cdot [(P_{O_2} - P_{th}) / (1\ \text{atm} - P_{th})]^{b}, && P_{O_2} \geq P_{th} \\ &= 0, && P_{O_2} < P_{th} \end{aligned}$$

The original definition of UPTD fixed the exponent $b = 1/1.2 = 0.833$ and the threshold $P_{O_2,}\ P_{th} = 0.5$ atm.

By inspection of the one set of published data available from multiple sources,[2–4]

$$\%\Delta VC = \begin{cases} a \cdot \text{UPTD} + c, & a \cdot \text{UPTD} + c < 0 \\ 0, & a \cdot \text{UPTD} + c \geq 0. \end{cases}$$

For Clark's data set[1–3], $a = -5.6 \cdot 10^{-3}$ %·min^{-1} and $c = -1\%$.
We considered this model in three versions: fitting only scaling factor a and offset c; fitting a, b, and c; and fitting all parameters a, b, c, and P_{th}. The UPTD model with 2, 3, or 4 fitted parameters is nearly linear after the effect of the threshold parameter. Although data from short exposures and those from P_{O_2} near 1 atm can be approximated, this model does not fit the data in general. Because it does not include a

recovery component, it cannot fit intermittent exposures without adjustment; the simple assumption of no change in short periods of normoxia is insufficient.

2. Proportional models assume that both the relation between %ΔVC and time and that between %ΔVC and P_{O_2} are linear. We fitted exponents of time and of P_{O_2} and found that only for some subsets of the data does the proportional model appear to apply. However, because this model is often quoted, we present it as previously published and based on a more limited data set than that available to us.[4,5]

Let F be the concentration of reactive oxygen species (ROS). As a concentration, F cannot be less than zero.

$$F = \begin{cases} a \cdot (P_{O_2} - P_{th}) \cdot t + F_0, & P_{O_2} \geq P_{th} - F_0 / (a_1 \cdot t) \\ 0, & P_{O_2} < P_{th} - F_0 / (a_1 \cdot t). \end{cases}$$

F can be related to ΔVC, as in the Harabin reduced (linear) model[4–6]

$$\%\Delta VC = -\alpha \cdot F, \qquad \text{(Model 2a)}$$

where the fitted parameter is $a' = -\alpha \cdot a$.
Harabin found $a' = 0.011$ $(\text{atm}\cdot\text{min})^{-1}$ with $P_{th} = 0.5$ atm.

Alternatively, the more complicated relation proposed by Vann[6] to limit $|\%\Delta VC| \leq 100\%$ can be used:

$$\%\Delta VC = -100\,[1 - 1.005^{-F}] \qquad \text{(Model 2b)}$$

Here, $a = 0.02$ $(\text{atm}\cdot\text{min})^{-1}$ and $P_{th} = 0.3$ to 0.4 atm, depending on the data set.

This linear model cannot describe the data for $P_{O_2} > 1.5$ atm. The linear recovery portion fits only the very slow recovery data of one early experiment.

3. The proportional rate of healing model proposed by Vann[6] assumes that ROS are created at a rate proportional to P_{O_2} and destroyed at a rate proportional to their concentration:

$$dF/dt = \begin{cases} a \cdot (P_{O_2} - P_{th}) - b \cdot F, & P_{O_2} > \text{threshold} \\ -b \cdot F, & P_{O_2} \leq \text{threshold}. \end{cases}$$

Vann proposed either a simple proportional relation between F and %ΔVC,

$$\%\Delta VC = -\alpha \cdot F, \text{ where one fits } -a \cdot \alpha,$$

where he found $a = 0.009$ (atm·min)$^{-1}$, $b = 2.1 \cdot 10^{-4}$ min^{-1}, and $P_{th} = 0.17$ atm, or the more complicated relation mentioned above to bound %ΔVC:

$$\%\Delta VC = -100\,[1 - 1.005^{-F}].$$

We propose a third sigmoidal version, listed under Model 6.

Vann also worked with a more limited data set than that available to us. Although the mechanism is conceptually appealing, the proportional model is curvilinear in time in the wrong direction for $P_{O_2} > 1.5$ atm. The recovery exponential function curves in the same direction as do the data but does not accommodate the different rates of recovery seen in different experiments.

4. An autocatalytic model is one in which the concentration of a reaction product becomes self-amplifying under specific conditions — in this case, when P_{O_2} exceeds a threshold.

We began with a model proposed by Harabin et al. in a central nervous system (CNS) oxygen risk model of the protective effect of air breaks in experimental animals.[7] In our application, though, the reaction products are ROS, and the reaction becomes self-amplifying when P_{O_2} exceeds parameter P_a, where $P_a > P_{th}$, the threshold for any effect of P_{O_2}. For $P_{O_2} < P_a$, the rate of destruction of ROS is proportional to their concentration but is also a function of P_{O_2}. The curvature with increasing time differs above and below P_a.

$\%\Delta VC = -\alpha \cdot F$, where the fitted parameter is $a' = -\alpha \cdot a$.

$$dF/dt = \begin{cases} a \cdot (P_{O_2} - P_{th}) + b \cdot F \cdot (P_{O_2} - P_a), & P_{O_2} > P_{th}, \\ b \cdot F \cdot (P_{O_2} - P_a), & P_{O_2} \le P_{th}. \end{cases}$$

After converting the CNS model to pulmonary use, we have proposed several further modifications: we fixed either P_{th} (Model 4a) or P_a (Model 4b), and we introduced two forms of dependence on exposure duration in the multiplier of the term that can change sign, valid when $P_{O_2} > P_{th}$:

$$dF/dt = a \cdot (P_{O_2} - P_{th}) + (b + c/T_{dur}) \cdot F \cdot (P_{O_2} - P_a), \qquad \text{(Model 4c)}$$

or

$$dF/dt = a \cdot (P_{O_2} - P_{th}) + [b + c \cdot (P_{O_2} - P_a)/T_{dur}] \cdot F, \qquad \text{(Model 4d)}$$

in which duration of exposure also changes the effective autocatalytic threshold.

In Model 4d we also introduced an exposure duration term to the recovery term,

$$dF/dt = [b + c \cdot (P_{O_2} - P_a) / T_{dur}] \cdot F, \qquad P_{O_2} < P_{th}.$$

Although this model provided curvatures in the same direction as the data, the model did not fit well to the data overall, particularly not to the intermittent data. However, a refinement within this class of model might be more successful.

5. An exponential model in which normalized P_{O_2} is raised to a power during periods of elevated P_{O_2} was proposed by Arieli[8–10] to fit the data for $P_{O_2} \geq 1.5$ atm. Recovery in Arieli's exponential model is a decaying exponential with the time constant a function of the P_{O_2} of injury. We fitted Arieli's exponential model and a number of modifications.

From the data for $P_{O_2} < 1.5$ atm, we used $P_{O_2} = 0.58$ rather than $P_{O_2} = 0.5$ as the transition between injury development and injury recovery. Models 5a and 5b differed only during recovery.

With P_{O_2} in the equations normalized by 1 atm, the published model is

$$\%\Delta VC = -a_1 \cdot P_{O_2}{}^{b} \cdot t^2 \qquad \text{(Models 5a and 5b)},$$

where published values[8–10] are $a_1 = -2.3 \cdot 10^{-6}$ min^{-2} and $b = 4.6$, and our fitted values are $a_1 = -2.7 \cdot 10^{-6}$ min^{-2} and $b = 2.7$ to 4.0, depending on the data set used.

We introduced a threshold when P_{O_2} is elevated,

$$\%\Delta VC = -a_1 \cdot (P_{O_2} - 0.5)^{b} \cdot t^2 \qquad \text{(Model 5c)};$$

set the exponent of time to normalized P_{O_2} to adjust curvature,

$$\%\Delta VC = -a_1 \cdot P_{O_2}{}^{b} \cdot t^{P_{O_2}} \qquad \text{(Model 5d)};$$

allowed a scaling factor on normalized P_{O_2} for finer model control of curvature,

$$\%\Delta VC = -a_1 \cdot (c \cdot P_{O_2})^{b} \cdot t^{c \cdot P_{O_2}} \qquad \text{(Model 5e)};$$

and tried piecewise integration including continuous recovery during and after exposure and for changes in P_{O_2},

$$\%\Delta VC = -a_1 \cdot [(c \cdot P_{O_2})^{b-1} / (c \cdot P_{O_2} + g)] \cdot [t_2^{c \cdot P_{O_2}} - t_1^{c \cdot P_{O_2}}]$$

$$+ (\%\Delta VC) \text{ at } t_1 \qquad \text{(Model 5f)}.$$

To accommodate intermittent exposures, all the models were computed with the accumulated duration at elevated P_{O_2} instead of time since the start of the current elevation in P_{O_2}, and either actual or moving averaged P_{O_2} was used in the calculations. With this modification, the models fit some of the intermittent data.

The curvature of the published model is in the correct direction for $P_{O_2} \geq 1.5$ atm but not for lower P_{O_2}. When the exponent on time is a function of P_{O_2}, the fits at lower P_{O_2} are improved with only slight degradation of those at higher P_{O_2}. Accumulated time at elevated P_{O_2} and moving average P_{O_2} cause these models to predict some but not all of the intermittent data; accumulated time differs from time since the start of the current P_{O_2} elevation only in models not linear in time.

The published recovery portion of the model assumes first-order kinetics,

$$dF / dt = -k \cdot F,$$

but with the rate parameter k a function of the prior P_{O_2}: for $P_{O_2} \leq 0.58$ atm,

$$\%\Delta VC = (\%\Delta VC)_0 \cdot e^{-[c + g \cdot P_{O_{2is}}]}, \qquad \text{(Model 5a)}$$

where $(\%\Delta VC)_0$ is the value after the exposure to $P_{O_2} > 0.58$ atm, and $P_{O_{2is}}$ represents the P_{O_2} of the initial step, the P_{O_2} that caused the injury. For the larger recovery data sets, $c = -4 \cdot 10^{-3}$ min^{-1}, $g = 4 \cdot 10^{-3}$.

We modified the recovery model, first with first-order kinetics but with rate dependence on duration of exposure (T_{dur}) and not on $P_{O_{2is}}$:

$$\%\Delta VC = (\%\Delta VC)_0 \cdot e^{-[c + g / T_{dur}] \cdot t}. \qquad \text{(Model 5b)}$$

For the larger recovery data sets, $c = -4 \cdot 10^{-3}$ min^{-1}, $g = 1.7$.

We modified that further by including an effect of the P_{O_2} during recovery:

$$\%\Delta VC = (\%\Delta VC)_0 \cdot e^{-[c - g \cdot (P_{O_2} - 0.5) / T_{dur}] \cdot t},$$

and we tried second-order kinetics,

$$dF / dt = -k \cdot F^2, \qquad \text{with } k \text{ depending on } T_{dur}:$$

$$\%\Delta VC = (\%\Delta VC)_0 / [1 - (c + g / T_{dur}) \cdot t \cdot (\%\Delta VC)_0].$$

The first-order models fit better than the second-order model.

Arieli's published recovery model accounts very well for the different rates of recovery after several, but not after all, the exposures. Counterintuitively, it implies that recovery should be faster from exposure to high P_{O_2} than from that to lower P_{O_2}, and that recovery will not occur if the exposure P_{O_2} is sufficiently close to atmospheric. Intriguingly, for the recovery data used to develop the model,[10] the duration of exposure was inversely proportional to the exposure P_{O_2}. The first of the modified recovery expressions uses the inverse of exposure duration, predicts recovery for all of the data available, and indicates more rapid recovery after short than after long exposures. The second modification allows the P_{O_2} during recovery to adjust the recovery rate.

Although only one experiment included recovery data in any condition except atmospheric air, this is the preferred recovery model.

6. Many dose responses are sigmoidal. We fitted %ΔVC to a Hill equation dose response:

$$\%\Delta VC = -g \cdot dose^b / (dose^b + a^b)].$$

The Hill equation is bounded between 0 and 1, and the inflection point at $dose = a$ is thus at $\%\Delta VC = g / 2$.

a) We used the proportional healing model concentration of ROS as the dose:

$$F = (P_{O_2} / c) \cdot (1 - e^{-(c \cdot t)}) + F_0 \cdot e^{-(c \cdot t)}.$$

b) We integrated the P_{O_2} difference from a threshold continuously from the start of the oxygen exposure until full recovery and considered that as the dose:

$IntO_2 = \int(P_{O_2} - P_{th})\, dt$, integrating from time = 0 to time = t.

$$\text{Dose} = \begin{cases} IntO_2 & , IntO_2 \geq 0 \\ 0 & , IntO_2 < 0. \end{cases}$$

c) We used the integrated difference from threshold as the dose when P_{O_2} was elevated, but we deviated from the sigmoidal curve to exponential recovery for P_{O_2} below threshold:

$$\%\Delta VC = (\%\Delta VC)_0 \cdot e^{-(c \cdot t)}, \qquad P_{O_2} < P_{th}.$$

Additionally, we fitted with fixed or fitted scaling factor g. With g fitted, the dose can be on either side of the inflection point for curvature in either direction.

The sigmoidal models generally underestimate %ΔVC after the first part of the exposure and do not match well to recovery data.

7. The kinetics of ROS production and removal may differ from the kinetics of injury by ROS concentration and recovery from injury. One model of that type is

$$dF / dt = a \cdot (P_{O_2} - P_{th}) - b \cdot F$$

$$d(\%\Delta VC) / dt = c \cdot F - g \cdot (\%\Delta VC).$$

The relative magnitudes of parameters a, b, c, and g control the curvature with increasing time. However, the data are not sufficiently detailed to distinguish among the parameters of this model.

8. In the injury memory model proposed here, acute injury I_1 is considered to be proportional to the concentration of ROS as given by the proportional healing model, but any acute model could be used. ΔVC is proportional to the sum of all acute injury within a time period τ, essentially over the body's memory for the acute injury:

$$dI_1 / dt = \begin{cases} a \cdot (PO_2 - P_{th}) - b \cdot I_1, & PO_2 > P_{th} \\ -b \cdot I_1, & PO_2 \le P_{th} \end{cases}$$

$\%\Delta VC = \alpha \int I_1 \cdot dt$, integrated over time from $(t - \tau)$ to t.

At constant PO_2, if $a' = a \cdot \alpha$, $PO_2 > P_{th}$, and $t > \tau$, then

$$\%\Delta VC = a' \cdot b^{-2} \cdot (PO_2 - P_{th}) \cdot \{e^{-[b \cdot t]} - e^{-[b \cdot (t-\tau)]}\} + a' \cdot b^{-1} \cdot \tau \cdot (PO_2 - P_{th}) + I_0 \cdot b^{-1} \cdot \{e^{-[b \cdot t]} - e^{-[b \cdot (t-\tau)]}\}.$$

This memory concept could be applied to any form of acute injury. With the proportional rate of healing model, the integration improves the curvature and fit only slightly.

9. Most inflammatory injury occurs sometime after the original insult. The delayed inflammation model presented here is based on a proportional rate of healing model. A similar technique could be used with any acute injury model.

Let τ_{io} = time lag from acute injury to onset of inflammation, and τ_{id} = duration of inflammation. Then

$$\%\Delta VC = -\alpha \cdot F + K_{inflam} \cdot \Sigma \%\Delta VC_a (\theta),$$

where θ in the summation term is a time value that runs from $t - \tau_{io} + \tau_{id}$ to $t - \tau_{io}$, $K_{inflam} > 0$ is the proportionality constant for delayed inflammatory injury, and the acute injury at any time, $\%\Delta VC_a$, is obtained from a selected acute model.

The delayed inflammation model was fitted for arbitrary lag times and inflammatory durations; the data do not permit fitting lags and durations. The model was also fitted with a 300-minute moving averaged PO_2 instead of instantaneous PO_2.

The inflammatory component makes only a small difference in the model fits. Averaging of PO_2 delays recovery slightly and changes the curvature of ΔVC early in the first 300 minutes of the steady exposure experiments from concave up to concave down, but it does not improve the fit in the intermittent experiments.

Discussion

Mechanisms

Many models in the literature have been proposed with putative ROS kinetics. However, the measured quantity, decreased VC, is many steps away from ROS concentration. VC may change because of normal physiological adjustments in blood distribution, regional injury from multiple oxygen-induced pathways, or inflammatory responses to previous insult, and any injury-induced changes will be opposed by compensatory mechanisms. Modeling from an *a priori* mechanism is unrealistic; only descriptive models can be expected to be useful. Further, mechanisms of injury may vary for different exposure conditions; no model should be used for higher P_{O_2} or for longer durations than have been measured, and it may be necessary to apply different models to accommodate the different effects of varied oxygen exposures.

Variability

The multiple adjustments, injury pathways, and compensatory mechanisms that affect VC may be responsible for the large variance of the data. For the data gathered at elevated P_{O_2} excluding intermittent exposures, the residual standard deviation (SD) of %ΔVC about the intersubject average is 7.44, and the residual SD around Model 5e is approximately 8. These values may be used to construct model prediction bands.

Best Candidate Models

Of all models fitted to the data, the best overall candidates during the development of injury are autocatalytic Model 4d and exponential Model 5e. Both of these models permit the curvature of ΔVC with time to differ for different elevations of P_{O_2}. Unfortunately, neither of these injury onset models corresponds to all data available. Currently, a useful injury onset model can be constructed only from the data fit for a particular P_{O_2}. More work concentrating on refinements of these ideas might produce a generalized injury onset model, but, in the absence of a universal model, a fit of either of these candidates to the historical data could be used to predict results from a similar P_{O_2}.

The best recovery model has first-order kinetics with recovery rate dependent on the duration of the previous exposure to elevated P_{O_2} and perhaps on the P_{O_2} during recovery; data for testing the importance of that term are limited. This recovery model may be useful in deciding what surface interval is needed for a chosen fractional recovery between dives.

We have found that many models, including those most familiar to the diving community, fail to represent available data. None of the UPTD concept,[1–3] the linear proportional,[4–6] or the proportional healing models[6] extends to the data accumulated since they were proposed. The proportional healing model, whether with *F* proportional to %ΔVC or with *F* related to %ΔVC through a logarithmic relation,[6] correlates weakly with some of the intermittent data, but it curves in the wrong direction for $P_{O_2} \geq 1.5$ atm and misses the different rates of recovery after different exposures. These familiar

models, if used at all, must be restricted to P_{O_2} very near 1 atm. Of the newly proposed models, if the proportional healing model is used to give the dose for a sigmoidal dose response curve, %ΔVC with increasing time curves in the correct direction for $P_{O_2} \geq 1.5$ atm but does not fit data for $P_{O_2} \geq 2$ atm. Sigmoidal dose response curves also fail for the other dose expressions we proposed.

Because the mean ΔVC after in-water resting exposures with $P_{O_2} = 1.3$ atm for up to 8 hours of exposure is near zero, none of the model predictions correlates with the mean ΔVC.

Conclusions

We have not found a universal model to relate %ΔVC to P_{O_2} and exposure time. The published models do not extend to data beyond those for which they were developed. Although a necessary condition of any universal model appears to be that the curvature with time can change as a function of P_{O_2}, those proposed models that do change curvatures still fail to explain all data. Recent experimental evidence indicates that the mechanisms of lung injury differ at high P_{O_2} from those at P_{O_2} near 1 atm.[11] Models that give %ΔVC as a function of P_{O_2} and exposure time should be used with great caution and only at the P_{O_2} for which they were developed.

The fraction of injury that remains after a recovery period appears to depend on the ratio of the recovery time to the total duration of the previous exposures to elevated P_{O_2}. This may be modified by the P_{O_2} during recovery, but we have few recovery data that are not in atmospheric air. Improved estimates of recovery time may be the most useful result of this modeling effort.

REFERENCES — EXECUTIVE SUMMARY

1. J. M. Clark and C. J. Lambertsen, *Pulmonary Oxygen Tolerance in Man and Derivation of Pulmonary Oxygen Tolerance Curves*, Institute for Environmental Medicine Report No. 1-70, University of Pennsylvania Medical Center, 1970.

2. H. Bardin and C. J. Lambertsen, *A Quantitative Method for Calculating Cumulative Pulmonary Oxygen Toxicity: Use of the Unit Pulmonary Toxicity Dose (UPTD)*, Institute for Environmental Medicine Report No. 4-70, University of Pennsylvania Medical Center, 1970.

3. W. B. Wright, *Use of the University of Pennsylvania, Institute for Environmental Medicine Procedure for Calculation of Cumulative Pulmonary Oxygen Toxicity*, NEDU TR 2-72, Navy Experimental Diving Unit, Jan 1972.

4. A. L. Harabin, L. D. Homer, P. K. Weathersby, and E. T. Flynn, *Predicting Pulmonary O_2 Toxicity: A New Look at the Unit Pulmonary Toxicity Dose*, NMRI Report 86-52, Naval Medical Research Institute, Dec 1986.

5. A. L. Harabin, L. D. Homer, P. K. Weathersby, and E. T. Flynn, "An Analysis of Decrements in Vital Capacity as an Index of Pulmonary Oxygen Toxicity," *J. Appl. Physiol.*, Vol. 63, No. 3 (1987), pp. 1130–1135.

6. R. D. Vann, *Oxygen Toxicity Risk Assessment*, Defense Technical Information Center, ADA299552, May 1988.

7. L. Harabin, S. S. Survanshi, P. K. Weathersby, J. R. Hays, and L. D. Homer, "The Modulation of Oxygen Toxicity by Intermittent Exposure," *Toxicology and Applied Pharmacology*, Vol. 93 (1988), pp. 298–311.

8. R. Arieli, "Oxygen Toxicity as a Function of Time and P_{O_2}," *J. Basic and Clin. Physiol. and Pharmacol.*, Vol. 5, No. 1 (1994), pp. 67–87.

9. R. Arieli, "Power Equation for All-or-None Effects of Oxygen Toxicity and Cumulative Oxygen Toxicity," *J. Basic and Clin. Physiol. and Pharmacol.*, Vol. 5, No. 3–4 (1994), pp. 207–225.

10. R. Arieli, A. Yalov, and A. Goldenshluger, "Modeling Pulmonary and CNS O_2 Toxicity and Estimation of Parameters for Humans," *J. Appl. Physiol.*, Vol. 92 (2002), pp. 248–256.

11. I. T. Demchenko, K. E. Welty-Wolf, B. W. Allen, and C. A. Piantadosi, "Similar but not the Same: Normobaric and Hyperbaric Pulmonary Oxygen Toxicity — the Role of Nitric Oxide," *Am. J. Physiol. Lung Cell Mol. Physiol.* (6 Apr 2007), *in press*.

INTRODUCTION

The degree of pulmonary oxygen toxicity expected from a particular exposure remains difficult to predict, and the mechanisms of the injury are poorly understood. An important step for predicting and understanding them would be to define a model of the response under all conditions. For this report we assessed the ability of some models to predict the average change in vital capacity (ΔVC) caused by various oxygen exposures.

A moderately large body of ΔVC data exists for periods during and after exposure to elevated oxygen partial pressure (P_{O_2}),[1–17] but other pulmonary data are sparse. Thus, we chose ΔVC to represent pulmonary oxygen toxicity, although other parameters might be at least equally appropriate.

Several predictive models have been proposed.[18–26] We have modified some and proposed others, and have compared the fits of all of these models, new or previously published, to the data that are available. The initial goal, an ambitious one, was to find a model to express average ΔVC in terms of P_{O_2} and exposure duration during the onset of injury and during recovery, even with intermittent exposure. Secondary, perhaps more realistic, goals were to describe which model might be best used to approximate a particular set of circumstances and which models do not apply

METHODS

Vital capacity data collected before, during, and after dry hyperbaric chamber exposures during which subjects had rested while breathing oxygen were assembled from literature sources. Additionally, previously unpublished VC measurements made before and after oxygen exposures were accumulated from experiments that had been conducted at the Navy Experimental Diving Unit (NEDU). Model equations in which ΔVC is a function of P_{O_2} and exposure time were fitted to the data from dry chamber exposures, and the predictions derived from them were compared to the dry data and to the measurements made before and after in-water exposures at NEDU.[16,17] Since all the in-water exposures were at similar P_{O_2}, parameters could not be fitted separately to "wet" data.

The available data (Table 1, Figure 1) and subsets were used to estimate parameters of all models. For each data group fitted, the numbers of data available for the models and the numbers of subjects from whom they came are listed in Table 2. The entire dry data set contains VC measurements from 35 different experimental conditions and 351 subject exposures and is available on compact disk from the NEDU Technical Library. In 282 of the subject exposures, measurements were made only before and after the oxygen exposures, not in the chamber during the exposures.

The intersubject variability in response was calculated by comparing ΔVC for an individual to the average ΔVC for that P_{O_2} and at each time.

Table 1.
Data sources

	Experiment Description	Number of subjects	Number of data	Reference
A	1 ata, 83% O_2, 50 hours No recovery	6	72	Ohlsson[1]
B	1 ata, 98% O_2, 72 hours Recovery	4	19 16	Caldwell[2]
C	2 ata, 100% O_2, 12 hours Recovery: 1 ata air	12	47 11	IFEM[3–7]
D	5 ata, air, 48 hours, P_{O_2} = 1 atm Recovery	12	265 84	Eckenhoff et al.[8] (IFEM)
E	Intermittent O_2, 2 ata, 15 hours 100% O_2, 20 min air, 5 min	5	37	Hendricks et al.[9] (IFEM)
F	Intermittent O_2, 2 ata, 15 hours 100% O_2, 60 min air, 15 min	6	39	Lambertsen and Clark[10,11] (IFEM Predictive Studies VI)
G	Intermittent O_2, 2 ata, 15 hours 100% O_2, 30 min air, 30 min	6 *avg. only*	10	Lambertsen and Clark[10,11] (IFEM Predictive Studies VI)
H	1.5 ata, 100% O_2, 18 hours Recovery: 1 ata, air	9	59 36	IFEM Predictive Studies V[6,12]
I	2 ata, 100% O_2, 9 hours Recovery: 1 ata, air	14 8	64 48	IFEM Predictive Studies V[6,12]
J	2.5 ata, 100% O_2, 6 hours Recovery: 1 ata, air	8	48 56	IFEM Predictive Studies V[6,12]
K	5 ata, normoxia, 2.2 ata, normoxia (IFEM) 1 ata, normoxia	6 4 2	162 132 23	Eckenhoff et al.[8] (IFEM) Fisher et al. 1970, as cited in Harabin et al.[13] Ohlsson[1]
L	2.25 ata, air	3	12	Fife et al. 1973, as cited in Harabin et al.[13]
M	Low total pressure >90% O_2, 0.25–0.30 atm 82% O_2, 0.62 atm	17 6	17 6	Morgan et al. 1961, 1963, and DuBois et al. 1963 Michel et al. 1960, as cited in Harabin et al.[13]
N	Disabled submarine (DISSUB) simulations, 10 profiles, recovery	156	542	NEDU[14]
O	DISSUB rescuer simulations, 8 profiles, recovery	126	246	NEDU[15]
P	In-water exposure data 20 fsw, LAR V, recovery 1.35 ata, 100% O_2, recovery	44 24	44 81	Marienau and Maurer[16] Shykoff[17]

ata = atmospheres absolute; fsw = feet of seawater
IFEM = Institute for Environmental Medicine, University of Pennsylvania

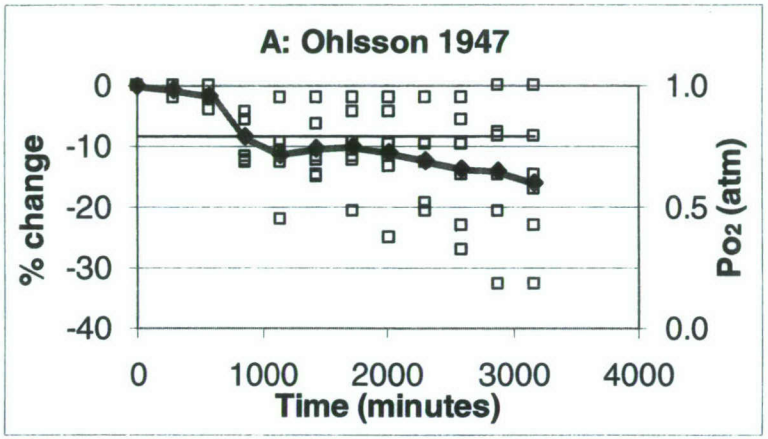

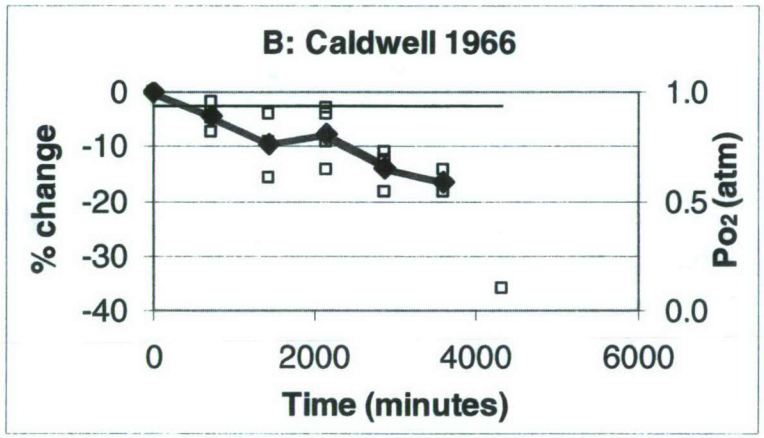

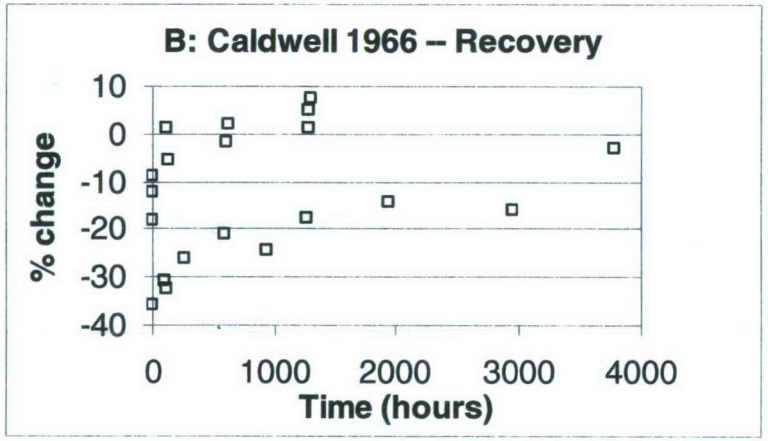

Figure 1. ΔVC as a function of time by experiment. Open squares represent one measurement in one subject. Filled diamonds and lines are cross subject averages; that is, the ΔVCs measured for each subject at that time are averaged. Thin solid line: P_{O_2} during exposure. The numbers of data averaged can vary from point to point. Subjects in Experiment B stopped exposures at different times. (Continued)

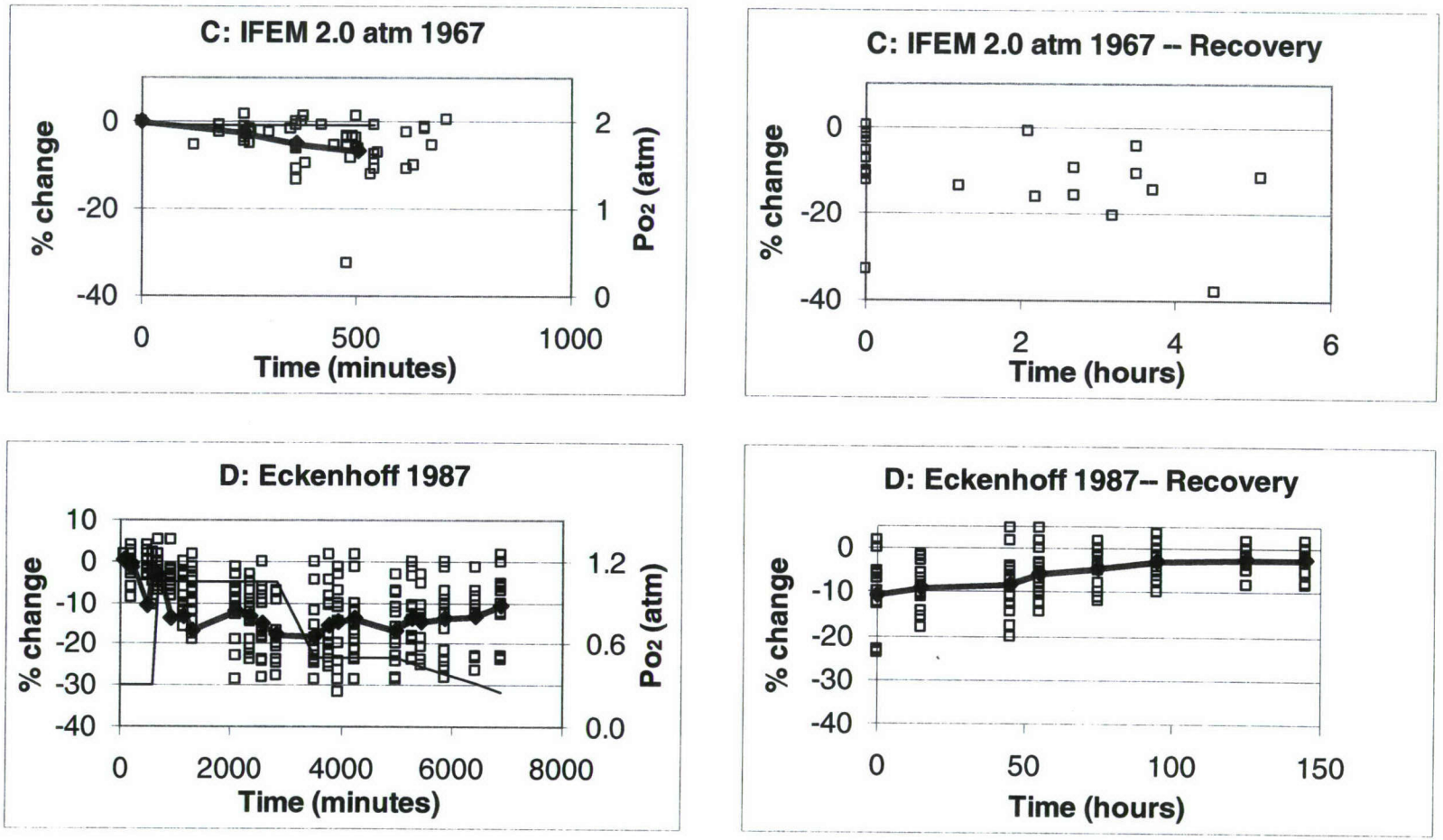

Figure 1. ΔVC as a function of time by experiment. Open squares represent one measurement in one subject. Filled diamonds and lines are cross subject averages; that is, the ΔVCs measured for each subject at that time are averaged. Thin solid line: P_{O_2} during exposure. The numbers of data averaged can vary from point to point. In Experiment C, subjects ended exposure after different times, and averaging is shown only until the first termination. (Continued)

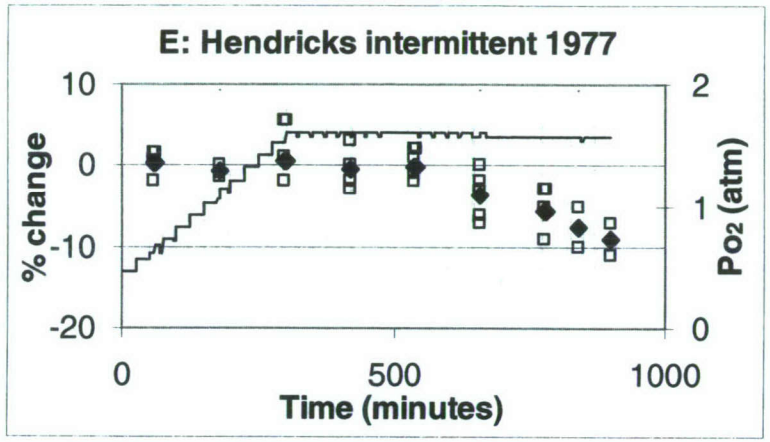

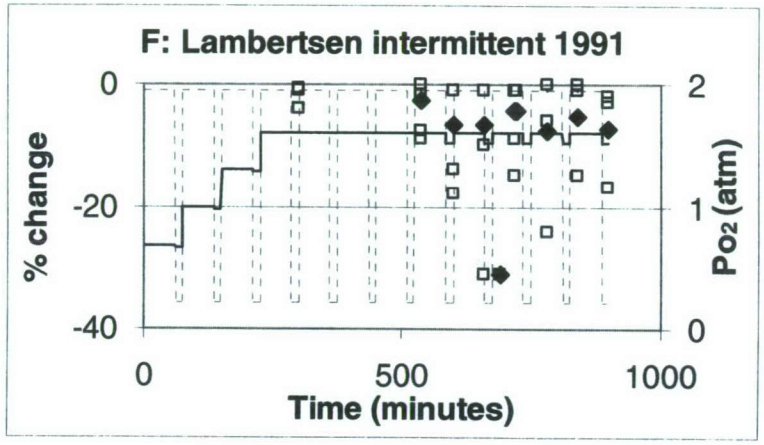

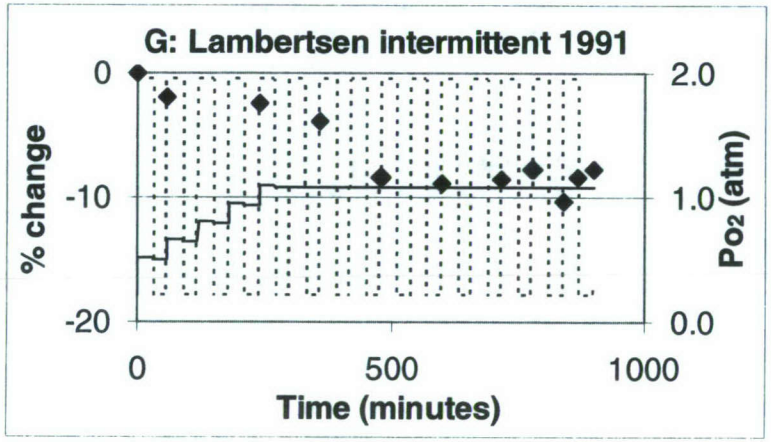

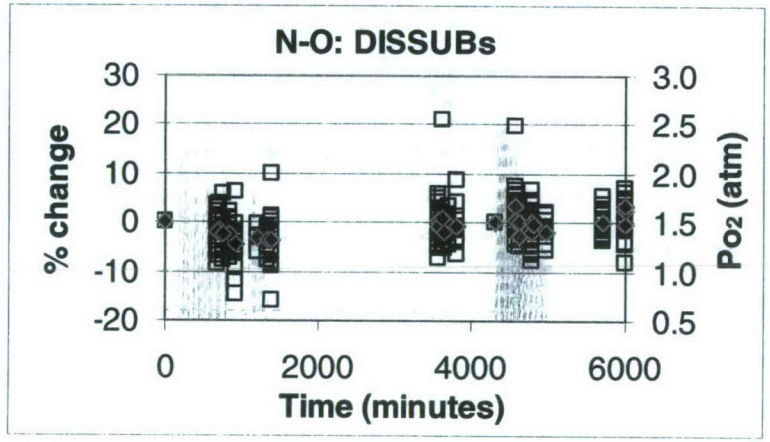

Figure 1. ΔVC as a function of time by intermittent exposure experiment. Open squares represent one measurement in one subject. Filled diamonds are cross subject averages. Dashed gray line represents instantaneous P_{O_2} and solid line P_{O_2} with a 300-minute moving average. (Continued)

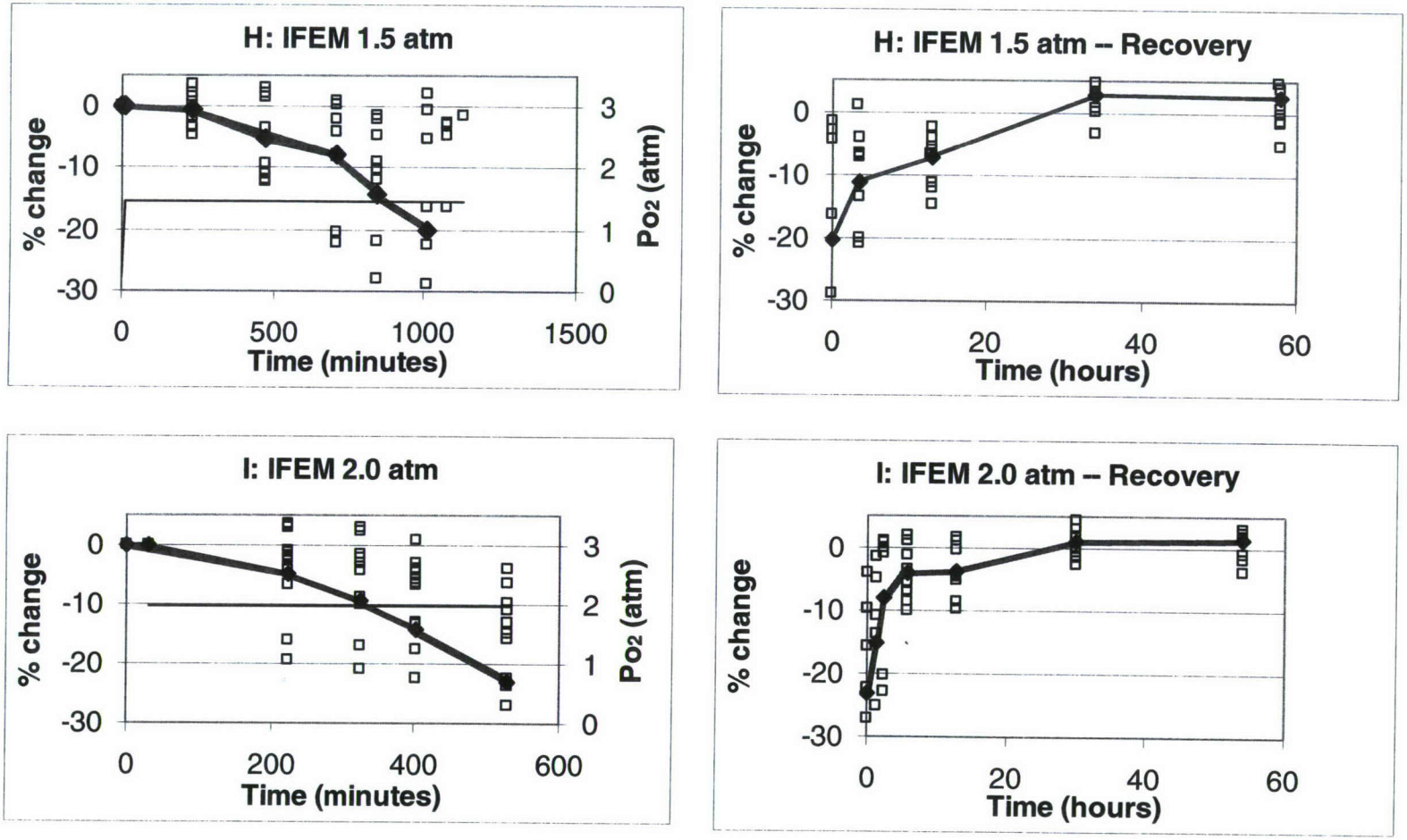

Figure 1. ΔVC as a function of time by experiment. Open squares represent one measurement in one subject. Filled diamonds and lines are cross subject averages; that is, the ΔVCs measured for each subject at that time are averaged. Thin solid line: P_{O_2} during exposure. The numbers of data averaged can vary from point to point. (Continued)

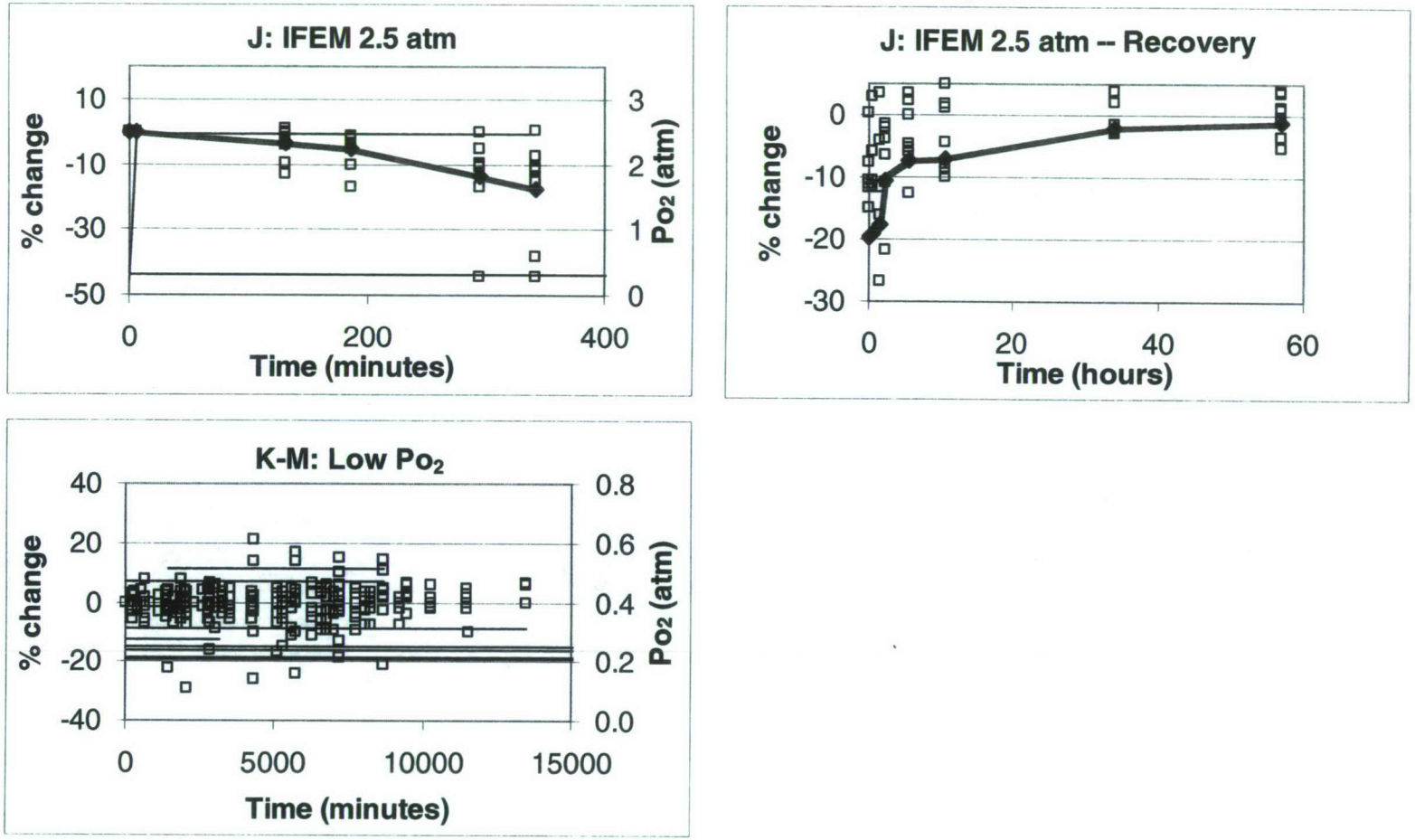

Figure 1. ΔVC as a function of time by experiment. Open squares represent one measurement in one subject. Filled diamonds and lines are cross subject averages; that is, the ΔVCs measured for each subject at that time are averaged. Thin solid lines: P_{O_2} during exposures.

Cumulative percentage ΔVC from baseline (%ΔVC) was used as the dependent variable to measure injury. Alveolar P_{O_2} and time were the independent variables. Parameters were calculated to minimize the sum of squares of the difference between calculated and measured ΔVC. The *a priori* model types that we tried to fit, all described in detail (see *Descriptions of Models*), included:

1. Unit Pulmonary Toxic Dose (UPTD) models (Fig. 2);
2. Proportional models, in which a factor causing %ΔVC is proportional to P_{O_2} and time (Fig. 3);
3. Proportional rates of healing models, in which a factor causing %ΔVC increases at a rate proportional to P_{O_2} and time and disappears at a rate proportional to its concentration (Fig. 4);
4. Autocatalytic models, in which a factor causing %ΔVC propagates more of itself if the P_{O_2} is sufficiently elevated, but in which the factor causing %ΔVC is eliminated in proportion to its concentration when P_{O_2} is below that critical value (Fig. 5);
5. Exponential models, in which %ΔVC is proportional both to P_{O_2} raised to an exponent and to the square of exposure time, but %ΔVC recovers by exponential decay (Fig. 6);
6. Sigmoidal dose response models, in which the dose is derived from the proportional healing model or is the time integral of P_{O_2} (Fig. 7);
7. A model in which injury is related to P_{O_2} with differing kinetics for generation of a factor causing %ΔVC and generation of %ΔVC (Fig. 8);
8. An "injury-memory" model, in which %ΔVC represents an accumulated result of a proportional rate of healing (Fig. 9); and
9. Delayed inflammation models that include secondary, inflammatory %ΔVC components proportional to the acute %ΔVC that occurred at a previous time.
   (a) The proportional healing model causes the acute %ΔVC (Fig. 10), and
   (b) the proportional healing model with P_{O_2} averaged over a period of time causes the acute %ΔVC (Fig. 11).

Additionally, using all dry data, we did separate stepwise linear regression analyses for onset of injury and for recovery to see which parameters of the set P_{O_2}, previous P_{O_2}, time at the P_{O_2}, the square of the time at the P_{O_2}, total pressure, and duration of the previous exposure to elevated P_{O_2} entered significantly into the linear relation with %ΔVC.

Unless it is otherwise noted in the model description, we used estimated alveolar, rather than inspired, P_{O_2} as the stimulus causing %ΔVC. To calculate alveolar P_{O_2} we used the alveolar gas equation

$$P_AO_2 = F_IO_2 \cdot (P_{tot} - P_{water}) - P_ACO_2 \cdot [F_IO_2 + (1 - F_IO_2)/RQ],$$

where P_AO_2 is alveolar O_2 partial pressure;
F_IO_2 is the inspired O_2 fraction;
P_{tot} is total pressure;

P_{water} is the saturation partial pressure of water at 37 °C, 47 Torr;
P_ACO_2 is alveolar CO_2 partial pressure, normally about 40 Torr; and
RQ is the respiratory quotient, the ratio of CO_2 produced to O_2 consumed. (We assumed RQ = 0.8.)

Because

$$P_IO_2 = F_IO_2 \cdot P_{tot},$$

$$P_AO_2 = P_IO_2 - F_IO_2 \cdot (P_{water} + P_ACO_2) - P_ACO_2 \cdot [(1 - F_IO_2)/RQ]$$

$$= P_IO_2 - 37 \cdot F_IO_2 - 50, \quad \text{expressed in Torr,}$$

$$= P_IO_2 - 0.04 \cdot F_IO_2 - 0.07, \text{ expressed in atm,}$$

where P_IO_2 is inspired O_2 partial pressure.

When F_IO_2 is low and total pressure is high, the difference between alveolar and inspired PO_2 is relatively small, but at high F_IO_2 and low total pressure it is important, as we can infer from the equations. For a person breathing atmospheric air at sea level, P_IO_2 is 160 Torr or 0.21 atm, and $P_AO_{2\,is}$ 100 Torr, or about 0.13 atm.

The inspired oxygen values are those reported by the experimenters. We cannot confirm that experimental systems did or did not control F_IO_2.

Methods of Fitting

Although some subjects participated in multiple experiments and the number of measurements per subject varied among experiments, for the most part data were considered to be independent. When results are listed as "weighted by datum," each measurement was given equal weight independent of the number of measurements on each subject. Some results where each subject was weighted equally ("weighted by data/subject") are presented. In those cases the weighting factor for each measured value was the number of measurements/subject, with separate counts during injury onset and during recovery.

We used Marquardt's algorithm to implement nonlinear regression in Pascal (Borland Delphi Professional ver. 4.0) and incorporated some library routines (Dmath ver. 2.0, J. DeBord). We included the simplex method as an option for fitting and sometimes used it to find starting parameters for a Marquardt's fit. The program was written to allow modular insertion of different model configurations and was tested with a simulated, externally generated data set with known parameter values.

Marquardt's lambda was set initially to $1 \cdot 10^{-2}$ and was constrained to a maximum value of $1 \cdot 10^{3}$. Numerical differentiation was used. One parameter at a time, a parameter estimate was multiplied by $(1 + 1.5 \cdot 10^{-8})$, the sums of squared differences from the data of the fitted model function were computed with the perturbed and the

unperturbed estimates, and the difference in the sum of squares caused by the parameter perturbation was divided by the magnitude of the perturbation, $1.5 \cdot 10^{-8}$, to obtain the estimate of the derivative with respect to that parameter for the particular parameter value. The iterations were considered to have converged when either the absolute or the fractional difference of all parameters between two iterations was less than $1 \cdot 10^{-7}$.

To verify that another minimum of the fitting surface could not be found near the initial fit, starting values for the parameters were varied by one order of magnitude in each direction from the first fit obtained with the entire data set, and the parameters were reestimated. Thus, we fitted a two-parameter model for nine starting values, a three-parameter model for 27 starting values, etc. If the model did not converge with these perturbed initial estimates, we tried smaller perturbations from the initial fitted values. If we had found a second minimum, we would have selected the one with the lower residual sum of squares. Because all the tested models generate simple error surfaces, we considered this number and range of checks on the fit to be sufficient.

We assessed fits with the statistical uncertainty of parameter estimates, the correspondence of fitted curves to measurements from specific experiments, and the magnitudes of coefficients of determination. Coefficients of determination are numerically identical to the regression coefficient r^2.

Coefficient of determination $r^2 = 1 -$ (Residual sum of squares)/(Total sum of squares)
$= 1 - \Sigma (y_{calc\,i} - y_i)^2 / \Sigma (y_i - y_{avg})^2$ summed for $i = 1 \ldots n$,

where $y_{calc\,i}$ = the ith calculated estimate of %ΔVC, and
$y_{avg} = \Sigma y_i / n$ for $i = 1 \ldots n$.

The coefficient of determination expresses the fraction of the total variance of the data explained by a calculated (model) fit. The coefficient of determination can be negative if the model inflates the variability of the data; the "squared" of the r^2 notation is misleading in that regard. Note that a few large deviations of the model from the fit can have a large effect on the value of r^2.

Correspondence of model fits and the highly intermittent data from the disabled submarine (DISSUB) experiments N and O were difficult to assess graphically. Correlation coefficients were calculated for those data.

The models differ in the number of parameters fitted and therefore in the degrees of freedom. The r^2 has been adjusted as

$$r^2_a = 1 - [(1 - r^2) \cdot (n_{obs} - 1) / (n_{obs} - n_{param})],$$

where n_{obs} indicates the number of VC measurements and n_{param} indicates the number of parameters fitted in the particular regression. In all cases, because $n_{obs} >> n_{param}$, the correction is small.

We calculated an intersubject average response as a function of time within each experiment by averaging the data from all subjects at each measurement time for a particular P_{O_2}. Subjects in some experiments ended oxygen exposures at differing times; we averaged recovery data by matching the times from the return to normoxic conditions.

When the intersubject average is the model, the coefficient of determination measures variability of the data about the average response; a data set where every subject had the same response yields $r^2 = 1$. Although standard deviation and coefficient of determination are good measures of dispersion if data are stationary, the ΔVC are functions of time and P_{O_2}. We therefore have chosen the coefficient of determination about the intersubject mean as the measure of dispersion for each experiment. We compared the coefficients of determination of the models to those for the averages to judge model performance for each experiment.

Because the data include values from a few experiments in which P_{O_2} changed more than once (e.g., Figure 1 D), the models were generalized to handle multiple steps of elevated P_{O_2}. The fitted value of VC after one segment of elevated P_{O_2} is the starting value, $\%\Delta VC_0$, for the further change of the next segment. However, the changes in that next segment affect the parameter values that determine the fitted $\%\Delta VC_0$. Although the problem could be solved by recalculating the segmental starting values at each change in parameter, we chose to solve it iteratively.

1. For the first elevation of P_{O_2} from room air, $\%\Delta VC_0 = 0$. The first estimate of parameters was found by using only the measurements from the first elevation of P_{O_2}. Parameter estimates were required to converge to within either an absolute or a fractional mean square difference of 1×10^{-7}.
2. Parameter estimates from Step 1 were used to calculate first estimates of $\%\Delta VC_0$ for subsequent changes in P_{O_2}.
3. The segmental $\%\Delta VC_0$ were held constant, and all model parameters were fitted to the entire data set under consideration until parameters converged to within 1×10^{-7}.
4. Using the parameters from Step 3, we recalculated $\%\Delta VC_0$ for all segments.
5. Iterations 3 and 4 were continued until the estimates of $\%\Delta VC_0$ for each increment of P_{O_2} change converged to either an absolute or a fractional mean square difference of $\%\Delta VC_0 \leq 1 \times 10^{-4}$, and parameters calculated with those $\%\Delta VC_0$ values converged to within 1×10^{-7}.

Continuous changes in P_{O_2} were handled as multiple steps, matching the fact that data were acquired discontinuously.

From one experiment (Set G, Table 1) only averaged data were available. When we used these data we considered the average ΔVC from the six subjects to have been obtained six times. The lack of individual data means that the variability of that data set is unknown.

Data Grouping

Several of the nine types of models in the study (see *Descriptions of Models*) have been proposed at least in part by other authors; the other types have not appeared in the literature. To fit their models, Harabin et al.[13,21] and Vann[22] used data sets A–D and K–M, but Harabin did not use the recovery data or initial measurements at P_{O_2} = 0.3 atm in set D, and Vann did not use the recovery data. Arieli[24–26] used data sets C, D, and H–J.

For fitting, we defined Data Group 1 to be all of data sets A–D and K–M (Harabin's data plus recovery and early exposure), Group 2 to be sets A–M, Group 3 to be sets A–D and H–M (all uninterrupted data), and Group 4 to be data sets A–O (all dry data). Data Group 4, which consists of Data Group 2 and the DISSUB simulation experiments, includes data from complicated intermittent profiles for which only the postexposure vital capacities are known. Note that Data Group 4 includes all other data groups, Data Group 3 includes all of Data Group 1, and Data Group 2 includes all of Data Group 3.

We fitted data for three recovery durations: no recovery, recovery time up to eight hours, and all recovery data. Table 2 shows the number of VC measurements in each data group.

Table 2.
Number of subjects and number of vital capacity differences used in fits for each data group and recovery duration

Data group	**Number of subjects**	**Number of vital capacity differences available**		
Letters refer to Table 1		**No recovery >30 min**	**Up to 8-hr recovery**	**All recovery**
1 = A–D, K–M	68	610	620	744
2 = A–M	117	878	1021	1220
3 = A–D, H–M	105	817	885	1084
4 = A–O	408	865	1208	1975
In-water = P	68	0	68	132

The number of measurements for in-water exposures is small, all exposures are at P_{O_2} between 1.3 and 1.5 atm, and only recovery data were obtained. Since the mechanisms of injury for divers in the water may not be identical to those for subjects in air, it seemed unwise to pool the data from in-water and dry exposures. Thus, parameters were not fitted to the data from wet exposures. Instead, ΔVC following in-water exposures was compared to that of model fits calculated by using parameters obtained from the dry data sets.

Descriptions of Models

Some of the models relate %ΔVC directly to P_{O_2}, while others assume that a product of a reaction with oxygen provokes the changes. For simplicity in this report, any or all of the harmful substances that may be produced in the presence of elevated P_{O_2} are termed reactive oxygen species (ROS). In this report, "ROS concentration" is a model construct. We have not measured ROS concentration, and we recognize that ROS of diverse types can have different effects.

In the model descriptions below, symbols are defined as follows:

F = the concentration of ROS;
t = elapsed time (min) at a constant P_{O_2} or during a ramp change in P_{O_2};
P_{th} = a threshold P_{O_2} below which no injury occurs;
t_{th} = a threshold time before which no injury occurs;
subscript $_0$ indicates an initial value for the segment at one condition of P_{O_2}, whether P_{O_2} is steady or is ramping up or down; and
%ΔVC = change in vital capacity, always from the measurement made before the oxygen exposure.

The parameters that we fitted are represented by the italic letters *a*, *b*, *c*, and *g*. P_{th}, t_{th}, and autocatalytic pressure threshold P_a also are fitted parameters of some models. To prevent confusion with the symbol for derivative, the base of natural logarithms, and the notation for a function, the letters *d*, *e*, and *f* are not used as parameter designators, and e, the base of the natural logarithms, is represented in roman type. All fitted parameters are positive real numbers; negative signs are stated explicitly.

The schematic diagrams of Figures 2–11 are designed to illustrate the model curvatures with time. No units are given, only the relation of the P_{O_2} steps to any threshold P_{O_2} values. Magnitudes depend on parameters.

1. Unit Pulmonary Toxic Dose (UPTD) Model

$$\begin{aligned} \text{UPTD} &= t \cdot [(P_{O_2} - P_{th}) / (1\ \text{atm} - P_{th})]^{b}, && P_{O_2} \geq P_{th} \\ &= 0, && P_{O_2} < P_{th} \end{aligned}$$

The original definition of UPTD fixed $b = 1/1.2 = 0.833$ and $P_{th} = 0.5$ atm.

By inspection of the one set of published data available from multiple sources,[13,19,20]

$$\%\Delta VC = a \cdot \text{UPTD} + c.$$

The UPTD model[13,18–21] is arguably the best-known model for estimating %ΔVC. We tried three versions of this model:

(a) with the original definition of UPTD, but fitted parameters *a* and *c* (that is, fitting the standard UPTD definition to %ΔVC);
(b) with fixed threshold, but fitted parameters *a*, *b*, and *c*; and
(c) with fitted parameters *a*, *b*, *c*, and P_{th}.

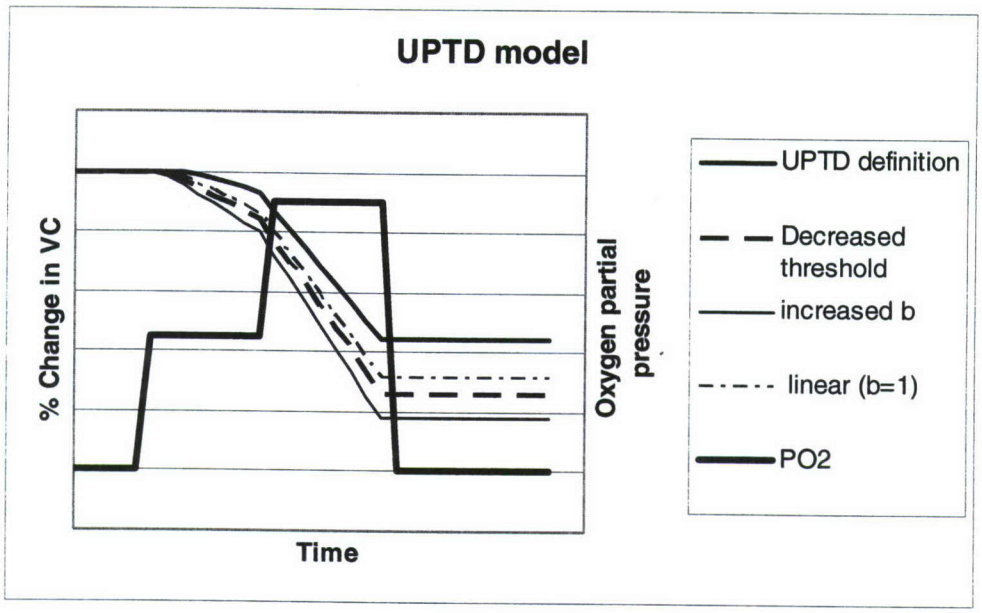

Figure 2. Schematic of Model 1, showing effects of varying parameters. After a latent period, the UPTD model shows a nearly linear decrement in VC with time when P_{O_2} is elevated. Recovery is not defined. Model behavior is depicted for P_{O_2} below threshold (no change), above threshold, and increasingly elevated above threshold.

2. Proportional and Related Models

Models in which %ΔVC is the product of a time term and a P_{O_2} term state that toxicity increases as either exposure time or P_{O_2} increases. The most general model of this type is

$$\%\Delta VC = a \cdot (P_{O_2} - P_{th})^b \cdot (t - t_{th})^c + \%\Delta VC_0, \qquad t \geq t_{th} \geq 0, \text{ and } c > 0.$$

Because exponents *b* and *c* need not be integers, the expression has general validity only if $P_{O_2} > P_{th}$. This restriction of the data caused the number of available data *n* to be a function of P_{th}; if $P_{O_2} < P_{th}$ on any iteration, the weighting factor on the measurement was set to 0, and otherwise the weight was set to 1 or to the number of subjects from whom data had been averaged to obtain the value. In other words, when $P_{O_2} < P_{th}$, it was treated as if the measurement had not been made. The number of measurements that are considered in the fit fluctuates with P_{th}, and the number in the final fit becomes a model result.

If the exponent *b* is unity, %ΔVC becomes directly proportional to the P_{O_2} difference from threshold, and P_{O_2} values below threshold permit healing.

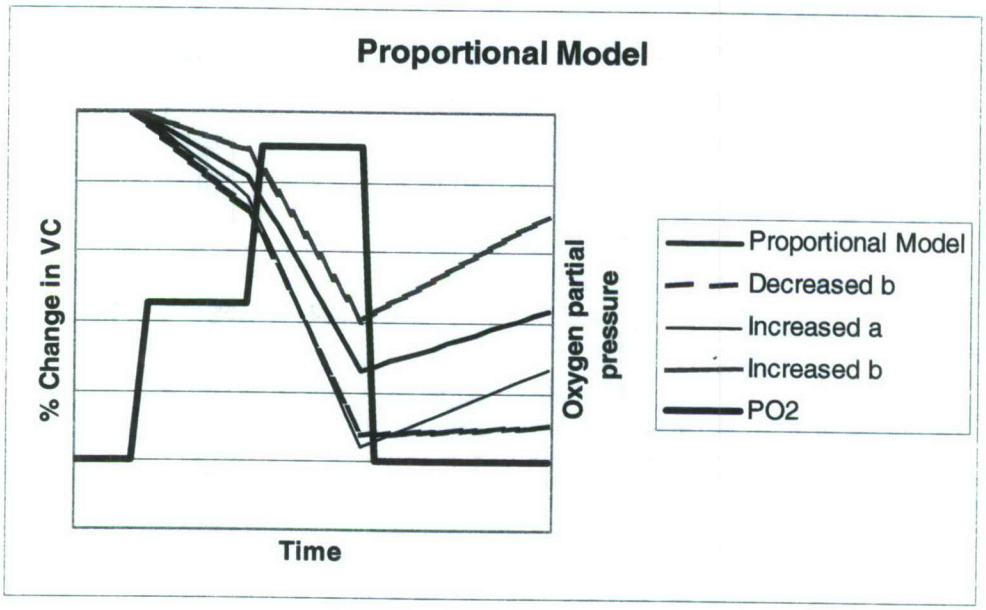

Figure 3. Schematic of Model 2a. The proportional model is linear in time, both in onset and in recovery. Model behavior is depicted for P_{O_2} below threshold *b*, elevated above threshold *b*, more elevated, and then in a recovery phase below threshold *b*. Effects of parameters are depicted.

If %ΔVC = $-\alpha \cdot F$, the differential form of the model with exponents *b* and *c* equal to one is

$$dF/dt = a_1 \cdot (P_{O_2} - P_{th}) = a \cdot P_{O_2} - g,$$

where $g = a \cdot P_{th}$ and $a_1 = a/\alpha$. The model hints at first-order kinetics for ROS production and zero-order kinetics for ROS destruction. For *t* at constant P_{O_2},

$$F = \begin{cases} a \cdot (P_{O_2} - P_{th}) \cdot t + F_0, & P_{O_2} \geq P_{th} - F_0/(a_1 \cdot t) \\ 0, & P_{O_2} < P_{th} - F_0/(a_1 \cdot t). \end{cases}$$

Because the quantity *F* is a concentration, it cannot be negative.

F can be related to ΔVC, as in the Harabin reduced (linear) model[13,21,22]

$$\%\Delta VC = -\alpha \cdot F, \qquad \text{(Model 2a)}$$

where the fitted parameter becomes $a' = \alpha \cdot a$.

Alternatively, the more complicated relation proposed by Vann[22] to limit $|\%\Delta VC| \leq 100\%$ can be used:

$$\%\Delta VC = -100\,[1 - 1.005^{-F}]. \qquad \text{(Model 2b)}$$

3. Proportional Rate of Healing Model

$$dF/dt = \begin{cases} a \cdot (P_{O_2} - P_{th}) - b \cdot F, & P_{O_2} > \text{threshold} \\ -b \cdot F, & P_{O_2} \leq \text{threshold} \end{cases}$$

This model, proposed by Vann,[22] sets the rate of ROS elimination to be proportional to their concentration F and sets the rate for ROS production to be proportional to P_{O_2} above a threshold. An implied mechanism is that ROS are unstable.

Again, the simplest relation between F and $\%\Delta VC$ is

$$\%\Delta VC = -\alpha \cdot F. \qquad \text{(Model 3a)}$$

The more complicated relation, which puts bounds on $\%\Delta VC$, can also be used:

$$\%\Delta VC = -100\,[1 - 1.005^{-F}]. \qquad \text{(Model 3b)}$$

A third version is presented in Model 6a, the sigmoidal model.

The solutions of the differential equation for t at constant P_{O_2} are

$$F = \begin{cases} (a/b) \cdot (P_{O_2} - P_{th}) \cdot [1 - e^{-(b \cdot t)}] + F_0 \cdot e^{-(b \cdot t)}, & P_{O_2} > \text{threshold} \\ F_0 \cdot e^{-(b \cdot t)}, & P_{O_2} \leq \text{threshold}. \end{cases}$$

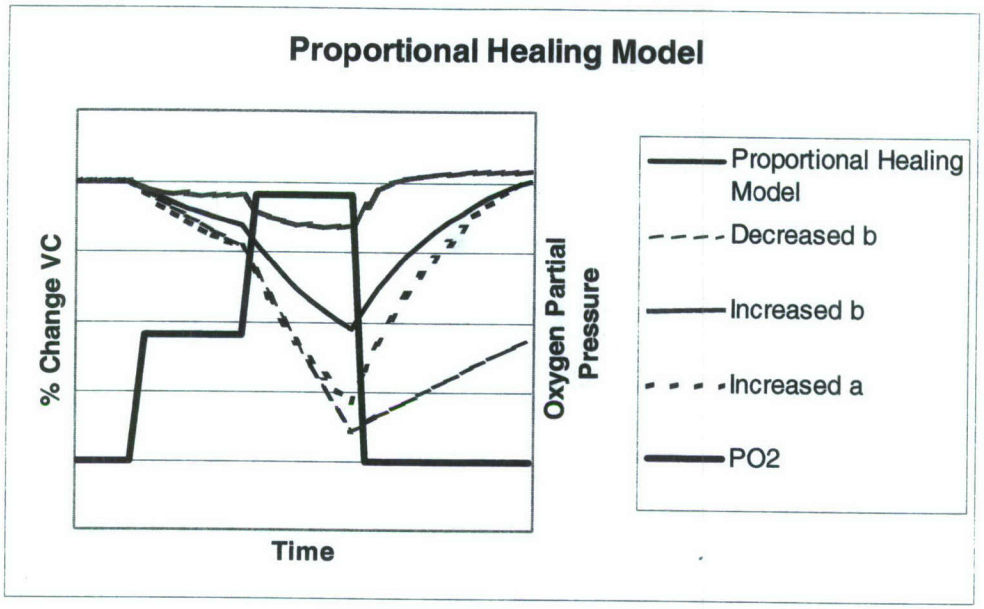

Figure 4. Schematic of Model 3a. The proportional healing model is depicted for P_{O_2} below threshold *b*, elevated above threshold *b*, more elevated, and then in a recovery phase below threshold *b*. Effect of parameters are depicted.

The proportional healing model (Fig. 4) demonstrates curvilinear responses as time increases at constant P_{O_2}. When P_{O_2} is above threshold *b*, injury increases at a rate proportional to the elevation in P_{O_2}, and healing proceeds at a rate proportional to injury. When P_{O_2} is below threshold, %ΔVC decays exponentially. A steady state in injury — shown in Figure 4's "Increased *b*" curve — is achieved after a time duration that depends on parameter values. Model 3b keeps recovery values at or below baseline, a restraint preventing overshoot like that shown in the "Increased *b*" tracing.

4. Autocatalytic Models

An autocatalytic reaction is one in which the concentration of a reaction product becomes self-amplifying under specific conditions. The model formulation that we have tested is that proposed by Harabin et al. in a central nervous system oxygen risk model of the protective effect of air breaks in experimental animals.[23] In our application, though, the reaction products are ROS, and the reaction becomes self-amplifying when P_{O_2} exceeds parameter P_a, where $P_a > P_{th}$. For $P_{O_2} < P_a$, the exponent of recovery is a function of P_{O_2}.

$$dF/dt = \begin{cases} a_1 \cdot (P_{O_2} - P_{th}) + b \cdot F \cdot (P_{O_2} - P_a), & P_{O_2} > P_{th}, \\ b \cdot F \cdot (P_{O_2} - P_a), & P_{O_2} \le P_{th}. \end{cases}$$

Parameter *b* can be replaced by a function of the duration of exposure and P_{O_2}.

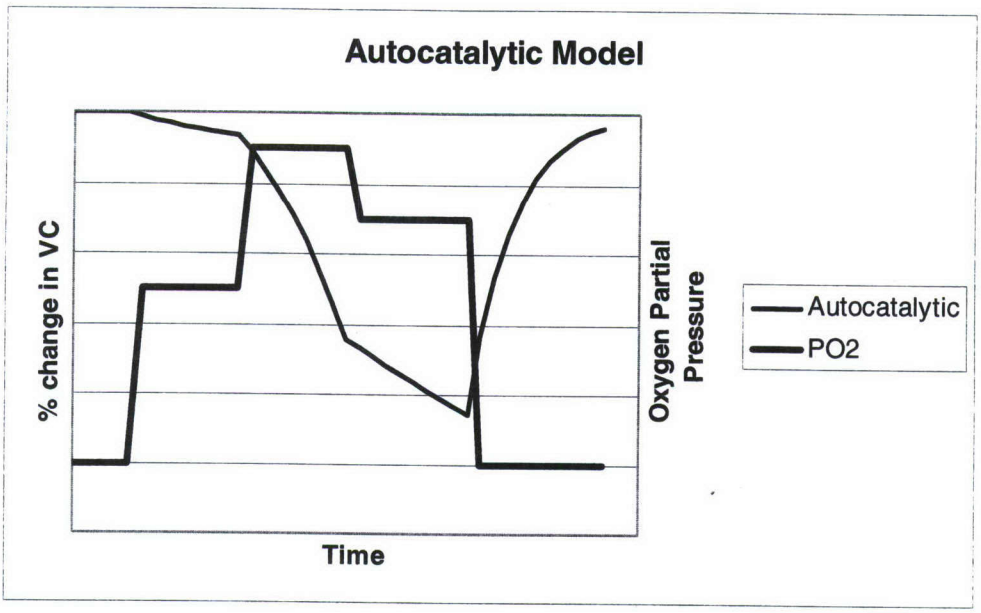

Figure 5. Schematic of Model 4. Steps in P_{O_2}, left to right, represent $P_{O_{22}} < P_{th}$, $P_{th} < P_{O_2} < P_a$, $P_{O_2} > P_a$, $P_{O_2} = Pa$, and $P_{O_2} < P_{th}$ when there is prior injury.

The autocatalytic model (Fig. 5) shows distinct behaviors for each different range of P_{O_2} diagrammed as a step change. P_{O_2} begins below the threshold for injury, P_{th}.

The first step indicates the model response for P_{O_2} between P_{th} and P_a, the P_{O_2} at which autocatalytic behavior begins. In this range the autocatalytic model reduces to a proportional healing model, but the time constant of healing depends on P_{O_2}. Any of the upwardly concave responses shown for elevated P_{O_2} in Figure 4 could occur in this P_{O_2} range.

The second step in Figure 5 represents $P_{O_2} > P_a$. In this P_{O_2} range, injury increases at a rate proportional to itself in addition to the increase proportional to the P_{O_2} elevation, an increase generating a downwardly concave curve. Changes in parameters modify the slope and curvature.

The third step in Figure 5 indicates the model response when $P_{O_2} = Pa$, when the model reduces to the proportional (linear) model: changes in parameters have the effects shown for the elevated P_{O_2} in Figure 3.

When P_{O_2} is below the injury threshold, recovery rate is proportional to injury, as in the proportional healing model. Adjusting parameters brings results similar to those shown in the recovery phase of Figure 4.

For constant P_{O_2}, the autocatalytic model becomes

$$F = \begin{cases} a_1 \cdot (P_{O_2} - P_{th}) / [b \cdot (P_{O_2} - P_a)] \cdot [1 - e^{b \cdot (P_{O_2} - Pa) \cdot t}] + F_0 \cdot e^{b \cdot (P_{O_2} - Pa) \cdot t}, & P_{O_2} \neq P_a \text{ and } P_{O_2} > P_{th} \\ F_0 \cdot e^{b \cdot (P_{O_2} - Pa) \cdot t}, & P_{O_2} \leq P_{th} \\ a_1 \cdot P_{O_2} \cdot t + F_0, & P_{O_2} = P_a \end{cases}$$

$\%\Delta VC = -\alpha \cdot F$, and the value a reported in Table 12 is $a = \alpha \cdot a_1$.

These expressions describe several response shapes, as illustrated in Figure 5. Note that the model predictions are concave upward with increasing t for $P_{th} < P_{O_2} < P_a$, linear for $P_{O_2} = P_a$, and concave downward for $P_{O_2} > P_a$.

5. Exponential Models

When P_{O_2} is elevated above the normal atmospheric value, Arieli et al.[24–26] modeled the damage caused by ROS as quadratic in time and higher than first order in the ratio of P_{O_2} to one atmosphere:

$$\%\Delta VC = -a \cdot (P_{O_2})^b \cdot t^2, \quad \text{where } P_{O_2} \text{ is numerically in atm and } P_{O_2} > 0.5 \text{ atm.}$$

If P_{O_2} drops to or below 0.5 atm, recovery begins at a rate dependent on the P_{O_2} of the previous segment. In this report, the previous P_{O_2} (presumably that at which injury occurred) is termed the initial P_{O_2} for the recovery segment and is symbolized as $P_{O_2\,is}$:

$$d(\%\Delta VC) / dt = -(c + g \cdot P_{O_2\,is}) \cdot \%\Delta VC,$$

where $P_{O_2\,is} > 0.5$ atm and $(c + g \cdot P_{O_2\,is}) \geq 0$.

The model assumes accumulation of injury only if $P_{O_2} > 0.5$ atm.

We considered modeling with a constant recovery rate, but inspection of the data (Fig. 1) shows a clear difference in rates of recovery among experiments. We introduced a model with ongoing removal of ROS even as ROS accumulates, models with different exponents of time, and models with different recovery kinetics.

a. We restated Arieli's exponential model to accommodate multiple changes in P_{O_2} by using the concept that elevated P_{O_2} generates ROS with concentration F, where $\%\Delta VC = -\alpha \cdot F$. At any change in P_{O_2}, ROS from the previous P_{O_2} condition are present in concentration F_0. F_0 will be zero only if the initial $P_{O_2} \leq 0.5$ atm and any previous accumulations have decayed. Healing depends on $P_{O_2\,is}$ once $P_{O_2} \leq 0.5$ atm:

$$F = \begin{cases} a_1 \cdot (P_{O_2} / 760)^{b} \cdot t^2 + F_0, & P_{O_2} > 0.5 \text{ atm} \\ F_0 \cdot e^{-(c + g \cdot P_{O_2 \text{ is}}) \cdot t}, & P_{O_2} \le 0.5 \text{ atm} \end{cases}$$

If $P_{O_{2is}} \le 0.5$ atm, the P_{O_2} from the previous segment with $P_{O_2} > 0.5$ is used. If $(c + g \cdot P_{O_2 \text{ is}}) < 0$, the term is set to 0; F cannot increase if $P_{O_2} < 0.5$.

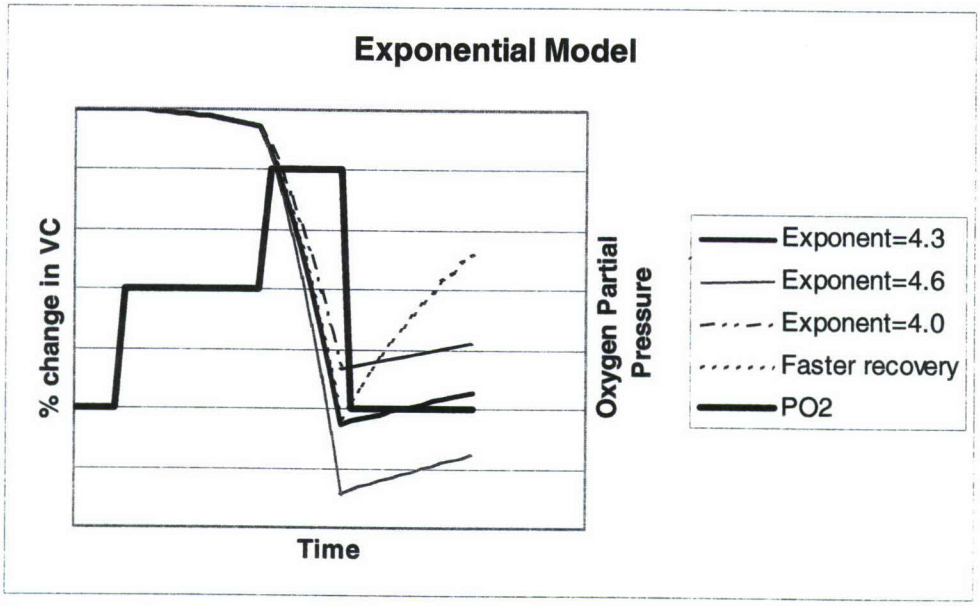

Figure 6. Schematic of Model 5. Left to right, P_{O_2} not elevated, normalized P_{O_2} = 1, normalized P_{O_2} = 2, P_{O_2} not elevated. Effects of varied exponents are shown.

The exponential model 5a (Fig. 6) is depicted for the first step of P_{O_2} = 1 atm and for the second step as P_{O_2} = 2 atm to represent all P_{O_2} values greater than 1 atm. The third step shows recovery. Note that the model prediction is independent of the exponent *b* when P_{O_2} = 1 atm but is very sensitive for the higher P_{O_2}. Recovery in Figure 6 is shown from only one $P_{O_2 \text{ is}}$.

b. The healing function is replaced by one in which the time constant is a function of the previous duration of exposure, T_{dur}, rather than the previous P_{O_2}:

$$F = \begin{cases} a_1 \cdot (P_{O_2} / 760)^{b} \cdot t^2 + F_0, & P_{O_2} > 0.5 \text{ atm} \\ F_0 \cdot e^{-(c + g/T_{dur}) \cdot t}, & P_{O_2} \le 0.5 \text{ atm} \end{cases}$$

c. The healing function is replaced by one in which the time constant is a function both of the previous duration of exposure, T_{dur}, and of the previous P_{O_2}. Also, the P_{O_2} threshold is subtracted when P_{O_2} is elevated:

$$F = \begin{cases} a_1 \cdot (P_{O_2}/760 - 0.5)^b \cdot t^2 + F_0, & P_{O_2} > 0.5 \text{ atm} \\ F_0 \cdot e^{-[c + g(P_{O_2 \text{ is}} - 0.5)/T_{dur}] \cdot t}, & P_{O_2} \le 0.5 \text{ atm} \end{cases}$$

d. Inspection of the data (Fig. 1) suggests that curvatures steepen when P_{O_2} increases. Further, recovery kinetics might be second order rather than first order. We normalized P_{O_2} by 1 atm and fitted:

$$F = \begin{cases} a_1 \cdot P_{O_2}^{\,b} \cdot t^{P_{O_2}} + F_0, & P_{O_2} < 0.5 \text{ atm} \\ F_0 / [1 - c + g/T_{dur}) \cdot t \cdot F_0], & P_{O_2} \le 0.5 \text{ atm} \end{cases}$$

e. In Model 5d the choice of normalizing factor for P_{O_2} is critical to the exponential fit. We added the normalizing factor as a parameter:

$$F = \begin{cases} a_1 \cdot (c \cdot P_{O_2})^b \cdot t^{c \cdot P_{O_2}} + F_0, & P_{O_2} < 0.5 \text{ atm} \\ F_0 / [1 - (c + g/T_{dur}) \cdot t \cdot F_0], & P_{O_2} \le 0.5 \text{ atm} \end{cases}$$

f. We considered the dynamic state in which removal of ROS occurs whenever $F > 0$, even as F is generated by separate mechanisms. Piecewise integration of a differential model was used to accommodate intermittent experiments. Generation of ROS was based on the system modeled in 5e, and removal followed first-order kinetics.

$$F = \begin{cases} a_1 \cdot [(c \cdot P_{O_2})^{b-1} / (c \cdot P_{O_2} + g)] \cdot [T_{dur2}{}^{c \cdot P_{O_2}} - T_{dur1}{}^{c \cdot P_{O_2}}] + F \text{ at } T_{dur1}, \\ \qquad P_{O_2} < 0.5 \text{ atm} \\ F_0 \cdot e^{-g \cdot t / T_{dur}}, & P_{O_2} \le 0.5 \text{ atm} \end{cases}$$

6. Sigmoidal Dose Response Models

We fitted the Hill equation, the typical sigmoidal dose response expression

$$\%\Delta VC = -[g \cdot dose^b / (dose^b + a^b)],$$

where parameter *a* is the dose at the inflection point of the curve, the dose where $\%\Delta VC = -0.5 \cdot g$, and parameter *b*, the Hill coefficient, determines the steepness of the sigmoidal change. %ΔVC is constrained to lie between 0 and *g*.

a. The dose may be considered to be *F*, the concentration of ROS from Model 3, the proportional healing model, in which case *F* changes with P_{O_2} and time according to

$$dF/dt = P_{O_2} - c \cdot F.$$

b. The dose may be the time integral of P_{O_2} above a threshold, $IntO_2$ beginning when vital capacity is at baseline:

$$IntO_2 = \int (P_{O_2} - P_{th})\, dt, \text{ integrating from time} = 0 \text{ to time} = t.$$

Because dose cannot be negative,

$$\text{Dose} = \begin{cases} IntO_2, & IntO_2 \geq 0 \\ 0, & IntO_2 < 0. \end{cases}$$

c. We also considered the case where the previous %ΔVC decays exponentially when $P_{O_2\,is}$ is below threshold:

$$\%\Delta VC = \begin{cases} -[g \cdot dose^b / (dose^b + a^b)] \text{ with } Dose = \int (P_{O_2} - P_{th})\, dt, & P_{O_2} \geq P_{th} \\ (\%\Delta VC)_0 \cdot e^{-ct}, & P_{O_2} < P_{th}. \end{cases}$$

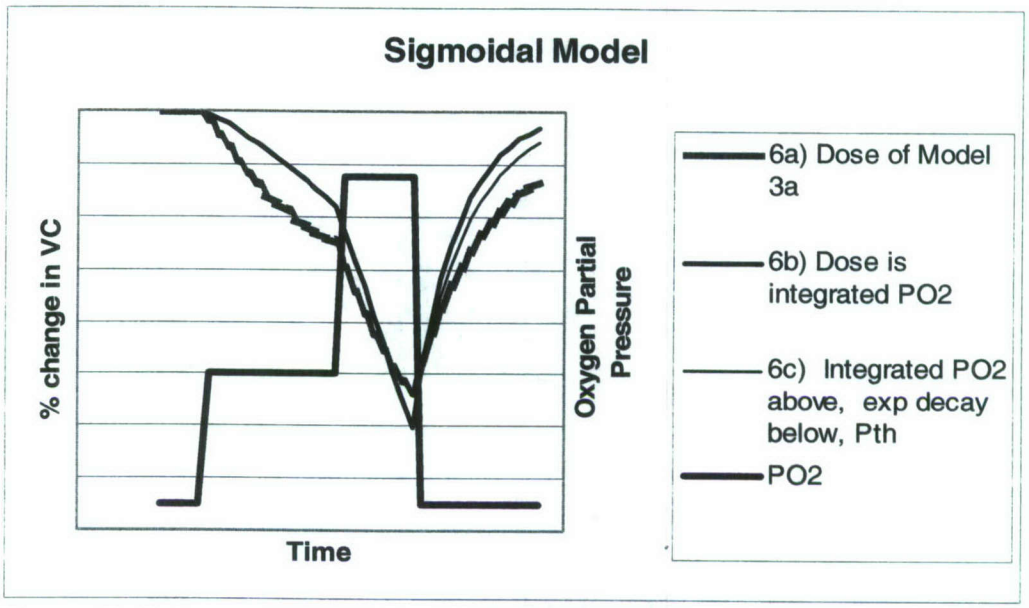

Figure 7. Schematic of Model 6. Sigmoidal dose response curves for Models 6a, 6b, and 6c are shown for two elevations of P_{O_2} above P_{th}. Models 6b and 6c are identical when $P_{O_2} > P_{th}$, but 6b has a decreasing dose, while 6c has exponential healing when P_{O_2} is below threshold.

7. Different Kinetics Model

As in Model 3, F may increase as a function of P_{O_2} during an oxygen exposure and decrease in proportion to its concentration, but a similar relationship with different kinetics may relate F to measurable injury (decrease in VC):

$$dF/dt = a \cdot (P_{O_2} - P_{th}) - b \cdot F$$

$$d(\%\Delta VC)/dt = c \cdot F - g \cdot (\%\Delta VC).$$

This model can have many responses, as shown in Figure 8, but has five parameters. Data with fine time resolution are needed to distinguish the two exponential components. If F reaches steady state extremely quickly, this model reduces to Model 3a, the proportional healing model.

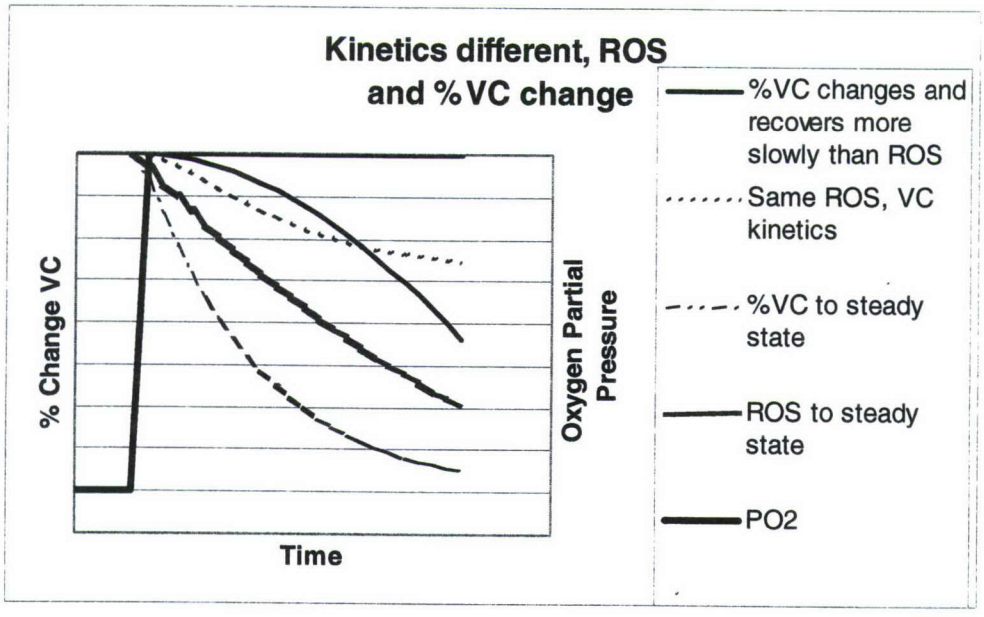

Figure 8. Schematic of Model 7, in which the kinetics of ROS production and removal differ from those for ΔVC, depicted for a single step change in P_{O_2}.

8. Injury-Memory Model

In the injury-memory model, Fig. 9, an initial injury I_1 is directly proportional to F, as is %ΔVC in Model 3a. However, ΔVC is considered to be secondary to I_1 and to be resolved more slowly. In effect, ΔVC has a "memory" for acute injury, because it is a moving average with a time window of length τ.

$$dI_1/dt = \begin{cases} a \cdot (P_{O_2} - P_{th}) - b \cdot I_1, & P_{O_2} > P_{th} \\ -b \cdot I_1, & P_{O_2} \le P_{th} \end{cases}$$

$$\%\Delta VC = \alpha \int I_1 \cdot dt\,, \text{ integrated over time from } (t-\tau) \text{ to } t.$$

At constant P_{O_2}, if $a' = a \cdot \alpha$, $P_{O_2} > P_{th}$, and $t > \tau$, then

$$\%\Delta VC = a' \cdot b^{-2} \cdot (P_{O_2} - P_{th}) \cdot \{e^{-[b \cdot t]} - e^{-[b \cdot (t-\tau)]}\} + a' \cdot b^{-1} \cdot \tau \cdot (P_{O_2} - P_{th}) + I_0 \cdot b^{-1} \cdot \{e^{-[b \cdot t]} - e^{-[b \cdot (t-\tau)]}\}.$$

If $t < \tau$, the effects of earlier segments at different P_{O_2} must be included. The model "forgets" oxidative injury that occurred when $t < t - \tau$. As can be seen in Fig. 9, this injury-memory model smoothes out short-term changes in P_{O_2}, a feature that is interesting when intermittent exposures are considered.

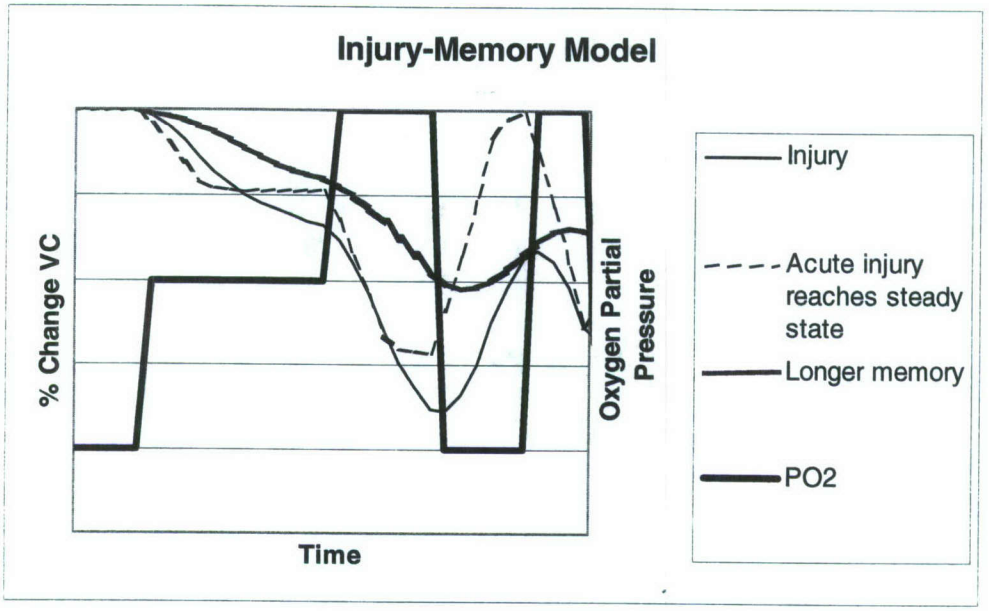

Figure 9. Schematic of Model 8, which represents an integration of the proportional healing model over a finite memory period. The ΔVC is the time-weighted moving average of the insult caused by elevated P_{O_2}. P_{O_2} is depicted from below injury threshold through two steps in elevation and then across an air break (intermittent exposure). Note the smoothing that the moving average causes on predicted ΔVC.

Rather than fitting τ as a Marquardt or simplex parameter, we fitted this model for discrete memory periods τ = 3, 6, 12, 24, 36, 48, 60, 72, 84, 96, or 120 hours and selected the value for the smallest least squares error. Although this fitting is more an exploration of the data than a complete fit, recovery data exist only at sparse intervals, a situation making fine distinctions difficult.

9. Delayed Inflammation Model

A second inflammatory injury follows most insults to the body. Although the injury-memory model addresses secondary injury, inflammation usually occurs after a delay, rather than immediately after the primary injury. In the delayed inflammation models, inflammation was modeled as being directly proportional to the acute injury but as occurring after an adjustable delay.

The delayed inflammation approach introduced an additional three parameters to alter the shape of the response for the late parts of P_{O_2} exposure and for early recovery.

Let τ_{io} = time lag from acute injury to onset of inflammation and τ_{id} = duration of inflammation. Then

$$\%\Delta VC = -\alpha \cdot F + K_{inflam} \cdot \Sigma \%\Delta VC_a\ (\theta),$$

where θ in the summation term is a time value that runs from $t - \tau_{io} + \tau_{id}$ to $t - \tau_{io}$, $K_{inflam} > 0$ is the proportionality constant for delayed inflammatory injury, and the acute injury at any time, $\%\Delta VC_a$, is obtained from a selected acute model. We used the proportional healing model.

The delayed inflammation model was fitted for specific lag times and inflammatory durations to explore their effects. This approach cannot find best-fit values between the values considered. The values for τ_{io} that were tested were 3, 6, 8, 12, 24, 36, 48, 60, 72, 84, 96, or 120 hours, and for τ_{id} they were 3, 6, 12, 24, 36, 48, 60, or 72 hours.

For each chosen combination of τ_{io} and τ_{id}, the same procedure was followed:

1. The model of acute injury — here, the proportional rate of healing model — was fitted.

2. For each measurement time, calculated acute injury $\%\Delta VC_a$ was summed from the time of the assigned onset of inflammation and throughout its assigned duration to find the term in the equation for $\%\Delta VC$. K_{inflam} was found by least-squares regression, while all other parameters were held constant.

3. K_{inflam} was held constant, and the parameters of the acute injury were adjusted with inflammation included.

4. Iteration of the second and third steps continued until K_{inflam} was within one percent of its previous value.

5. The combination of inflammatory lag and duration that gave the largest coefficient of determination (r^2) and smallest sum of squared error was selected as the best fit.

Model 9a uses the instantaneous P_{O_2} value, as in the previous model fits. Model 9b uses a time-averaged oxygen dose in an attempt to explain the results of intermittent exposures.

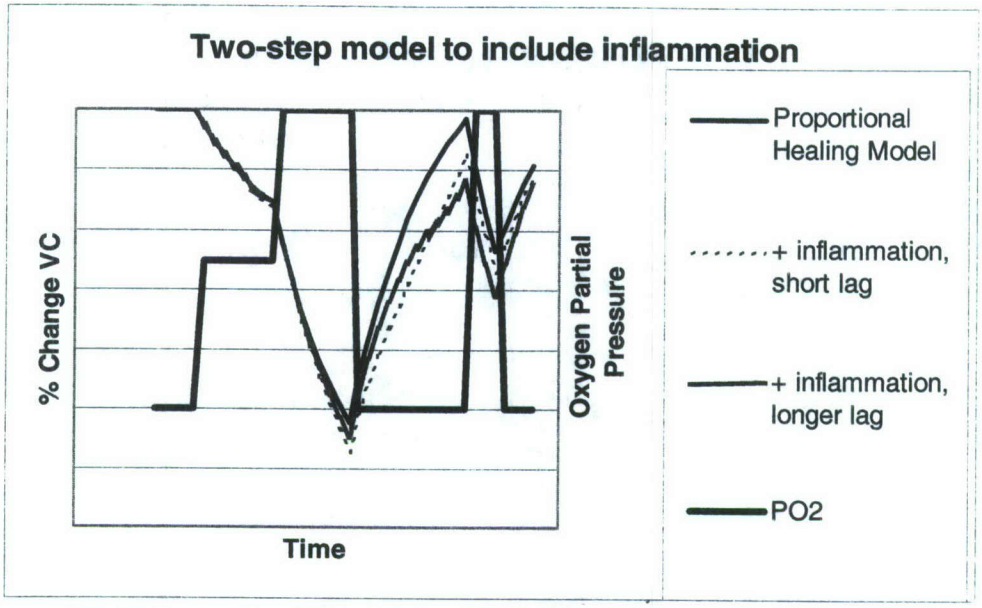

Figure 10. Schematic of Model 9a. The inclusion of inflammation that occurs after a short time lag modifies the later portions of prolonged exposures to constant P_{O_2} and can prolong recovery, as shown.

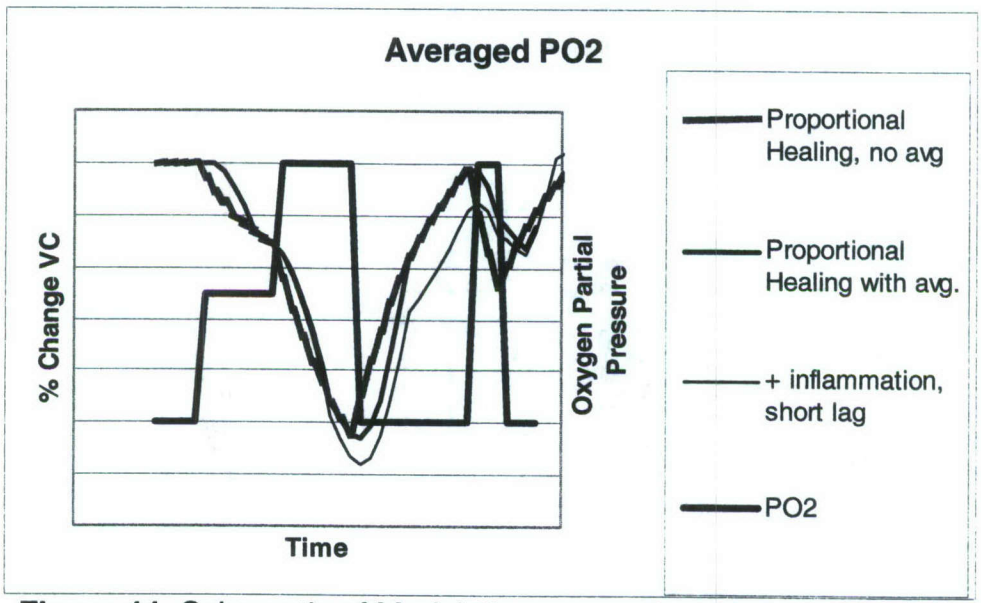

Figure 11. Schematic of Model 9b, a proportional healing model with averaged P_{O_2}. If the concentration of ROS is proportional to the average P_{O_2} over a period of time, the onsets of injury and recovery are slowed. Short intermittent periods simply reduce the effective exposure.

RESULTS

A "perfect" regression model cannot do better than to match the average response; no model will explain the often large differences in responses across subjects. As shown in Figure 1, where both average responses across subjects and individual data are plotted for some of the experiments, individual responses to oxygen vary highly. Table 3 lists the variability for specific experiments and for the four data groups we have used. For the data groupings, about half the total variability is among subjects: models can be expected to explain less than half the scatter in the data.

Table 3.
Coefficient of determination of average responses, listed by recovery duration

	Data Source	Coefficients of determination (r^2) for intersubject averages			
		Weighted by datum			Weighted by subject
Recovery duration included (hr)		*0*	*8*	*all*	*8*
A	Ohlsson[1]	0.32	0.32	0.32	0.32
B	Caldwell[2]	0.83	0.83	0.95	0.79
C	2 atm IFEM[3–7]	0.20	0.35	0.36	0.42
D	Eckenhoff et al.[8] (IFEM)	0.42	0.42	0.43	0.44
E	Intermittent 20:5 Hendricks et al.[9] (IFEM)	0.63	0.67	0.67	0.42
F	Intermittent 60:15 Lambertsen and Clark[10,11] (IFEM)	0.30	0.30	0.30	0.81
H	1.5 atm IFEM[6,12]	0.36	0.35	0.44	0.33
I	2.0 atm IFEM[6,12]	0.26	0.22	0.29	0.24
J	2.5 atm IFEM[6,12]	0.36	0.16	0.22	0.21
P	Wet data	0.41	0.42	0.36	0.42
Group 1	Experiments A–D, K–M	0.57	0.58	0.58	0.55
Group 2	Experiments A–M	0.45	0.43	0.45	0.39
Group 3	No intermittent experiments	0.45	0.42	0.45	0.39
Group 4	All dry data	0.46	0.44	0.49	0.47

Weighting by subject yields values slightly different from those of weighting by datum, because some data sets include more measurements from some subjects than from others.

Goodness of fits by the models are given in Table 4 as model r^2 expressed as percentages of the coefficients of variability for the average responses given in Table 3. The ratio indicates the degree to which a model explains the dependence of intersubject average %ΔVC on time and P_{O_2}. For the average of all data independent of time and P_{O_2}, $r^2 = 0$ — and $r^2 < 0$ if the model increases the overall variance.

Table 4.
Model performance: Percentage variance explained relative to intersubject average.
Parentheses when the model increased the variance. **Bold** for values >70%.

a) Recovery times up to 8 hours

Model	**Number of parameters**	***(r^2 of model) / (r^2 of average)***			
(0.5 hr < Recovery ≤ 8 hr)		Group 1	Group 2	Group 3	Group 4
1. UPTD		*No recovery in model*			
2. Proportional					
a – no limit	2	62%	33%	33%	35%
a weighted by subject		4%	1%	4%	1%
b – log limit		61%	33%	33%	34%
3. Proportional healing					
a – no limits		**79%**	56%	60%	52%
a weighted by subject	3	35%	42%	42%	51%
b – log limit		**78%**	**70%**	**74%**	53%
4. Autocatalytic*		P_{O_2}	50%	52%	43%
weighted by subject	3	range too small	47%	47%	50%
5. Exponential[1]					
a – Recovery depends on prior P_{O_2}	4	**74%**	53%	61%	56%
b – Recovery depends on exposure duration	4	60%	56%	62%	59%
e – Exponent of time is f(P_{O_2})	5	68%	69%	69%	67%
6. Sigmoidal –					
a. dose as in 3a, $g = 100$	3	**73%**	54%	54%	54%
g fitted	4	no fit	51%	34%	no fit
b. integrated P_{O_2}, $g = 100$	3	64%	58%	67%	48%
c. with exponential decay, $g = 100$	4	no recovery	51%	55%	41%
7. Concentration of ROS may be changing at constant P_{O_2}	5	Too many parameters to fit for these data			
8. Injury-Memory	3+1 #	**78%**	42%	50%	21%
9. Two-stage models					
a. Proportional healing	3+1+2 #	Reduced to Model 3a	59%	**70%**	55%
b. Proportional healing with averaged P_{O_2}	3+1+2+1		58%	67%	59%
c. Averaged P_{O_2}, no inflammation	3+0+0+1		58%	68%	60%

* The threshold was set equal to air at 1.0 atm.
[1] Injury develops if $P_{O_2} > 0.5$ atm.
The "+1" parameter refers to memory, while the "+1+2" refers to the scale factor of inflammation and the lag and memory for it. "+1+2+1" means scale factor, lag, and memory for inflammation, and the memory for P_{O_2}.

Table 4. (continued)

b) Injury development only. No recovery.
Parentheses when the model increases the variance. **Bold** for values ≥70%.

Model	**Number of parameters**	***(r^2 of model) / (r^2 of average)***		
No recovery		Group 1	Group 2	Group 3
1. UPTD *(No recovery time)* – original definition		38%	32%	35%
a – UPTD fitted to %ΔVC	2	**84%**	67%	67%
b – exponent fitted	3	**84%**	66%	**72%**
c – exponent and threshold fitted	4	**83%**	58%	**73%**
2. Proportional				
a – no limit	2	66%	33%	35%
b – log limit		65%	32%	35%
c – Harabin linear parameters		57%	26%	28%
3. Proportional healing				
a – no limits	3	**82%**	**71%**	**75%**
b – log limit		**81%**	**70%**	**74%**
5. Exponential[1]				
a,b – Quadratic in time	2	**76%**	25%	66%
e – Exponent of time f(P_{O_2})	3	67%	52%	**71%**
6. Sigmoidal –				
a. dose as in 3a $g = 100$	3	**76%**	61%	55%
g fitted	4	didn't fit	57%	52%
b. integrated P_{O_2}	3	69%	58%	**74%**
7. Concentration of ROS may be changing at constant P_{O_2}	5	Too many parameters to fit for these data		
8. Injury-Memory	3 + 1 #	**81%**	56%	66%

[1] Injury develops if $P_{O_2} > 0.5$ atm.
The "+1" parameter refers to memory.

Model Fits

Model 1. UPTD (No recovery data used in fitting)

$$\%\Delta VC = a \cdot t \cdot [(P_{O_2} - P_{th}) / (1\ \text{atm} - P_{th})]^b + c + \%\Delta VC_0,$$

where $\%\Delta VC_0$ is the change caused by a previous elevation in P_{O_2}, if such a change has occurred.

a. We use the original UPTD definition[19,20] — that is, exponent $b = 1/1.2 = 0.833$ and $P_{th} = 0.5$ atm — and fit *a* and *c*.

b. We redefine UPTD by fitting *a*, *c*, and *b* with fixed P_{th}.

c. We redefine UPTD by fitting *a*, *c*, *b*, and P_{th}.

Figure 12 illustrates the correspondence of the fitted UPTD model to the averages of the observed values for different experimental exposures. Fits are shown with the classic parameters and with parameters from Models 1a, 1b, and 1c fitted to Data Group 3 weighted by datum but with no recovery (Appendix, Tables A1–A3). Models 1b and 1c are almost superimposed. Recovery is not considered in this model; for comparison to the intermittent exposure data, %ΔVC is held constant during periods with $P_{O_2} < 0.5$ atm.

The UPTD model does not generally fit the data well. However, with some of the fitted parameters it corresponds to some %ΔVC, particularly over the early parts of the experiments. Surprisingly, the correspondence is good to the first third of intermittent Exposure G. The correlation coefficients between any of these model predictions and measured data for highly intermittent Experiments N and O, the DISSUB data, are less than 0.1 (Model 1a: 0.09, Model 1b: 0.08, Model 1c: 0.08, Classic parameters: 0.04).

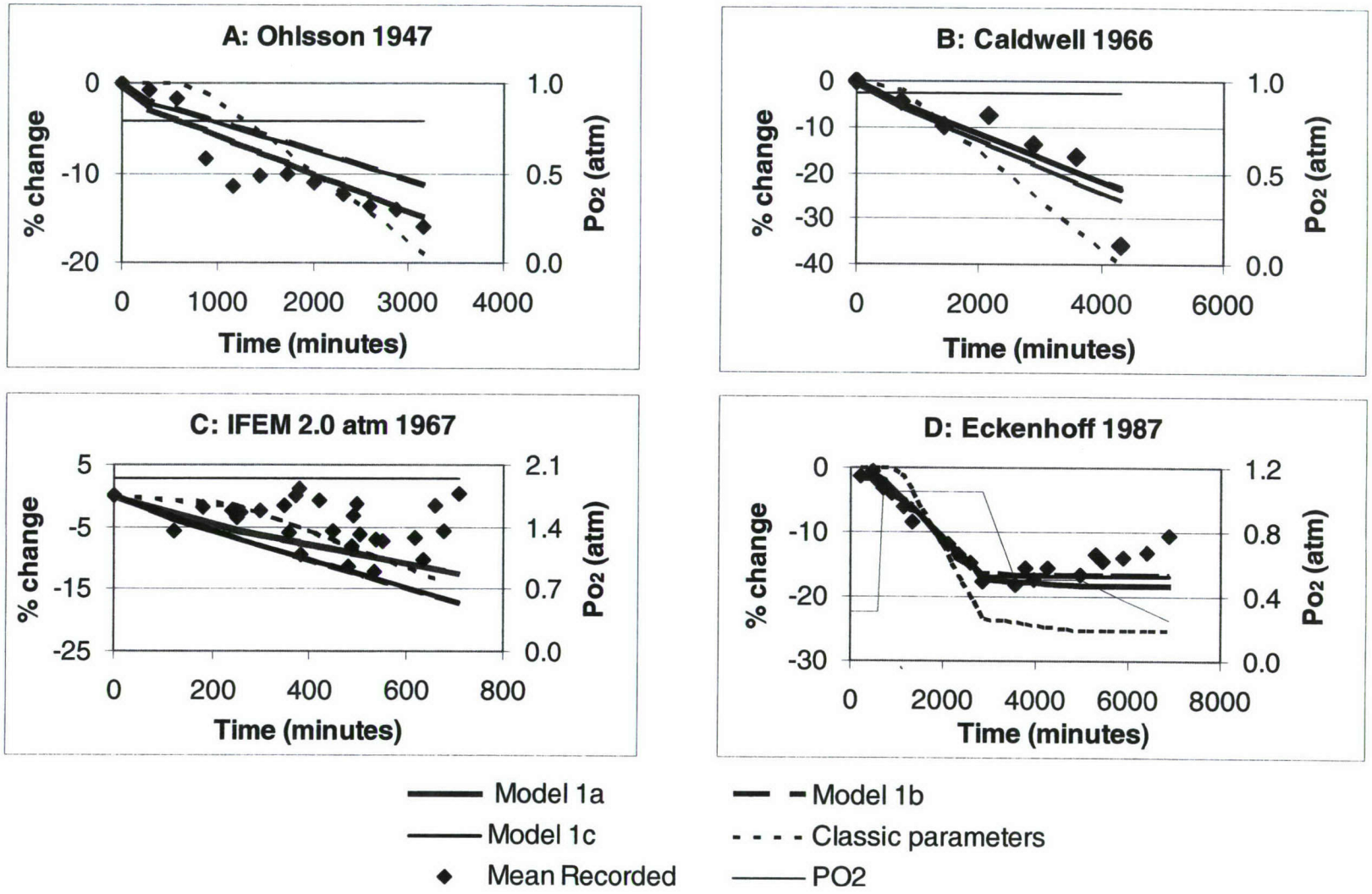

Figure 12. Model 1, UPTD Models.
Correspondence to data, experiments A–D.

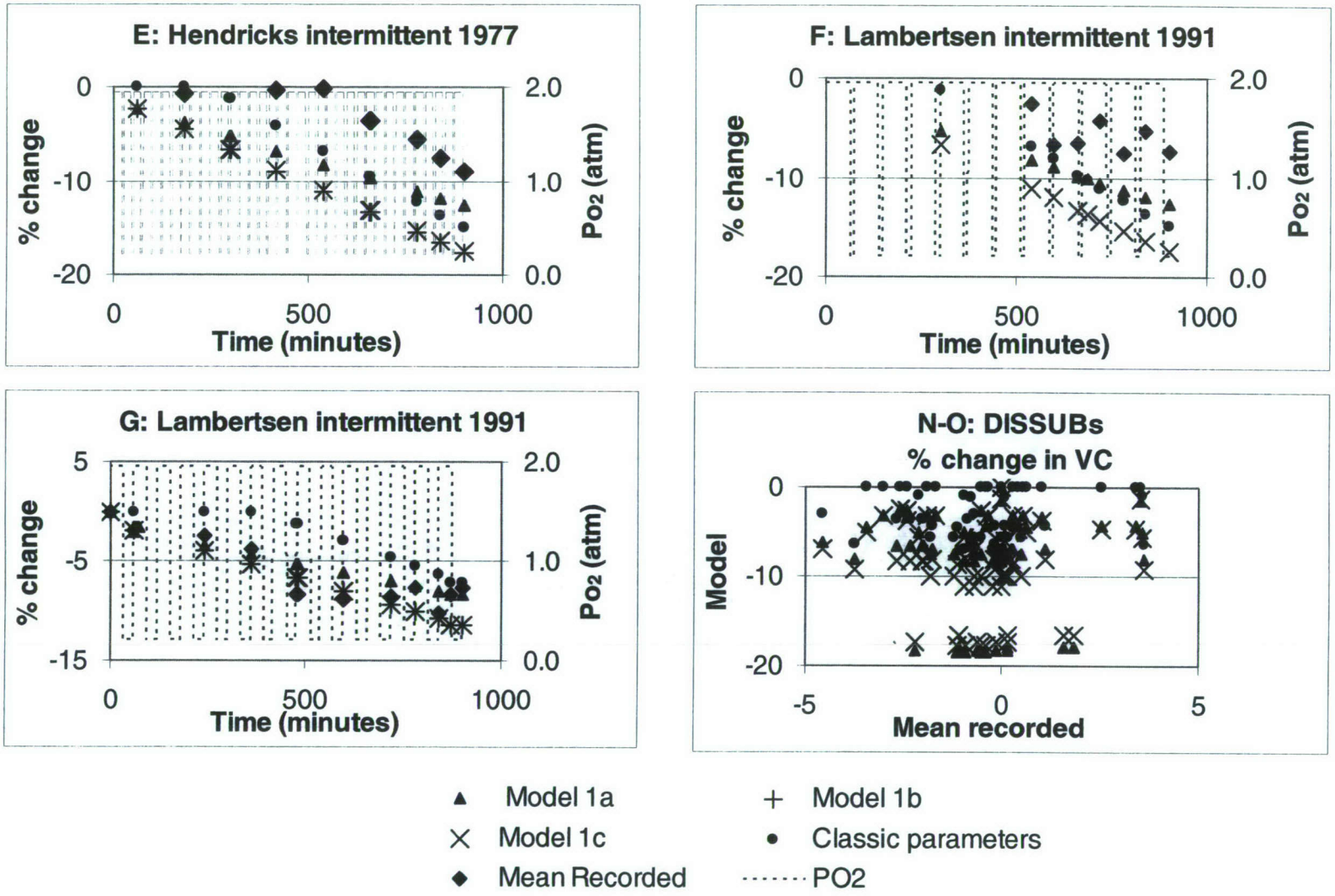

Figure 12 (continued). Model 1, UPTD Models.
Correspondence to data, intermittent experiments E–G and N–O. Profiles N and O are given as a correlation plot, because the many P_{O_2} changes make other depiction difficult.

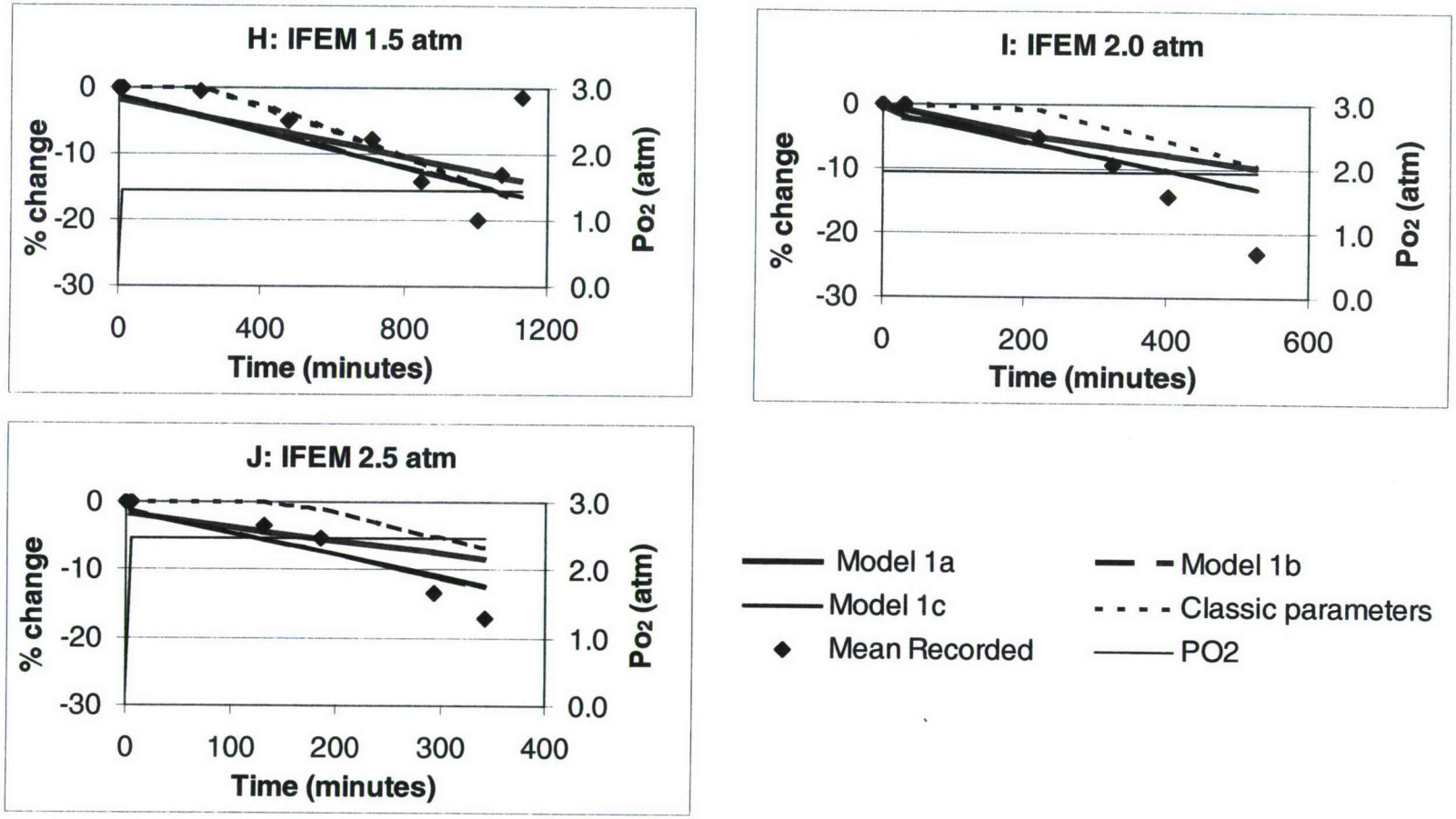

Figure 12 (continued). Model 1, UPTD Models.
Correspondence to data, experiments H–J.

Model 2. Proportional and Related Models

a. Testing Proportionality

We began with the general model of the type for which %ΔVC increases with either time or P_{O_2},

$$\%\Delta VC = a \cdot (P_{O_2} - P_{th})^b \cdot (t - t_{th})^c + \%\Delta VC_0, \qquad t > t_{th},\ P_{O_2} > P_{th}$$

For this model, partial pressures and times are normalized to one atmosphere and one hour. Pressures are numerically equal to the values in atmospheres and times to those in hours but are dimensionless. Normalization is necessary if the exponential form is to make sense, and the smaller numeric values of the bases for exponentiation (e.g., hours rather than minutes) make the results stable in the presence of noise in the data.

Because the fit was not improved by the presence of a nonzero t_{th}, the parameter was dropped from the model, to yield:

$$\%\Delta VC = a \cdot (P_{O_2} - P_{th})^b \cdot t^c + \%\Delta VC_0, \qquad P_{O_2} > P_{th}.$$

As described in *Methods*, the number of data for which this model is valid, n, is a function of P_{th}. Values of n are listed in the Appendix in Table A4 for the corresponding optimized P_{th}. Parameter values vary with data group, but the exponent on time, c, is not different from 1. For Data Group 1, where most P_{O_2} values lie near 1 atm, the model is linear in P_{O_2}.

If exponent c is set to one, the model becomes linear in time:

$$\%\Delta VC = a \cdot (P_{O_2} - P_{th})^b \cdot t + \%\Delta VC_0, \quad P_{O_2} > P_{th}.$$

This is similar to Model 1c, except that the intercept term of Model 1 has been set to zero and the coefficient a in this model includes the (1 atm – P_{th}) term of Model 1. Furthermore, while for Model 1 we assume no further ΔVC when $P_{O_2} < P_{th}$, for the four-parameter model we omit all data where $P_{O_2} < P_{th}$. Fitted parameters are listed in the Appendix in Table A5.

For Data Group 3, the data set with the larger range of P_{O_2}, r^2 is slightly higher with $c = 1$ than with c allowed to float, and the exponent b is not significantly different from 1, a result implying that the proportional model is reasonable. However, the fit with Data Group 1 does not appear to recommend a proportional model.

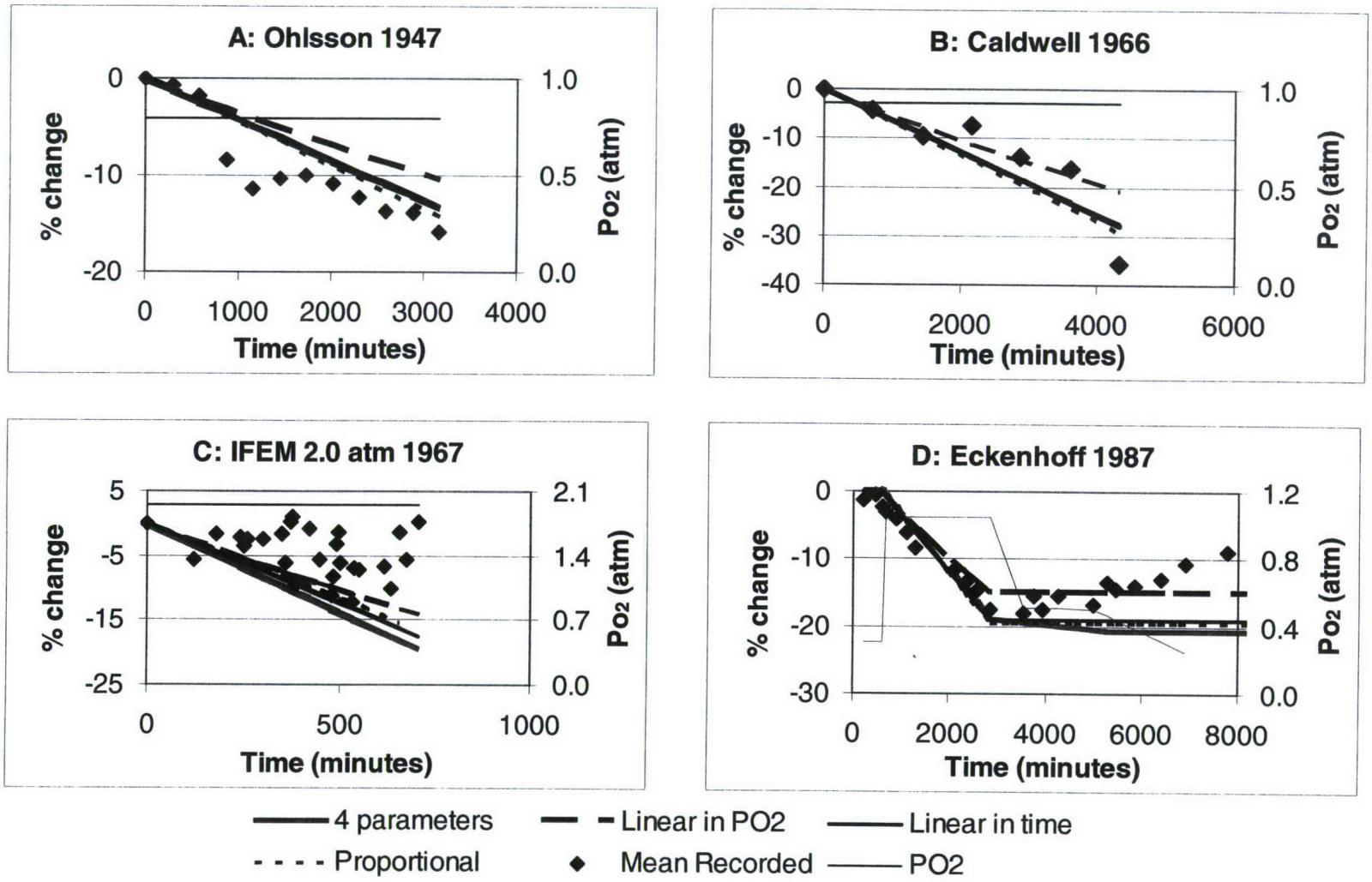

Figure 13. Testing for proportionality.
Correspondence of different models to data, Experiments A–D.

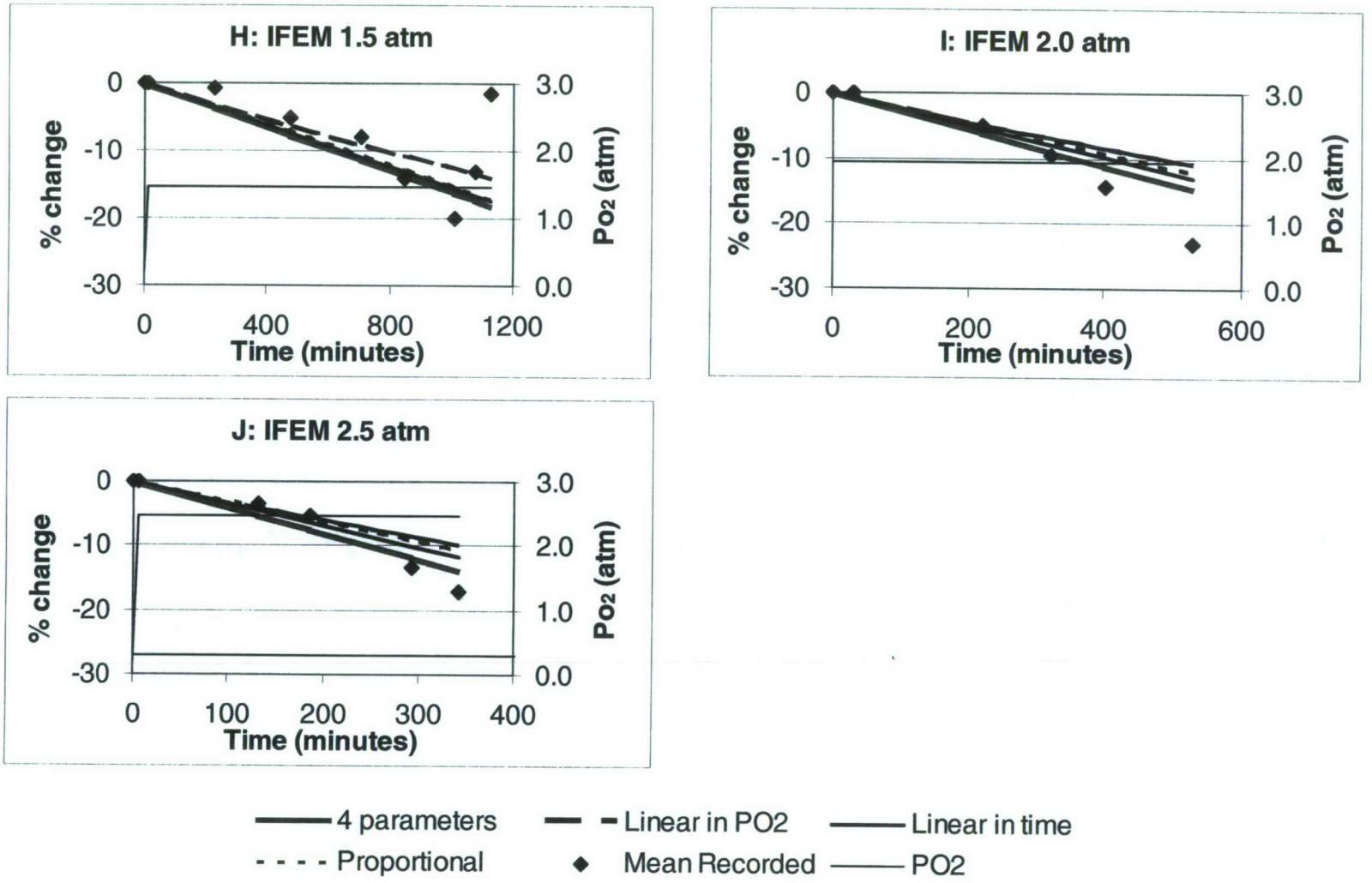

Figure 13 (continued). Testing for proportionality.
Correspondence of different models to data, Experiments H–J.

If we set $b = 1$ and let c float, the equation, now linear in P_{O_2}, can apply for all values of P_{O_2}, including $P_{O_2} < P_{th}$. However, we restrict the fit to $P_{O_2} > P_{th}$ to remain consistent. For both data groups, exponent c is significantly <1 when b is set to 1 (Table A6). For Data Group 1, this version is identical to the four-parameter version (Table A4).

b. Proportional Model

The proportional model sets both b and $c = 1$. With the fit restricted to data for which $P_{O_2} > P_{th}$, the fitted parameters become those in Table A7. The decrease in r^2 caused by forcing linearity is slight for Data Group 3 but is notable for the smaller Data Group 1 (Tables A4 and A6).

The small effects of the differences in the parameters for Data Group 3 are depicted in Figure 13. This linear model corresponds to only the early portions of experiments that are curvilinear in time. However, the proportional model has been published by others,[13,21] with the following proposed mechanism. If we consider F instead of %ΔVC directly, the equation can be written

$$F = a_1 \cdot (P_{O_2} - P_{th}) \cdot t + F_0.$$

This is the integration of the differential equation

$$dF / dt = a_1 \cdot (P_{O_2} - P_{th}), \qquad F \geq 0.$$

If we remove the restriction on P_{O_2}, when $P_{O_2} < P_{th}$ the free radical concentration F decreases, and healing occurs.

We considered two forms of this model, both previously published:[13,21]

a) %ΔVC = $-\alpha \cdot F$ and the parameter a in Table A7 is $a = -\alpha \cdot a_1$, and

b) %ΔVC = $-100\,[1 - 1.005^{-F}]$.

Figure 14 shows the match of the proportional models, Models 2a and 2b, to the observed data. Recovery (healing) is shown in separate panels on a longer time scale. In some experiments where exposure lengths varied among subjects, multiple recovery lines result from the different calculated values at the end of the exposures.

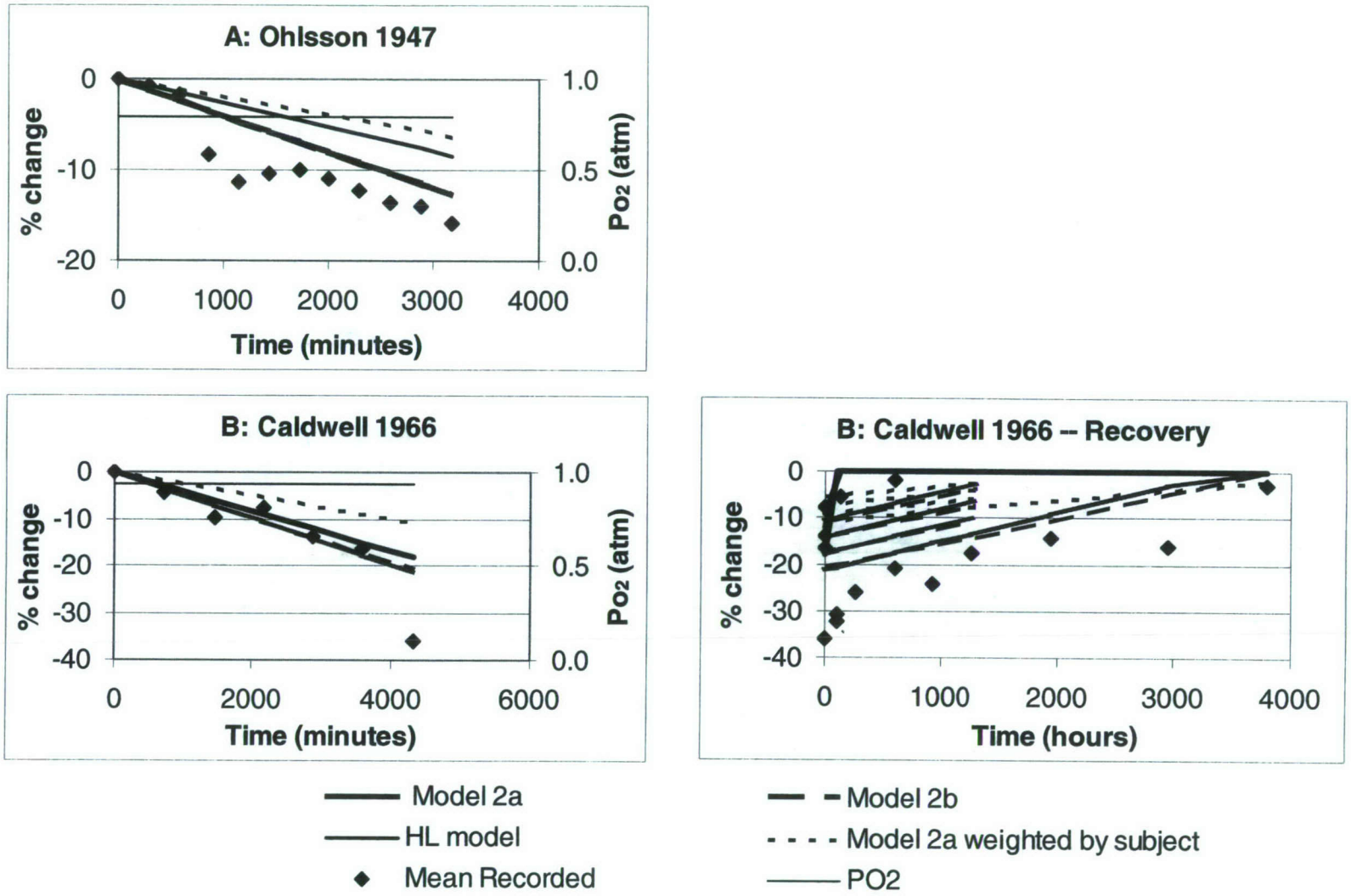

Figure 14. Proportional Models 2a and 2b.
Correspondence to data, Experiments A and B. Recovery breathing room air.

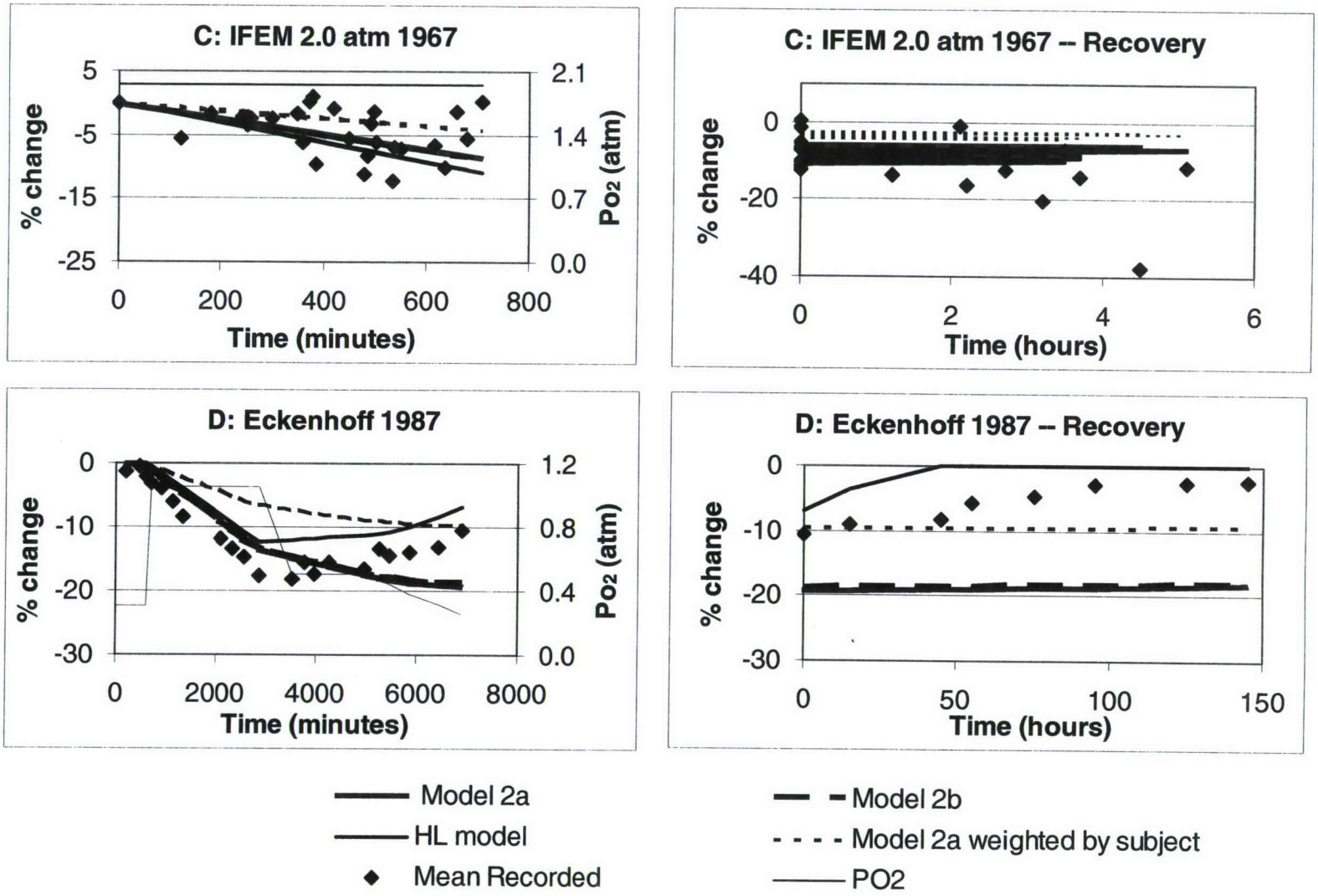

Figure 14 (continued). Proportional Models 2a and 2b by experiment.
Correspondence to data, Experiments C and D. Recovery breathing room air.

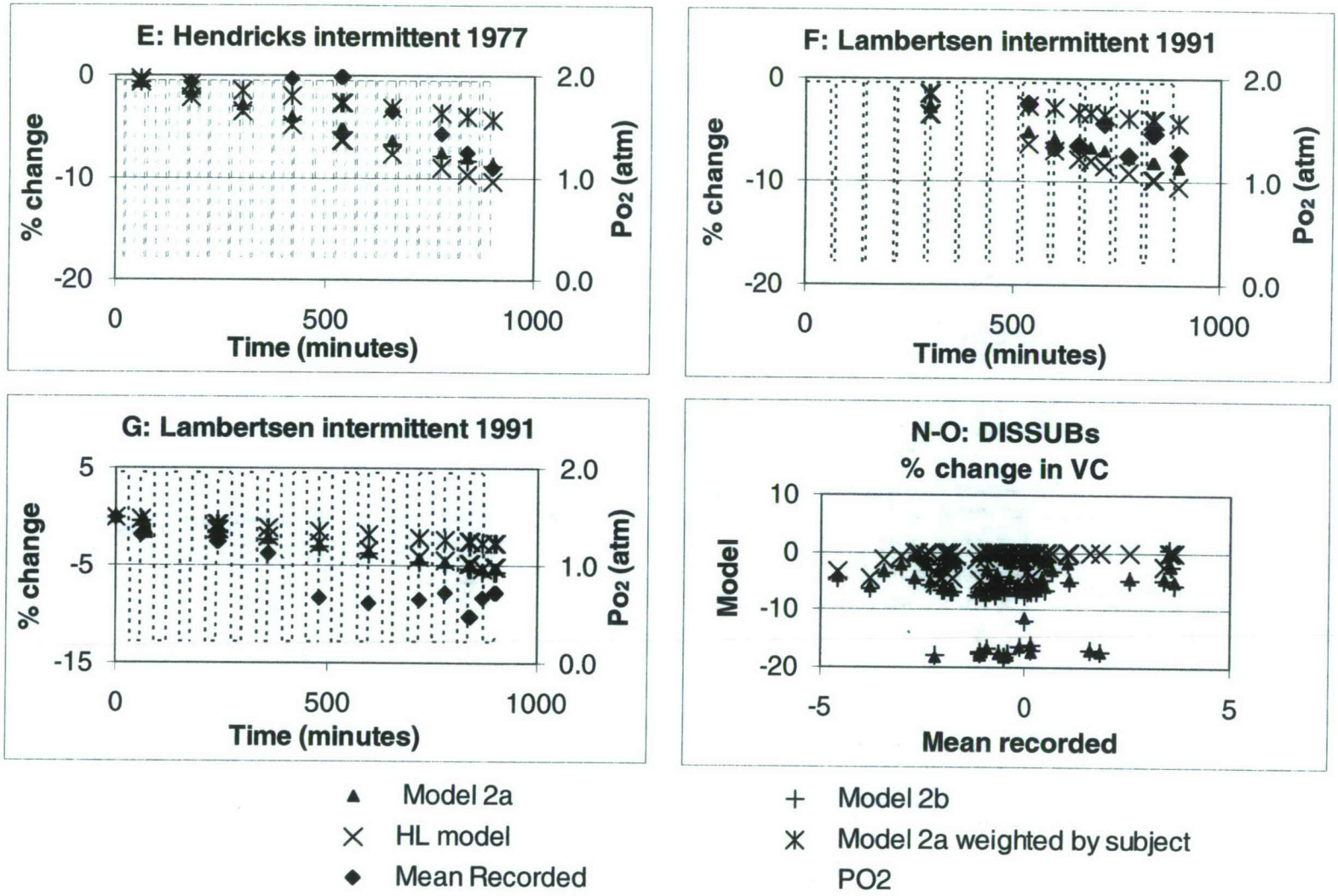

Figure 14 (continued). Proportional Models 2a and 2b by experiment.
Correspondence to data, intermittent experiments E–G, N, and O. Profiles N and O are given as a correlation plot because the many P_{O_2} changes make other depiction difficult.

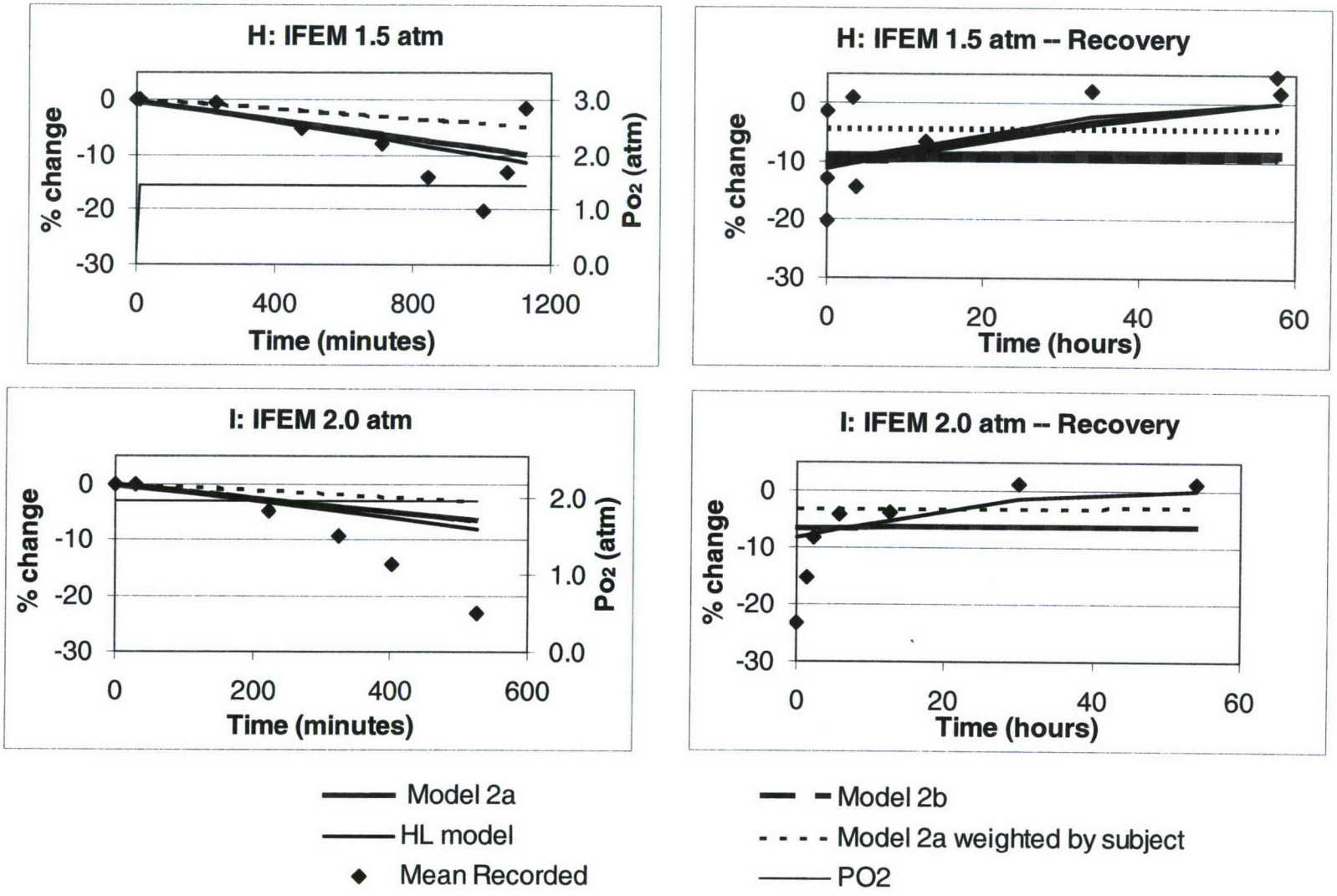

Figure 14 (continued). Proportional Models 2a and 2b by experiment.
Correspondence to data, Experiments H and I. Recovery breathing room air.

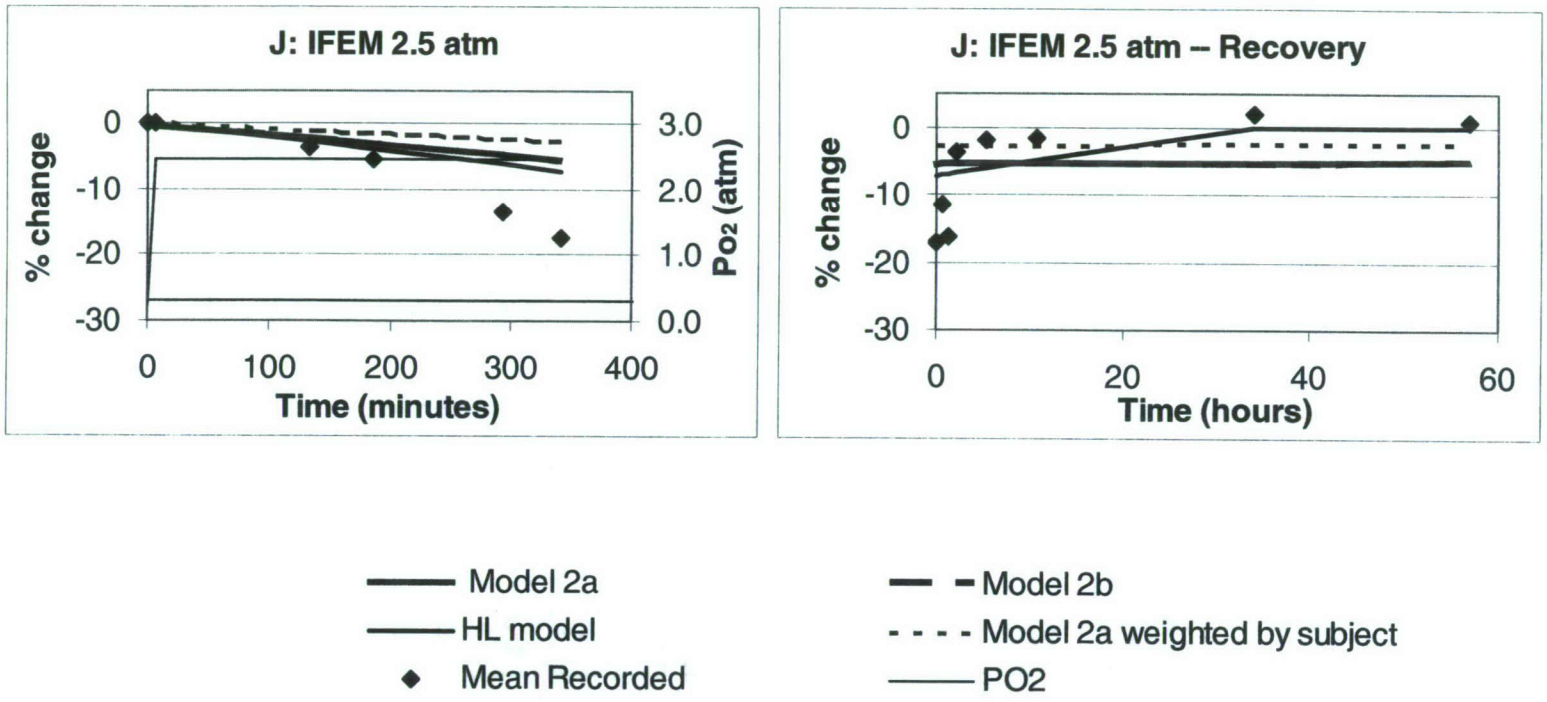

Figure 14 (continued). Proportional Models 2a and 2b by experiment. Correspondence to data, Experiment J. Recovery breathing room air.

Parameters fitted to Data Group 4 with eight hours of recovery are used in the figure for both models (Tables A7, A8), as are the Harabin linear model parameters.[13,21] For injury onset, the proportional models are linear in time. They do not correspond well to the intermittent data of Experiments E–G, and, like the UPTD models, they correspond only to the early data of experiments H–J. Recovery is poorly represented for all but some of the data of Experiment B. In the complex, intermittent DISSUB Experiments N and O, correlations between fitted models and average data were low: correlation coefficients for the data and Model 2a were 0.07; for the data and Model 2b, 0.08; and for the data and the Harabin linear parameter the fit was 0.10.

Model 3. Proportional Rate of Healing Models

$$\text{If } dF/dt = \begin{cases} a_1 \cdot (PO_2 - P_{th}) - b \cdot F, & PO_2 > \text{threshold} \\ -b \cdot F, & PO_2 \le \text{threshold}, \end{cases}$$

a. $\%\Delta VC = -\alpha \cdot F$

b. $\%\Delta VC = -100\,[1 - 1.005^{-F}]$

Figure 15 illustrates the performance of the proportional healing Models 3a and 3b with the parameters fitted for Data Group 4 and all recovery data (Tables A9 and A10). The fits with Vann's parameters[22] for Model 3a are also shown. These models are curvilinear, concave up with time during onset of injury, while Experiments H–J are concave down, and the modeled recovery is too rapid for some experiments and too slow for others. However, for the DISSUB data of Experiments N and O, correlations between the average responses and the models were moderately good, with correlation coefficients for Model 3a, 0.41; for Model 3b, 0.40; and for Vann's parameters, 0.32.

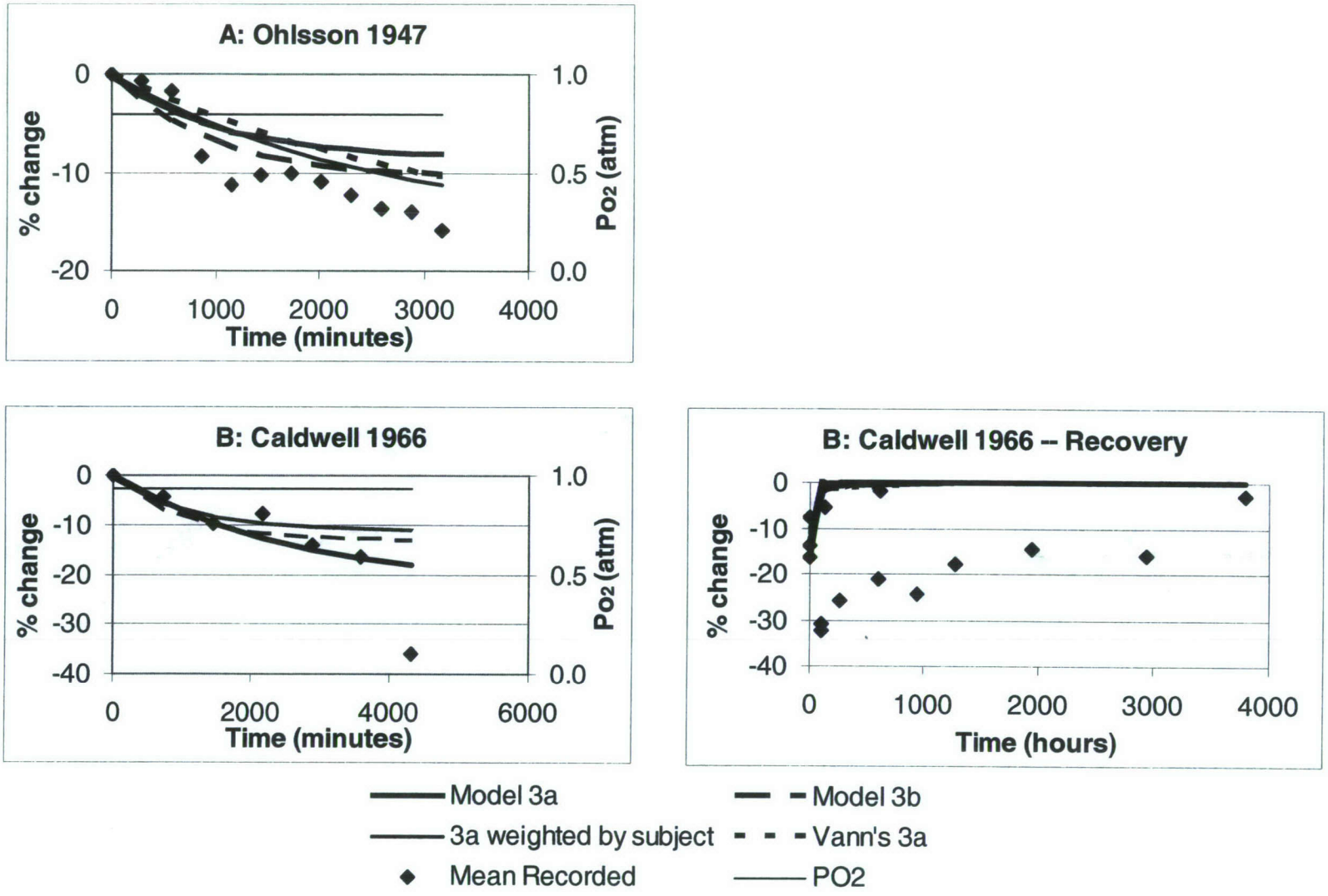

Figure 15. Proportional rate of healing Models 3a and 3b.
Correspondence to data, Experiments A and B. Recovery while breathing room air.

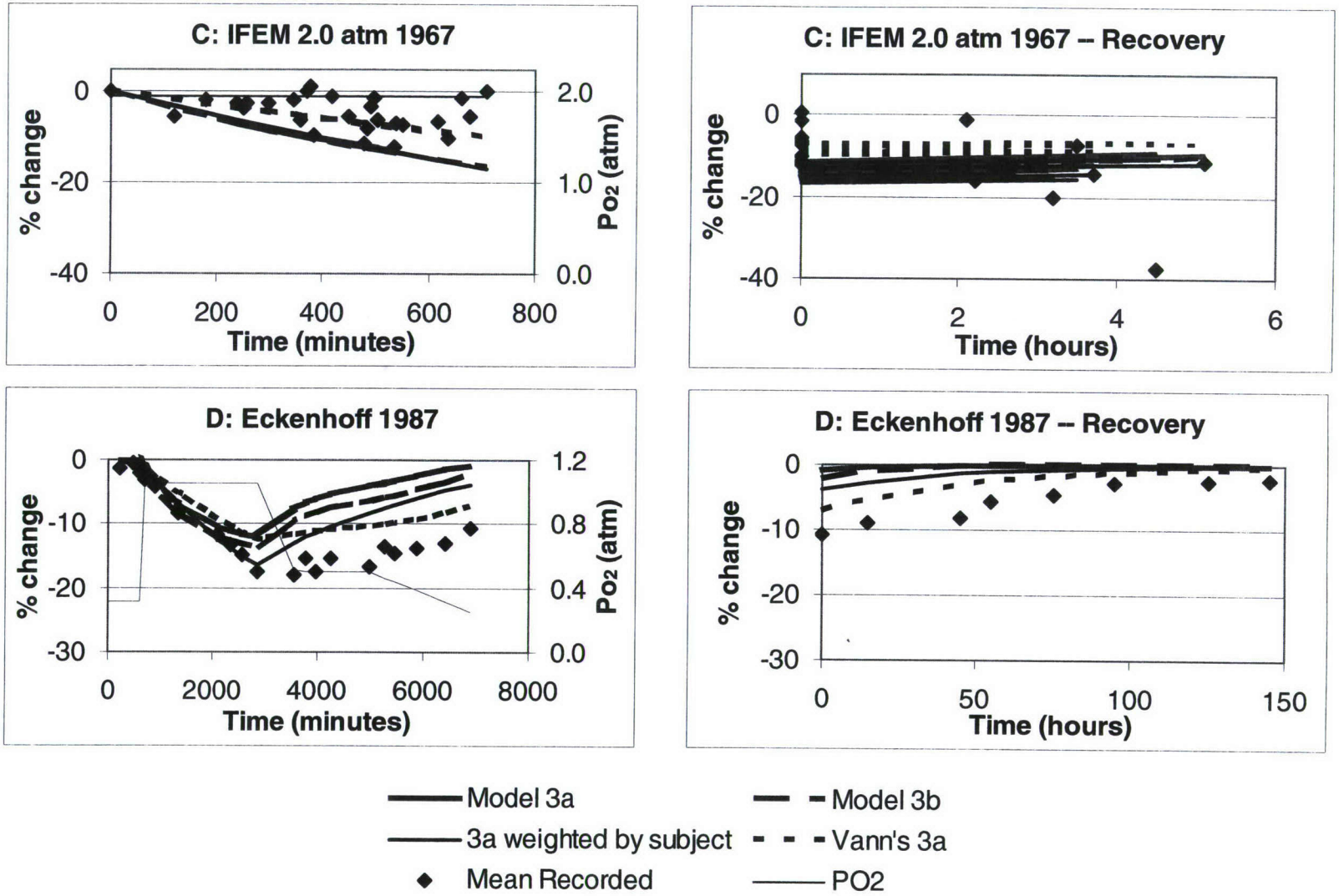

Figure 15 (continued). Proportional rate of healing Models 3a and 3b. Correspondence to data, Experiments C and D. Recovery breathing room air.

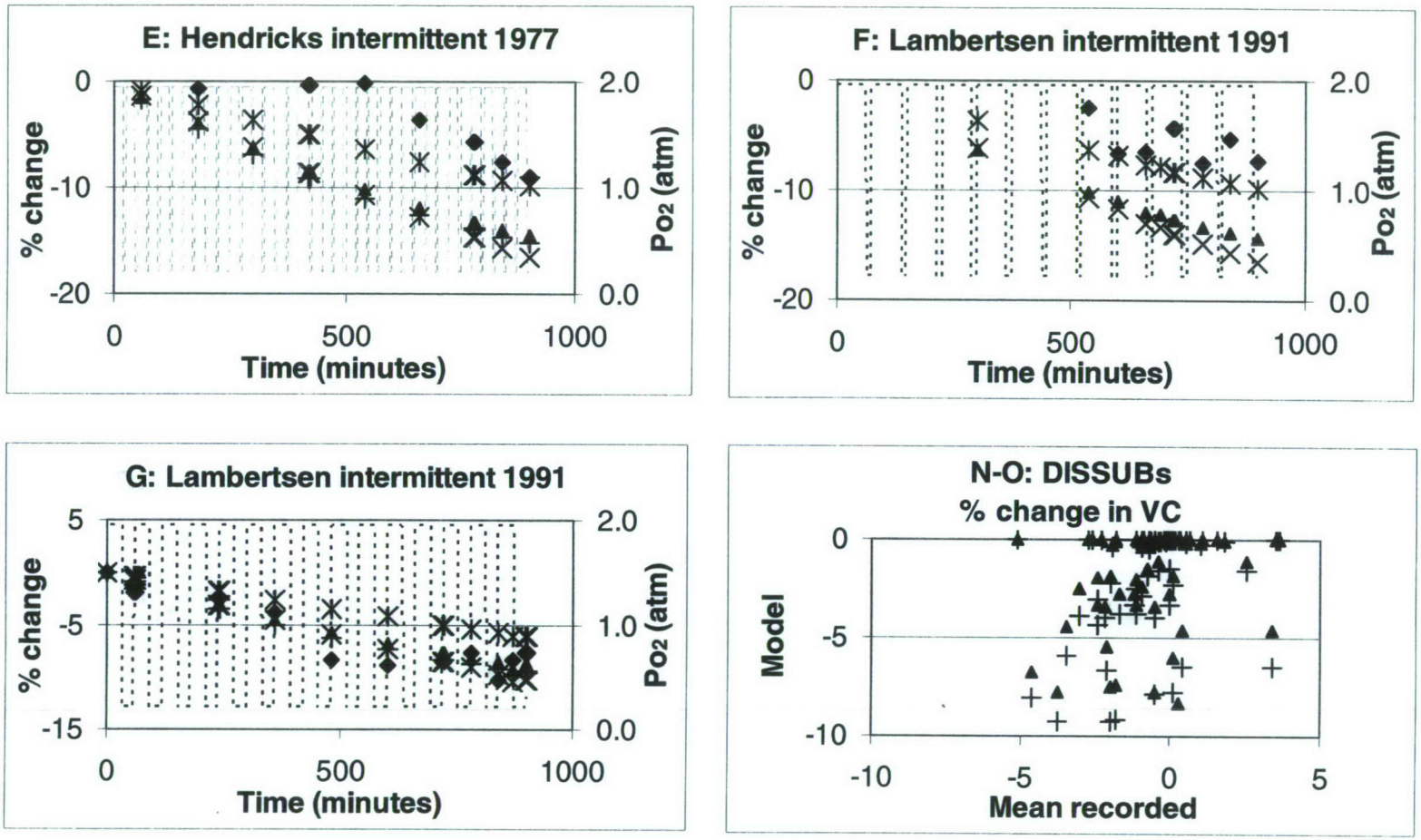

Figure 15 (continued). Proportional rate of healing Models 3a and 3b.
Correspondence to intermittent data, Experiments E–G, N, and O. Experiments N and O are shown as a correlation plot.

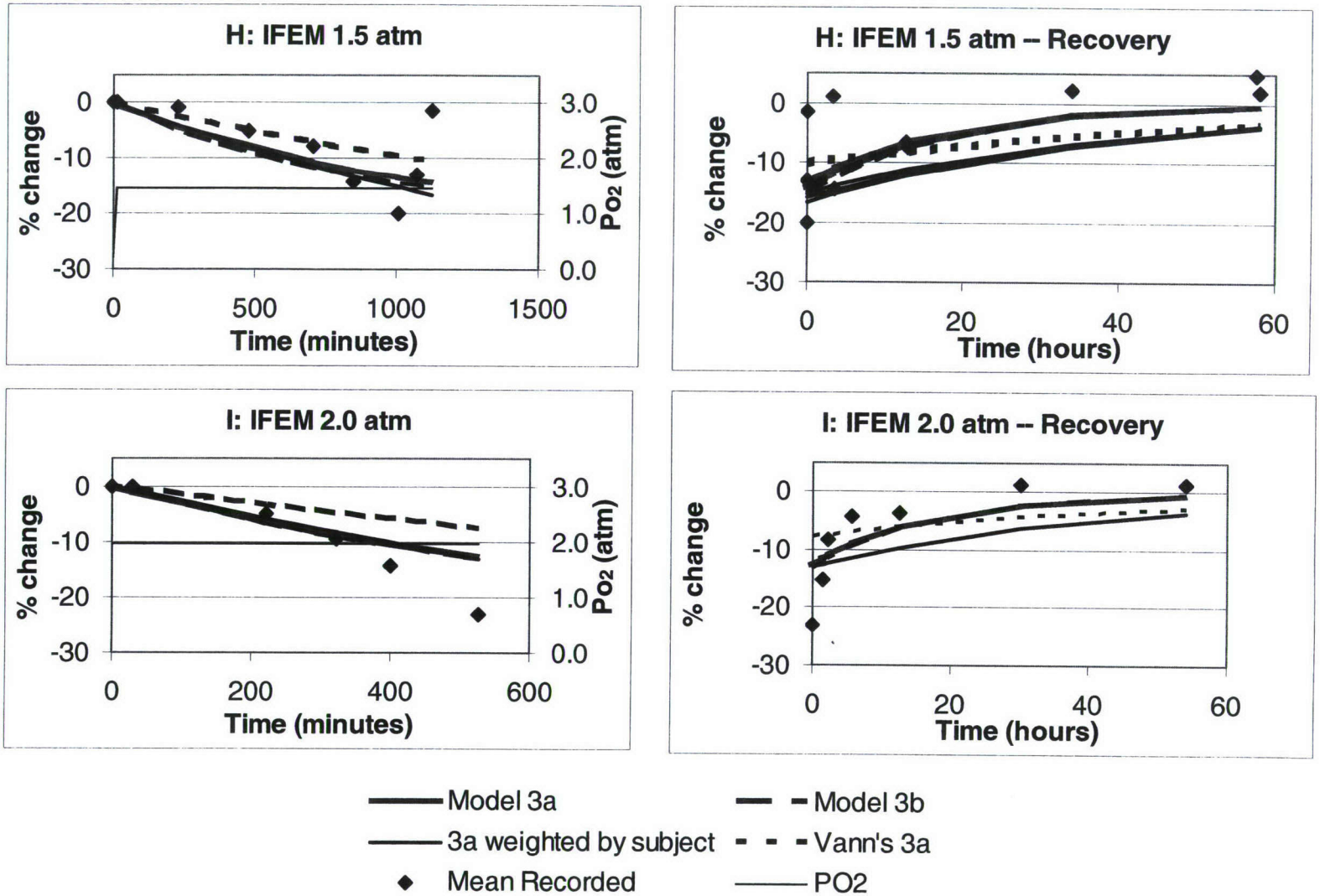

Figure 15 (continued). Proportional rate of healing Models 3a and 3b. Correspondence to data, Experiments H and I. Recovery breathing room air.

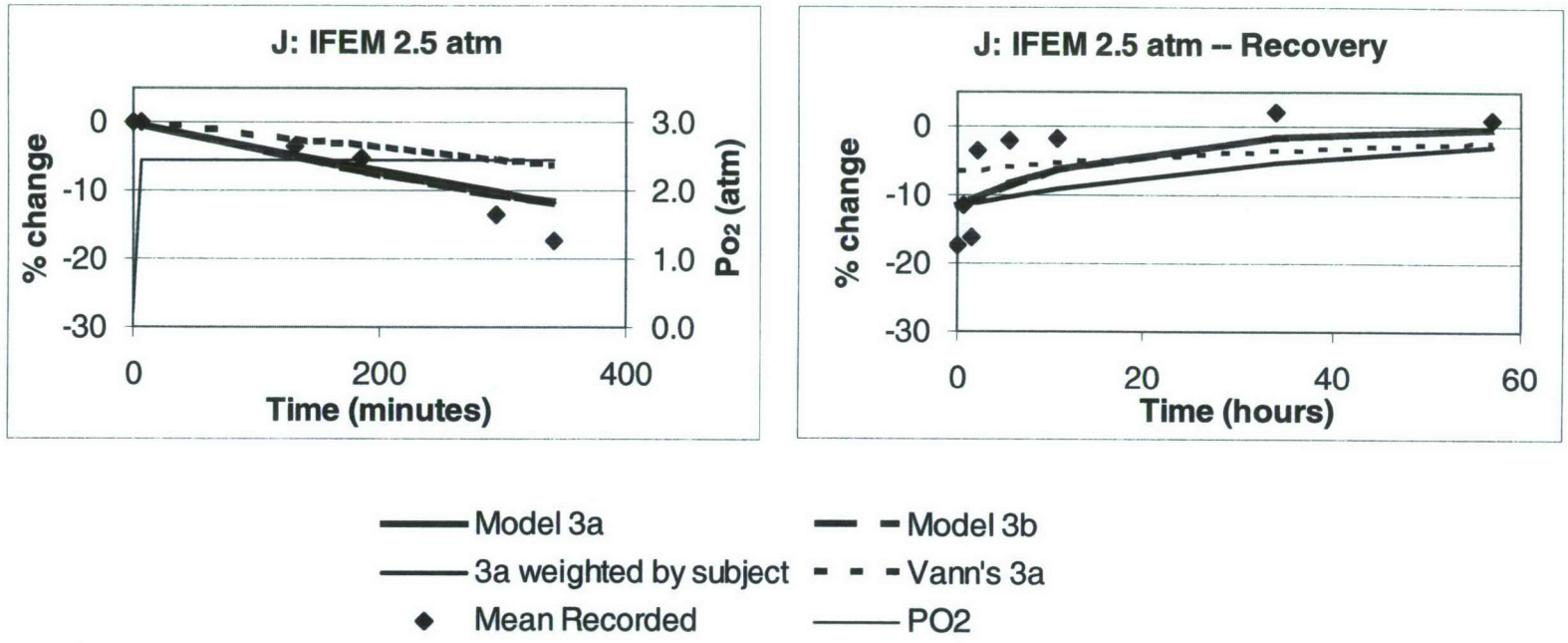

Figure 15 (continued). Proportional rate of healing Models 3a and 3b. Correspondence to data, Experiment J. Recovery breathing room air.

Model 4. Autocatalytic Models

$$dF/dt = a_1 \cdot (P_{O_2} - P_{th}) + b \cdot F \cdot (P_{O_2} - P_a)$$

$$\%\Delta VC = -\alpha \cdot F \qquad \text{Let } a = -\alpha \cdot a_1.$$

Model 4a: P_{th} set to 110 Torr. Model 4b: P_a set to 760 Torr.

Note that the time constant of recovery is $1 / [b \cdot (P_{O_2} - P_a)]$, not $1 / b$. For Model 4a, the exponents of recovery while breathing air at sea level pressure, $b \cdot (110 - P_a)$, range from $-8 \cdot 10^{-4}$ min^{-1} to $-1.2 \cdot 10^{-3}$ min^{-1}, concordant with those found for the proportional healing model.

In the absence of recovery data, neither Model 4a nor Model 4b could be fitted with any confidence in the parameters.

After further inspection of the data, we introduced two modifications consistent with the idea that recovery rates vary with the duration of the previous exposure. Here T_{dur} is the duration of exposure to elevated P_{O_2}:

Model 4c:

$$dF/dt = a_1 \cdot (P_{O_2} - P_{th}) + (b + c/T_{dur}) \cdot F \cdot (P_{O_2} - P_a), \qquad P_a = 760 \text{ Torr},$$

and Model 4d:

$$dF/dt = \begin{cases} a_1 \cdot (P_{O_2} - P_{th}) + [b + c \cdot (P_{O_2} - P_a) / T_{dur}] \cdot F, & P_{O_2} > P_{th} \\ 0, & 200 \text{ Torr} < P_{O_2} < P_{th} \\ [b + c \cdot (P_{O_2} - P_a) / T_{dur}] \cdot F, & P_{O_2} < 200 \text{ Torr}, \end{cases}$$

where P_{th} = 330 Torr and P_a = 760 Torr.

Figure 16 compares some autocatalytic models to the data. With Model 4a, the fitted autocatalytic threshold P_a is above P_{O_2} in Experiments A, B, and D, and thus those model curves are concave up; P_a is very close to P_{O_2} in Experiments C and H, and thus those model responses are almost linear; and P_a is below the P_{O_2} of Experiments I and J, and thus the model is concave down. With Models 4b and 4d, the selected autocatalytic threshold P_a is below P_{O_2} in Experiments C–J, and those responses are slightly concave down. Of the autocatalytic models, Model 4d corresponds most closely to the continuous exposure data. All models overestimate ΔVC for intermittent exposure Experiments E and F. For the DISSUB data, the correlation coefficient of Model 4a to the average data is 0.39; of Model 4b it is 0.01, and of Model 4d it is 0.08.

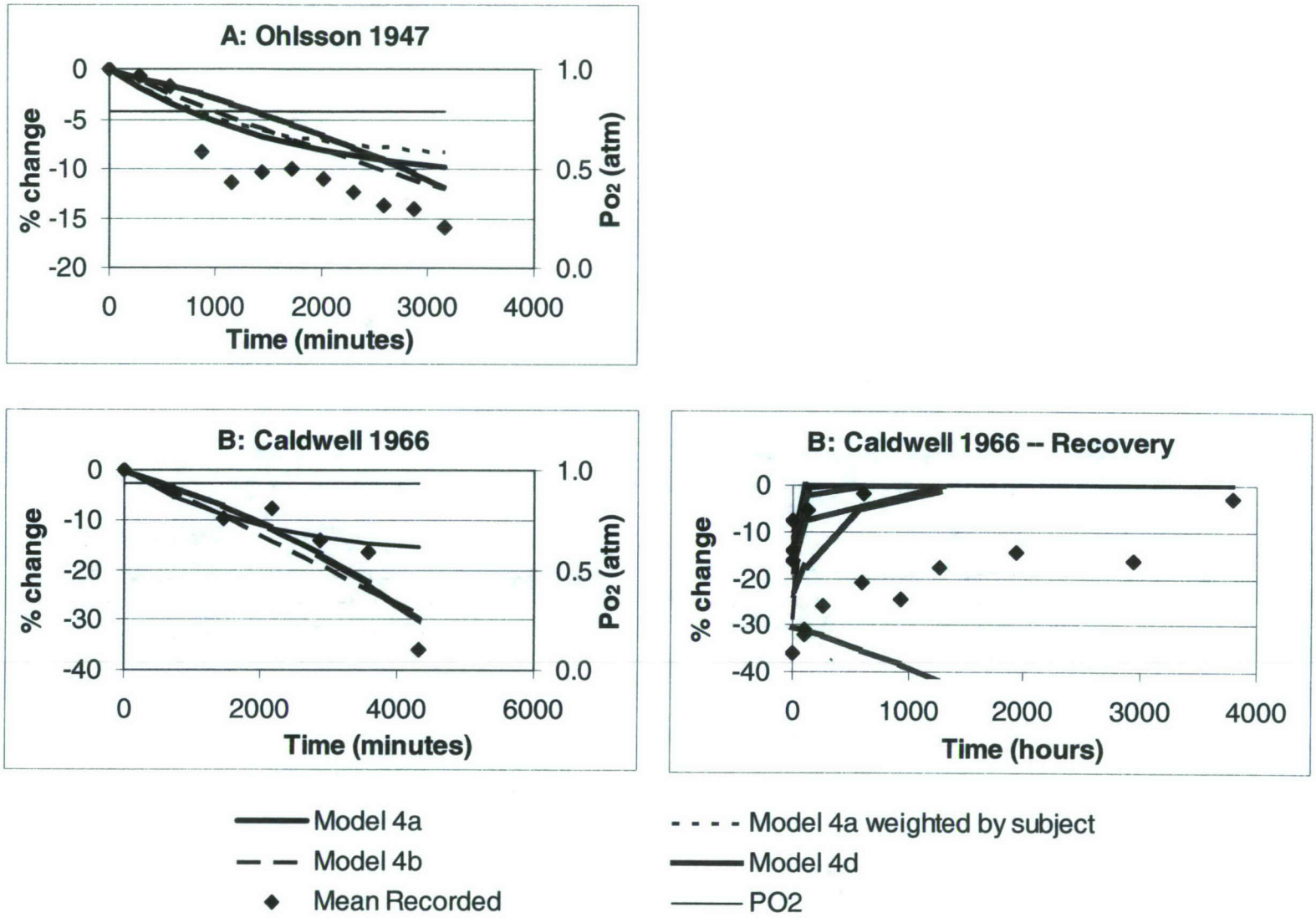

Figure 16. Autocatalyic Model 4.
Correspondence to data, Experiments A and B. Recovery with room air.

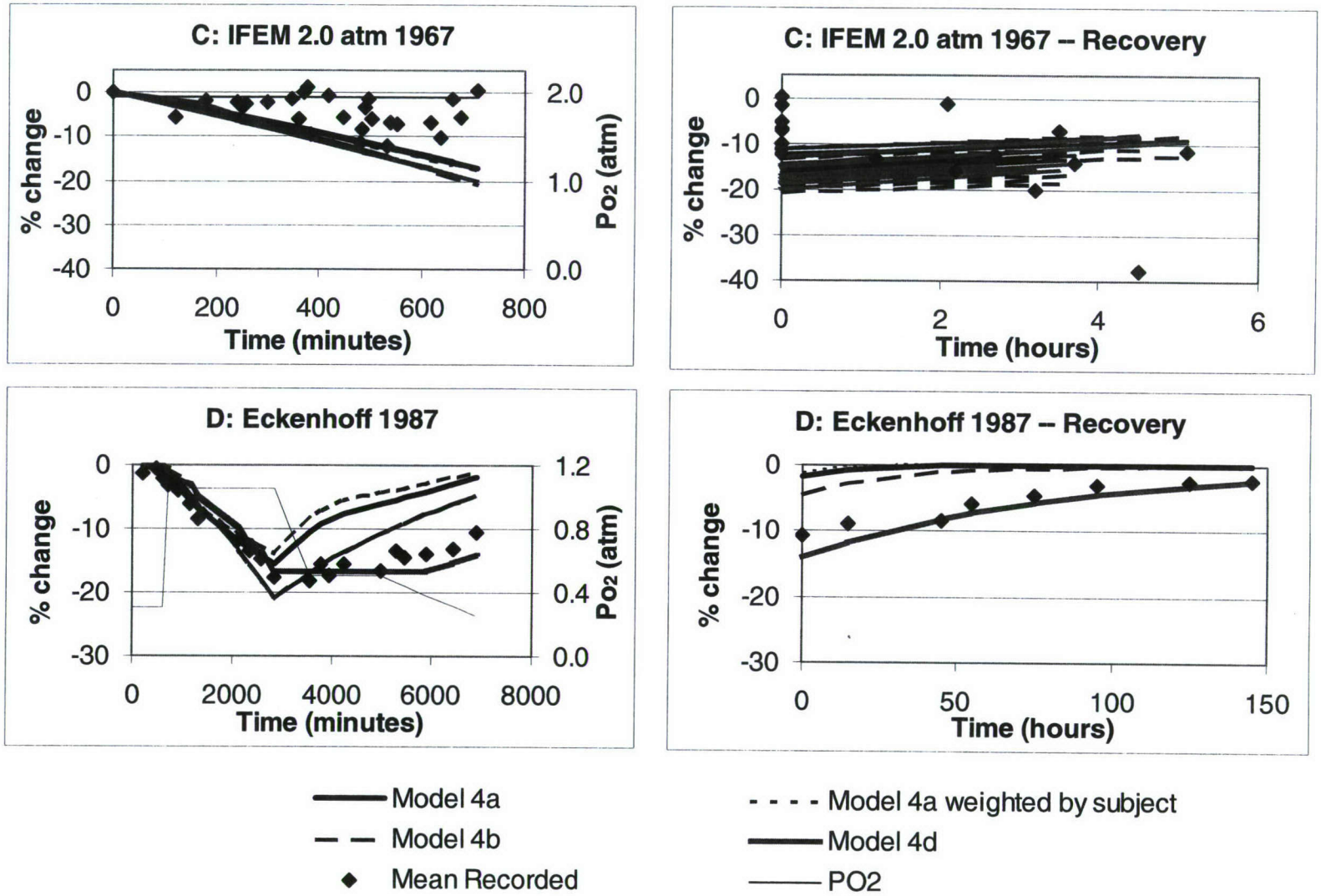

Figure 16 (continued). Autocatalyic Model 4.
Correspondence to data, Experiments C and D. Recovery with room air.

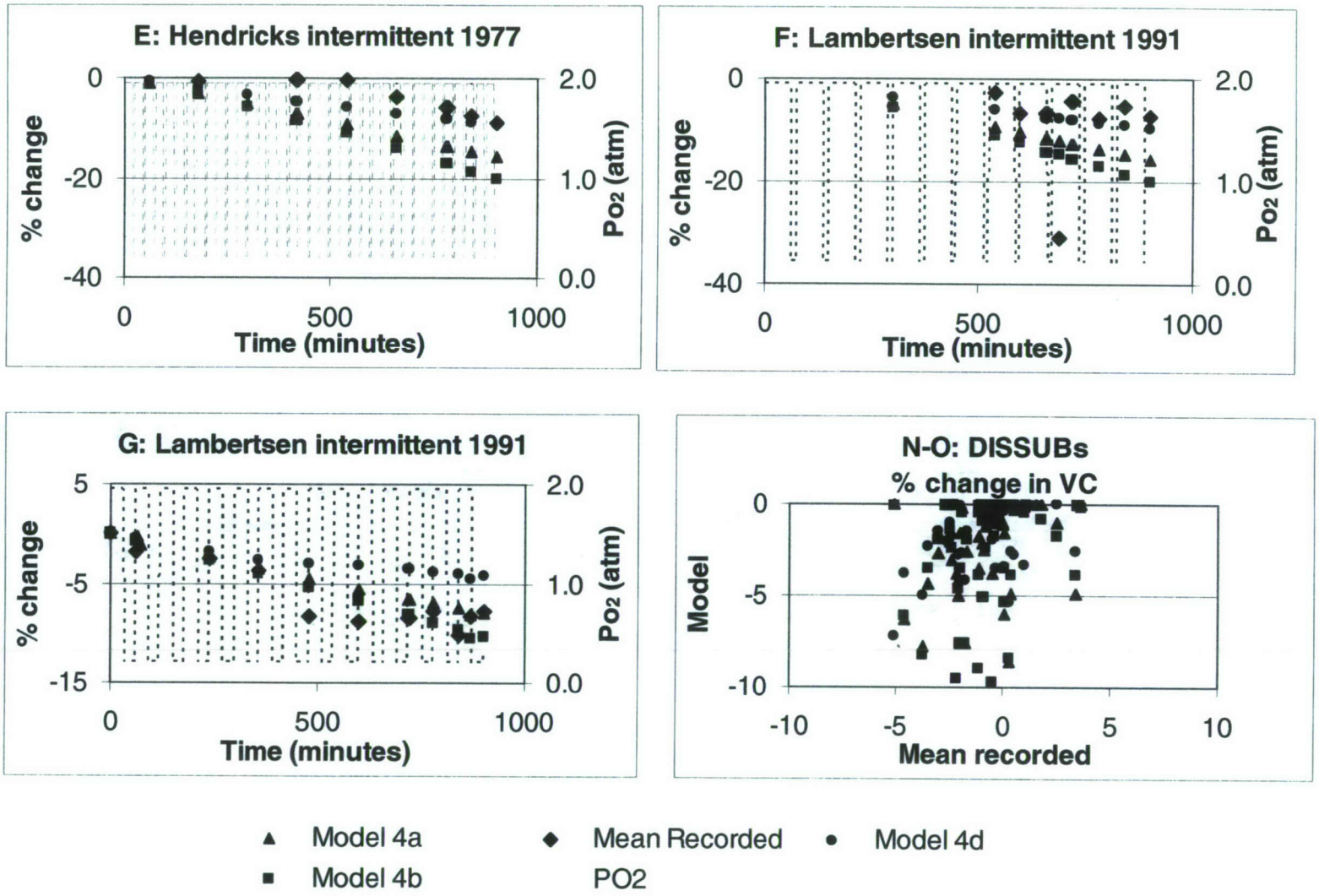

Figure 16 (continued). Autocatalyic Model 4 by experiment.
Correspondence to data, intermittent Experiments E–G, N, and O. DISSUB experiments are shown in a correlation plot.

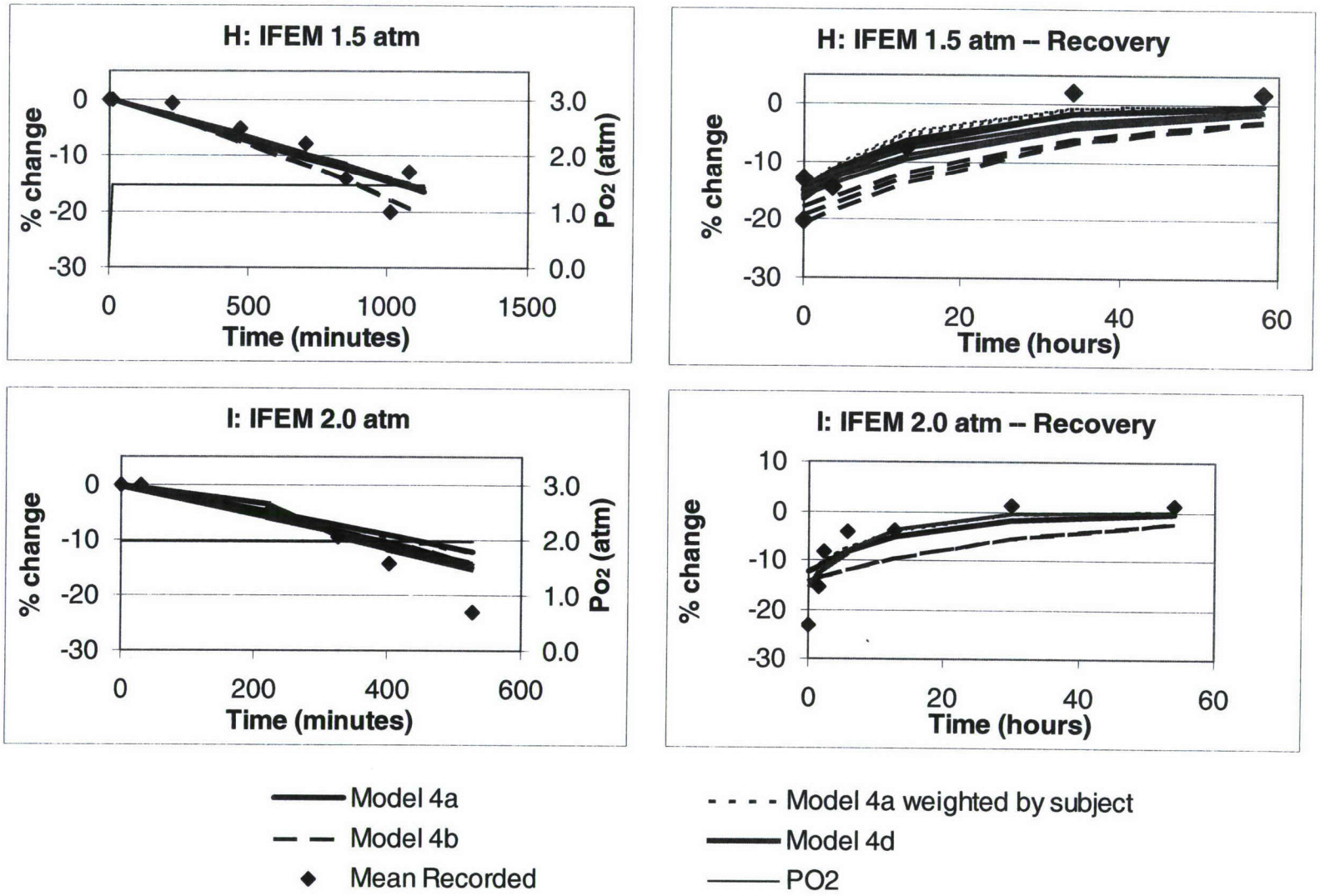

Figure 16 (continued). Autocatalyic Model 4 by experiment.
Correspondence to data, Experiments H and I. Recovery with room air.

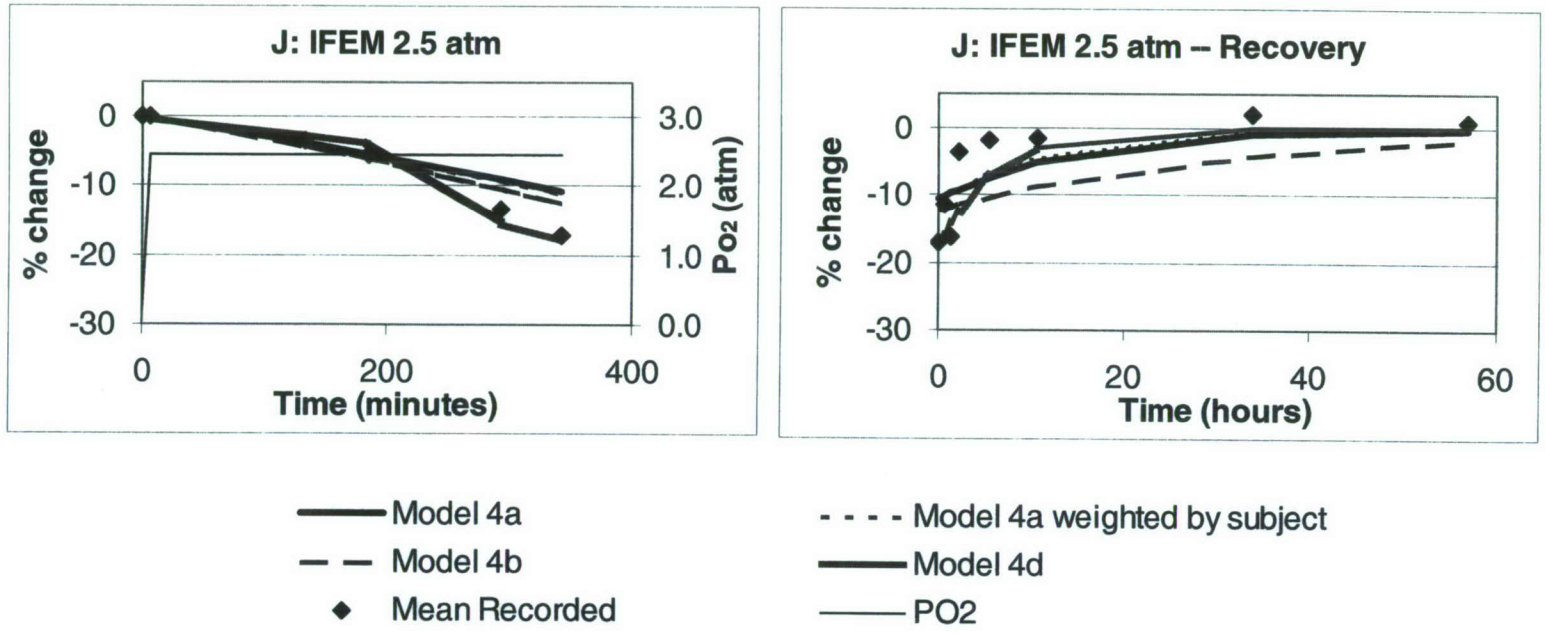

Figure 16 (continued). Autocatalyic Model 4 by experiment.
Correspondence to data, Experiment J. Recovery with room air.

Model 5.
Exponential Models

$$\%\Delta VC = -\alpha \cdot F, \text{ where}$$

a. $$F = \begin{cases} a_1 \cdot PO_2^{\,b} \cdot t^2 + F_0, & PO_2 > 0.58 \text{ atm} \\ F_0 \cdot e^{-[c + g \cdot PO_{2is}] \cdot t}, & PO_2 \le 0.58 \text{ atm.} \end{cases}$$

b. $$F = \begin{cases} a_1 \cdot PO_2^{\,b} \cdot t^2 + F_0, & PO_2 > 0.58 \text{ atm} \\ F_0 \cdot e^{-[c + g / T_{dur}] \cdot t}, & PO_2 \le 0.58 \text{ atm.} \end{cases}$$

c. $$F = \begin{cases} a_1 \cdot (PO_2 - 0.5)^b \cdot t^2 + F_0, & PO_2 > 0.58 \text{ atm} \\ F_0 \cdot e^{-[c - g \cdot (PO_2 - 0.5) / T_{dur}] \cdot t}, & PO_2 \le 0.58 \text{ atm.} \end{cases}$$

d. $$F = \begin{cases} a_1 \cdot PO_2^{\,b} \cdot t^{PO_2} + F_0, & PO_2 > 0.58 \text{ atm} \\ F_0 / [1 - (c + g / T_{dur}) \cdot t \cdot F_0], & PO_2 \le 0.58 \text{ atm} \end{cases}$$

e. $$F = \begin{cases} a_1 \cdot (c \cdot PO_2)^b \cdot t^{c \cdot PO_2} + F_0, & PO_2 > 0.58 \text{ atm} \\ F_0 / [1 - (c + g / T_{dur}) \cdot t \cdot F_0], & PO_2 \le 0.58 \text{ atm} \end{cases}$$

f. $$F = \begin{cases} a_1 \cdot [(c \cdot PO_2)^{b-1} / (c \cdot PO_2 + g)] \cdot [T_{dur2}^{\,c \cdot PO_2} - T_{dur1}^{\,c \cdot PO_2}] + F \text{ at } T_{dur1}, \\ \qquad PO_2 > 0.58 \text{ atm} \\ F_0 \cdot e^{-g \cdot t / T_{dur}}, & PO_2 \le 0.58 \text{ atm} \end{cases}$$

Models 5a and 5b are identical when $PO_2 > 0.58$. Models 5d and 5e are identical in form when $PO_2 < 0.58$ atm, but F_0 may differ between the two. Note that the PO_2 at which recovery begins was increased from 0.5 atm to 0.58 atm; data of Experiment D drove the change. However, the threshold in Model 5c was not increased.

For the long, steady exposure data, the periods with elevated PO_2 and the recovery periods were assessed separately for Models 5a–e, but both phases were combined to assess fits to intermittent exposure data of any model or to the fits of Model 5f.

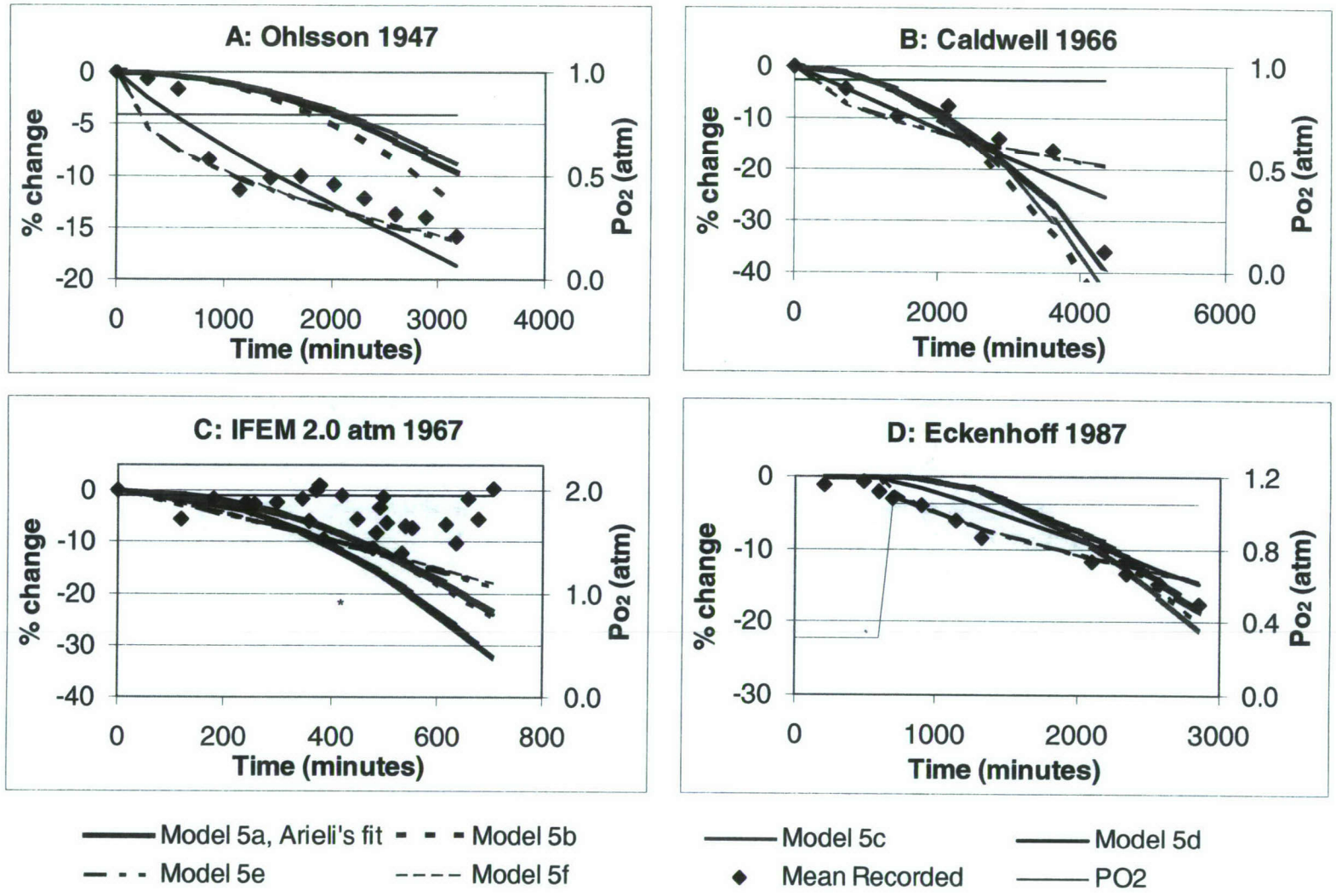

Figure 17. Exponential Model 5 at elevated P_{O_2}, by experiment. Correspondence to data, Experiments A–D.

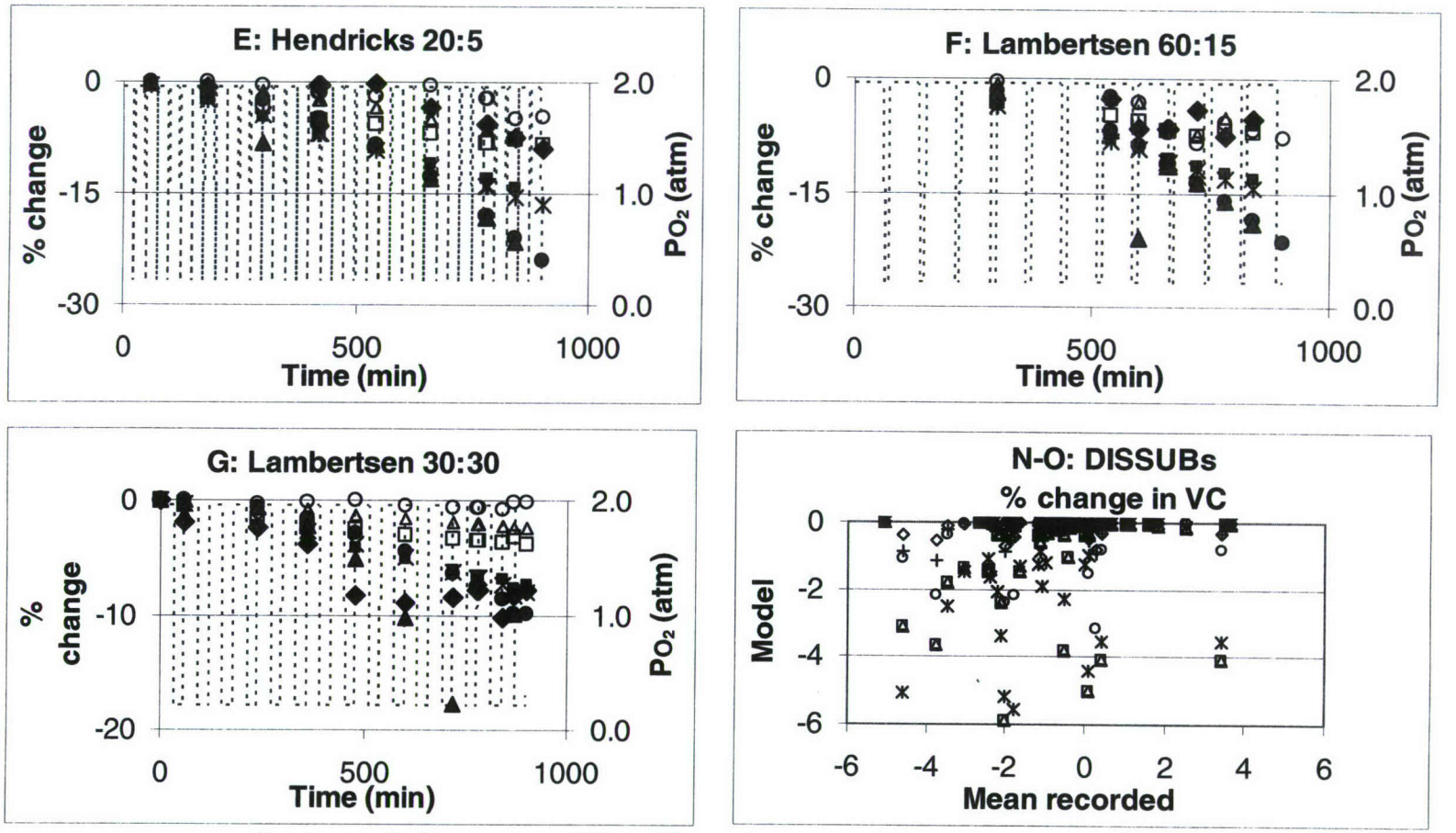

Open symbols: averaged P_{O_2}. Closed symbols: P_{O_2}not averaged (see text).

○, ● Model 5b; Δ, ▲ Model 5d; □, ■ Model 5e, * Model 5f, ♦ Mean recorded---- P_{O_2}

Figure 17 (continued). Exponential Model 5 at elevated P_{O_2}, by experiment.
Correspondence to intermittent exposure, Experiments E–G. Time is accumulated duration at elevated P_{O_2}. Correlation plot, Experiments N and O.

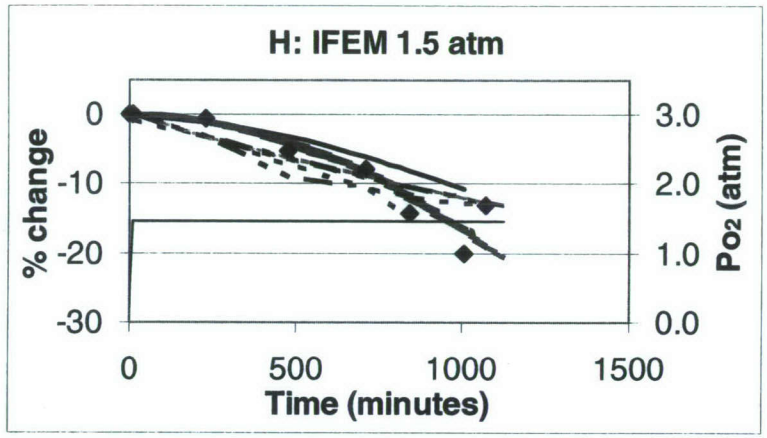

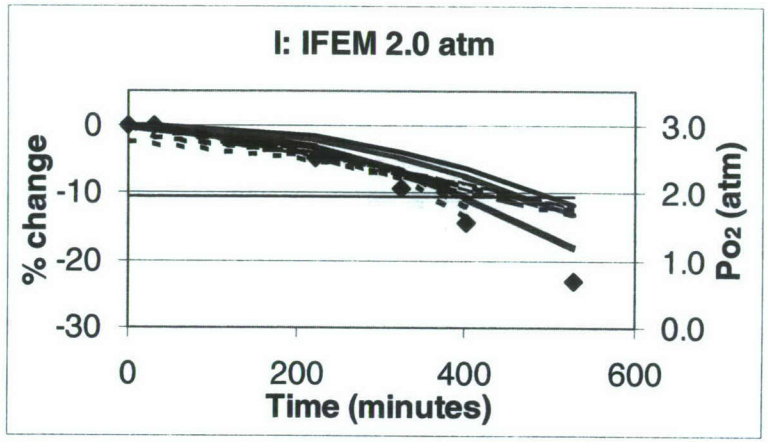

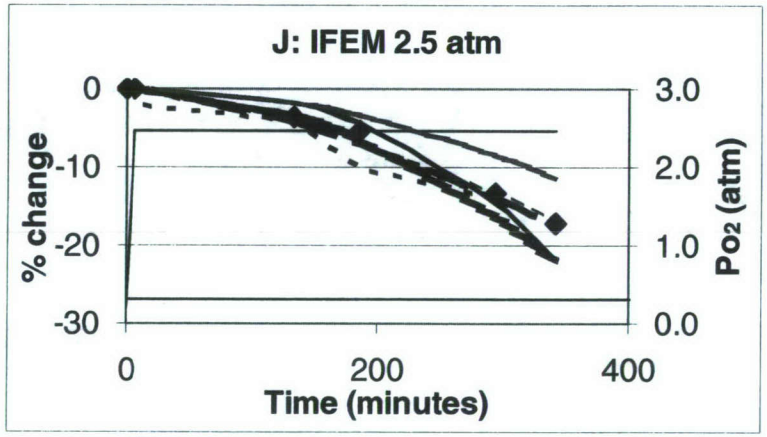

Figure 17 (continued). Exponential Model 5 at elevated P_{O_2}, by experiment. Correspondence to data, Experiments H–J.

Elevated P_{O_2}

Models 5a and 5b are identical during exposure to elevated P_{O_2}. Figure 17 shows the portion of the record when P_{O_2} was elevated, with parameters for Models 5b–e as fitted for Data Group 3 without recovery (Table A14); Model 5a with the parameters fitted by Arieli,[24–26] $a = -2.3 \cdot 10^{-6}$ min^{-2}, $b = 4.6$; and Model 5f fitted to Data Group 3 with all recovery (Table A16).

The subtraction of a threshold from P_{O_2} in Model 5c slightly degrades the model fit indicated by r^2. Model 5e, where the exponent of time is P_{O_2} with a scaling factor, accounts for somewhat more variance than the others. Because Model 5f with its simultaneous healing term must be fitted to the combined onset and recovery data (Table A15), direct goodness-of-fit comparisons cannot be made. The "by eye" assessments (Figure 17) vary among experiments.

Models 5a–5c are concave downward at all P_{O_2} during injury onset. However, the model curvature is too steep for some data and perhaps not steep enough for others. Models 5d–5f represent attempts to improve the match to curvature during injury onset by using an exponent proportional to P_{O_2}. P_{O_2} was normalized to 1 atm and time to one minute in Model 5d, but the normalizing factor on P_{O_2} was permitted to float in Model 5e. The factor for time can be absorbed in the scaling constant a, but that for P_{O_2} as an exponent cannot. For Experiments A–C, Model 5d corresponds more closely to the data than do Models 5a–5c, but 5e and 5f correspond still better to the data. (The point representing the longest exposure in Experiment B, the point for which Models 5a–5c appear superior to the others, represents just one measurement in one subject.) For Experiment D, Models 5e and 5f correspond well to the data for the first 2400 minutes, after which Models 5a–5c fit better. For Experiment H, Models 5a–5c provide better fits than do Models 5d–5f. Experiment I is best matched by Model 5a, and Experiment J is best fit by Models 5e and 5f.

Elevated P_{O_2} Coupled with Recovery

For intermittent exposures the onset and recovery phases cannot be separated. The model performances are shown in Figure 17, where other experimental data and models are shown only for elevated P_{O_2}. If each intermittent step is considered to restart the clock for injury onset, Models 5a–5e predict no changes; the results are not shown. If accumulated times at elevated P_{O_2} are used instead of the time since the last air break, the models overestimate the ΔVC, as shown in Figure 17, Panels E–G, by filled symbols. (To use the accumulated time, piecewise changes have to be calculated across each step of elevated or normoxic P_{O_2}.) If time-averaged rather than instantaneous P_{O_2} is used with accumulated time, the model results more closely approach the intermittent data; in Figure 17 E–G, the open symbols show the results of averaging over the previous 120 minutes, an arbitrary time choice. Averaging for 90 minutes provided closer correspondence to the data of Experiment G than that obtained with 120 min averaging, but such 90-minute averaging underestimated the values of

Experiments E and F. The use of time averaging removes the recovery phase from consideration during these intermittent exposures, because the average P_{O_2} increases during the first averaging period and then remains greater than 0.5 atm.

For the DISSUB Experiments N and O, the correlation coefficients of models with time-averaged P_{O_2} and accumulated time to data averaged across subjects were 0.37 for Model 5a with Arieli's parameters, 0.22 for Model 5b, 0.23 for Model 5c, 0.01 for Model 5d, 0.21 for Model 5e, and 0.03 for Model 5f.

Recovery

Table A15 lists parameters fitted to those of the long exposure experiments that include recovery measurements. The parameters used for Figure 18 are those fitted to Data Group 3.

To avoid influences of the earlier elevated P_{O_2} portions of the models, the measured values at the end of exposure were used as F_0, a different value for each subject. Normalized by those starting values, results are shown from 1 (no recovery) and approaching 0. Second-order recovery does not collapse to a single curve, because its functional relation with F_0 is additive as well as multiplicative.

In Experiment B (Fig. 18) Model 5a does not recover, Model 5b matches the slowest recovery data, Model 5c matches the fastest recovery data, the second-order Models 5d and 5e fall between the slow and fast recovery data, and the integrated Exponential Model 5f matches the fastest recovery data. The recovery data of Experiment C are sparse and confusing. All Model 5s fall within the data scatter for Experiment D, although Model 5a fails to recover from $P_{O_{2is}} = 1$ atm with the coefficients fitted by Arieli et al.[24–26] For Experiments H–J, Models 5a–5f fit similarly well in general, although some starting values cause the second-order model to recover very slowly.

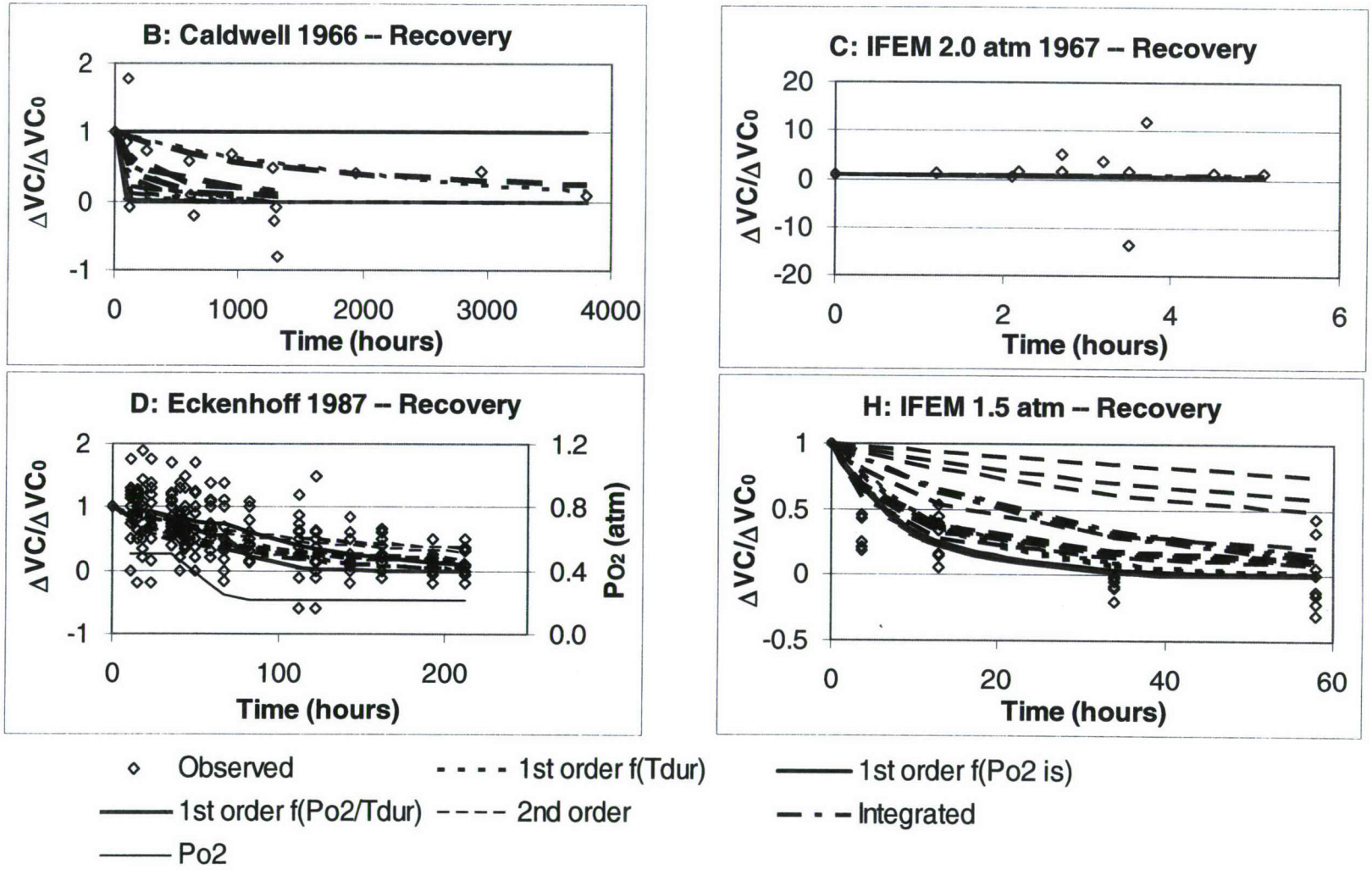

Figure 18. Recovery in Exponential Model 5, Experiments B–D and H. Correspondence to recovery data.

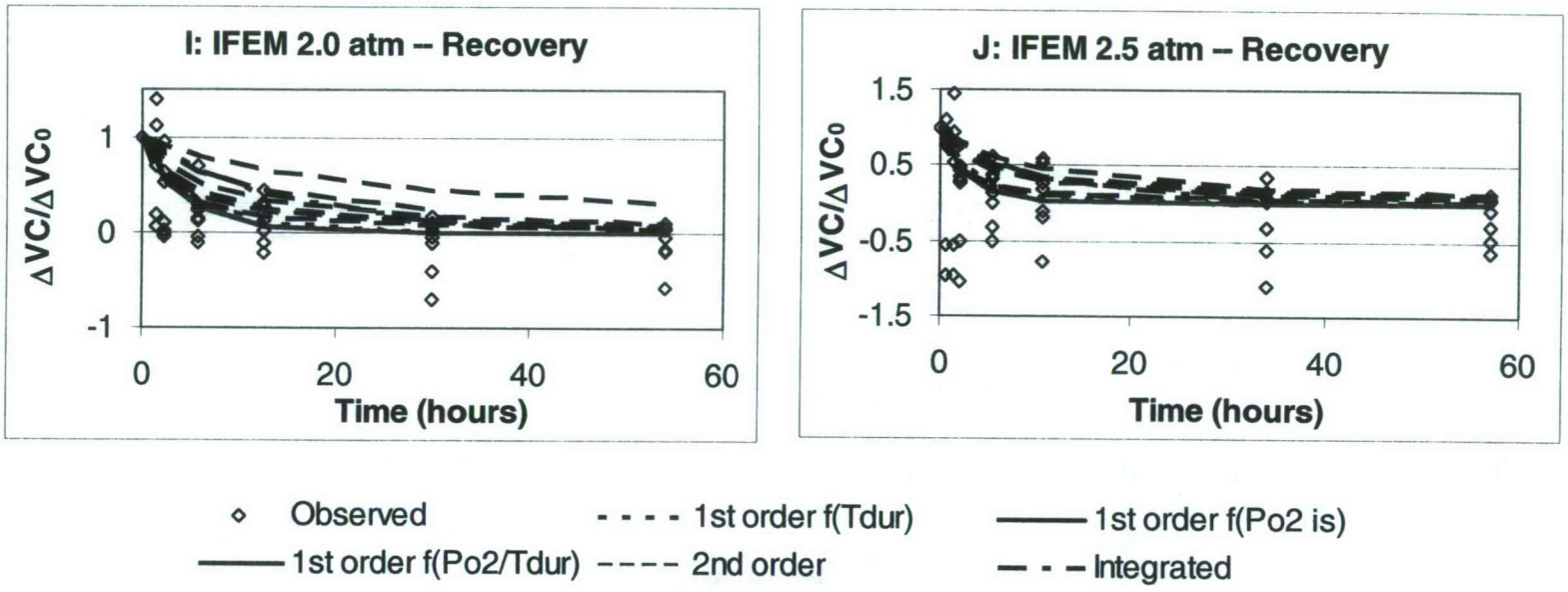

Figure 18 (continued). Recovery in Exponential Model 5, Experiments I and J. Correspondence to recovery data.

Model 6. Sigmoidal Dose Response Models

a. The Hill equation, scaled by parameter g, in this case has F from Model 3 as the dose:

$$\%\Delta VC = -g \cdot [F^b / (F^b + a^b)],$$

where $F = (P_{O_2} / c) \cdot (1 - e^{-(c \cdot t)}) + F_0 \cdot e^{-(c \cdot t)}$.

The Hill equation is bounded between 0 and 1, and the inflection point at $F = a$ is thus at $\%\Delta VC = g / 2$.

Because all %ΔVC are less than 50%, parameter a, the dose at the inflection point of the dose response curve, must be greater than the largest dose F when $g = 100$. However, even with $F < a$, %ΔVC can have an inflection point when plotted against time, because F is curvilinear in time. %ΔVC as a function of time is concave downward at small $(c \cdot t)$. As time increases, %ΔVC as a function of time becomes progressively linear, then almost constant as F approaches a plateau at P_{O_2}/c. However, with the range of values for c presented in Table A17, F would have reached 99% of its steady state value only after 4,620 to 18,420 minutes (77 to 307 hours) at constant P_{O_2}, times that lie outside the range of the data.

The model also was fitted with parameter g fitted (Table A18). Parameter a falls at %ΔVC between 7.5% and 11% depending on g, and measured data fall on both sides of the inflection. With these parameters, dose F would have reached 99% of its steady state value after 4620 to 7920 minutes (77 to 132 hours) at constant P_{O_2}.

b. The scaled Hill equation here has its dose given as the integral of the difference of P_{O_2} from a threshold, the cumulative dose model:

$$IntO_2 = \int (P_{O_2} - P_{th})\, dt, \text{ integrating from time} = 0 \text{ to time} = t$$

$$\text{Dose} = \begin{cases} IntO_2, & IntO_2 \geq 0 \\ 0, & IntO_2 < 0 \end{cases}$$

$$\%\Delta VC = -g \cdot [\text{dose}^b / (\text{dose}^b + a^b)]$$

c. The scaled Hill equation here has the dose given as the integral of the difference of P_{O_2} from a P_{O_2} threshold greater than threshold, but only exponential healing applies when P_{O_2} is less than threshold:

$$\%\Delta VC = \begin{cases} -g \cdot [\text{dose}^b / (\text{dose}^b + a^b), & P_{O_2} \geq P_{th} \\ (\%\Delta VC)_0 \cdot e^{-(c \cdot t)}, & P_{O_2} < P_{th} \end{cases}$$

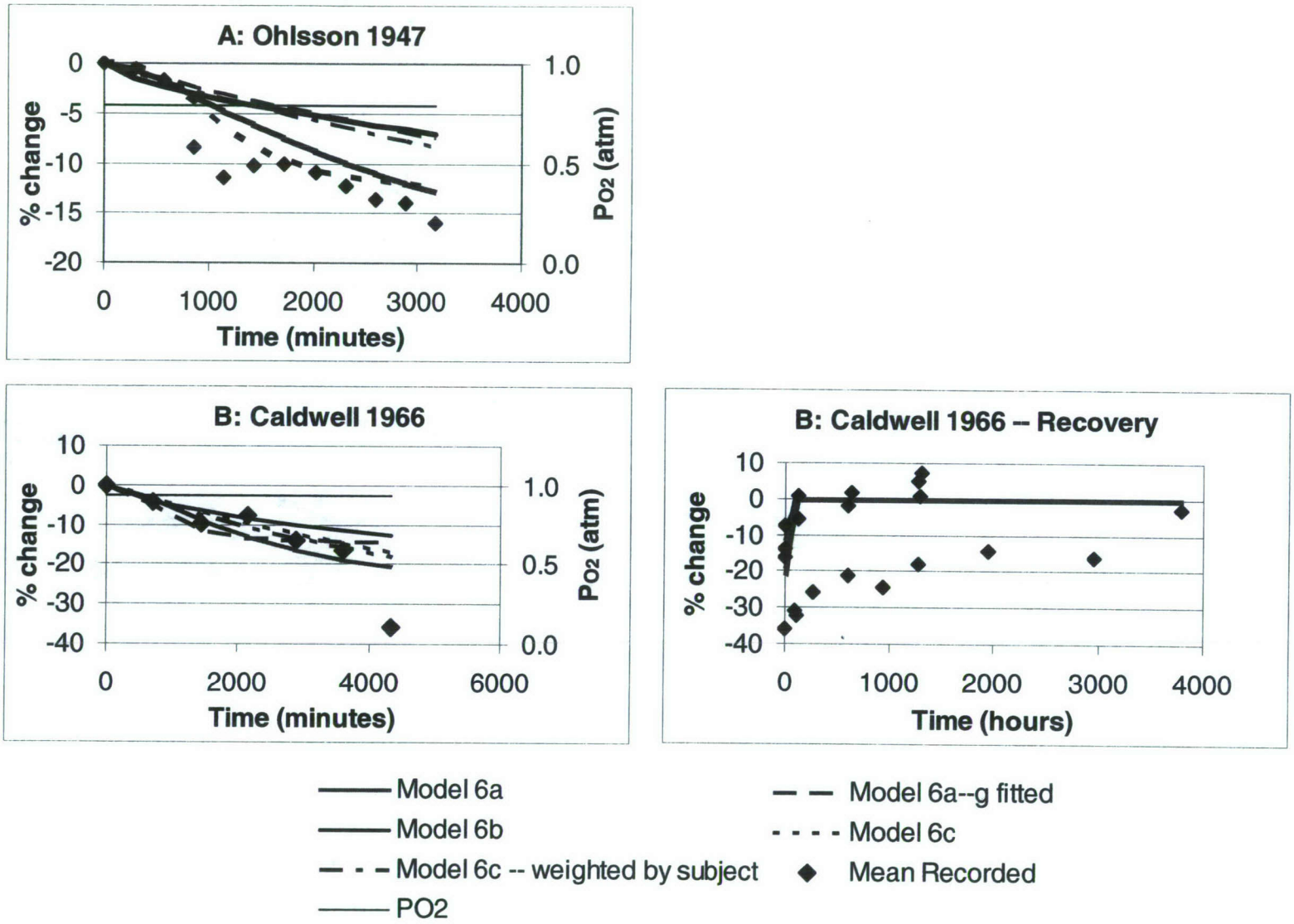

Figure 19. Sigmoidal Models 6a–6c, including fixed or fitted parameter *g*. Recovery with room air. Correspondence to data, Experiments A and B.

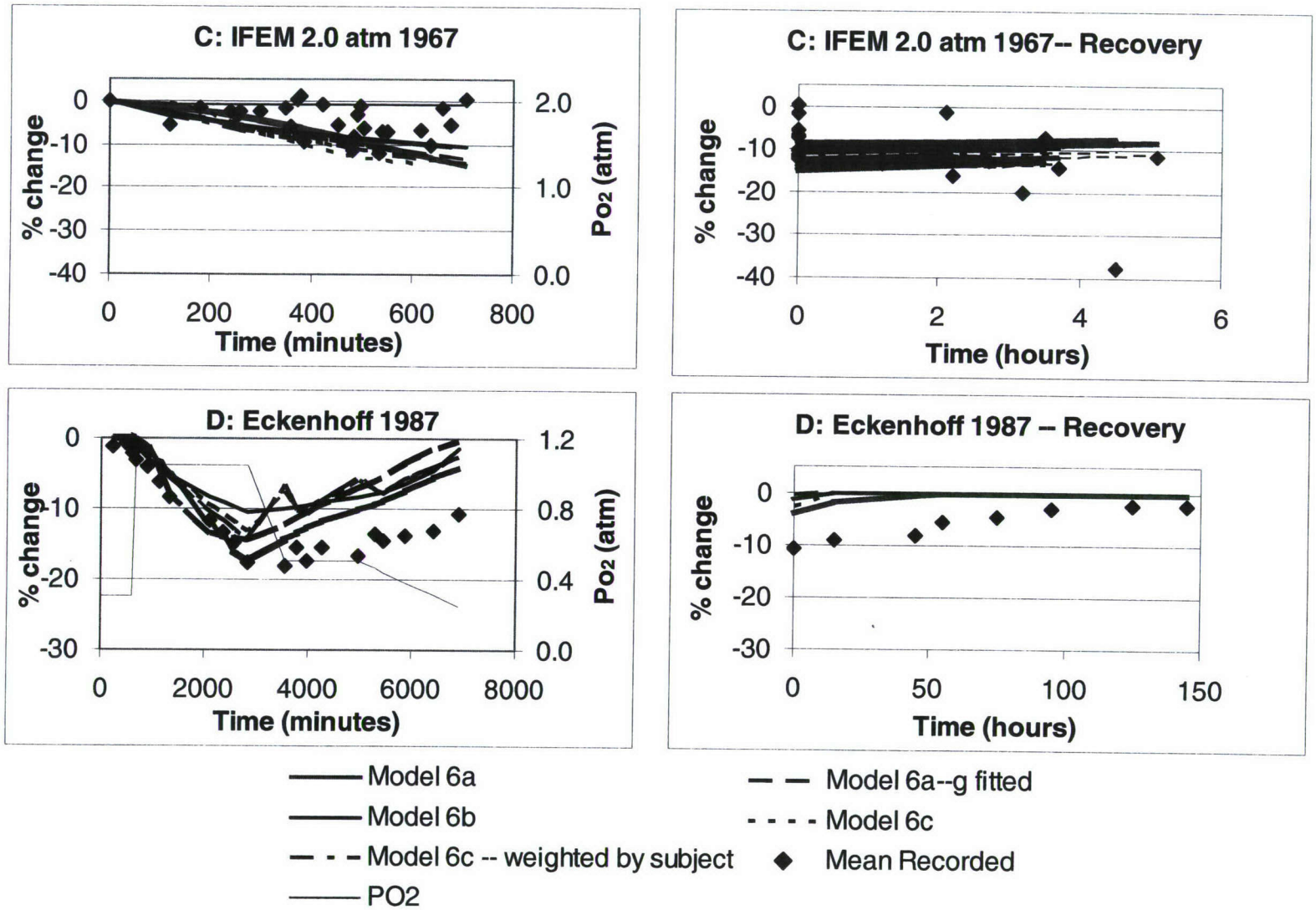

Figure 19. Sigmoidal Models 6a–6c, including fixed or fitted parameter *g*. Recovery with room air. Correspondence to data, Experiments C and D.

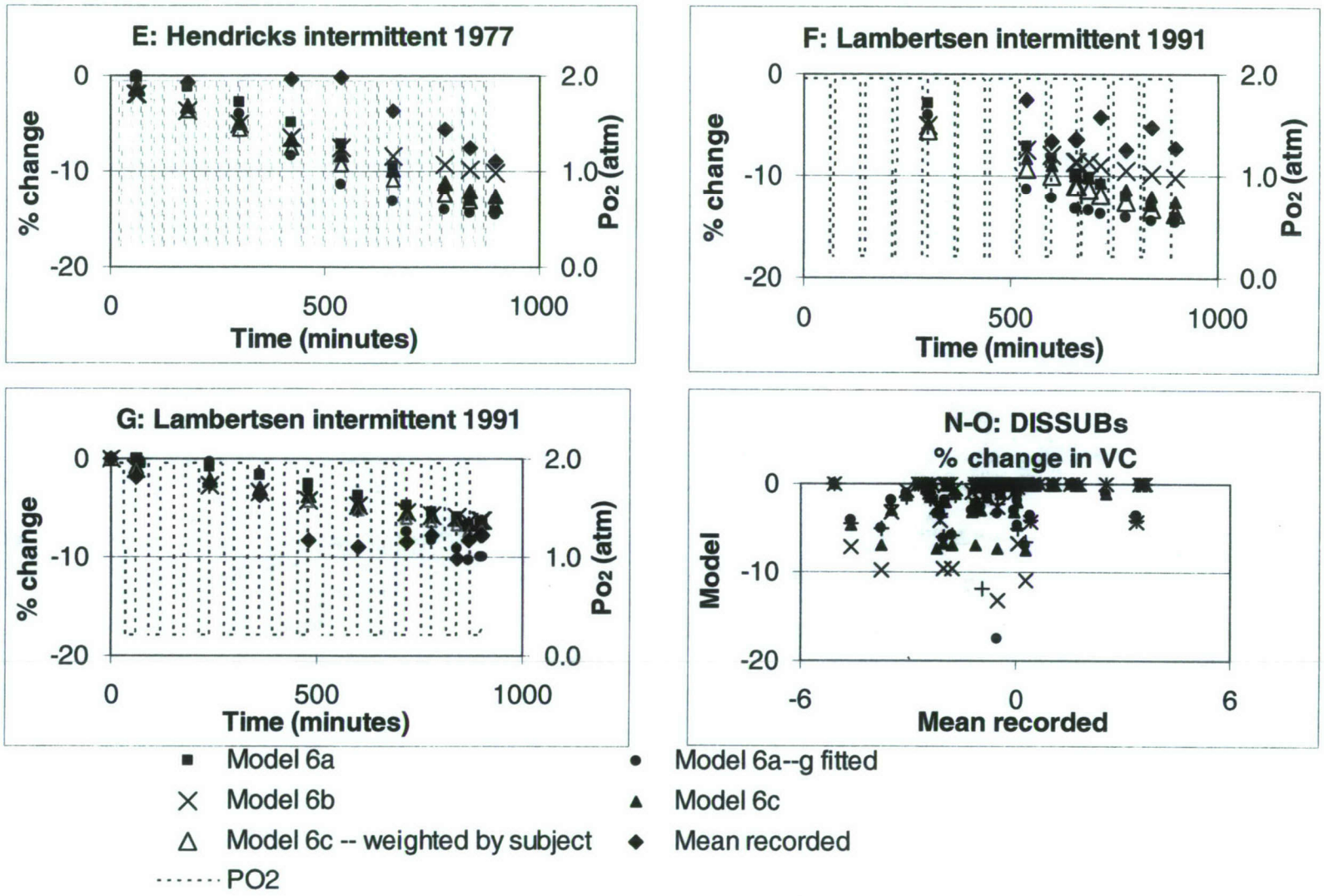

Figure 19 (continued). Sigmoidal Models 6a–6c.
Correspondence to data, intermittent Experiments E–G, N, and O. DISSUB experiments N and O are shown as a correlation plot.

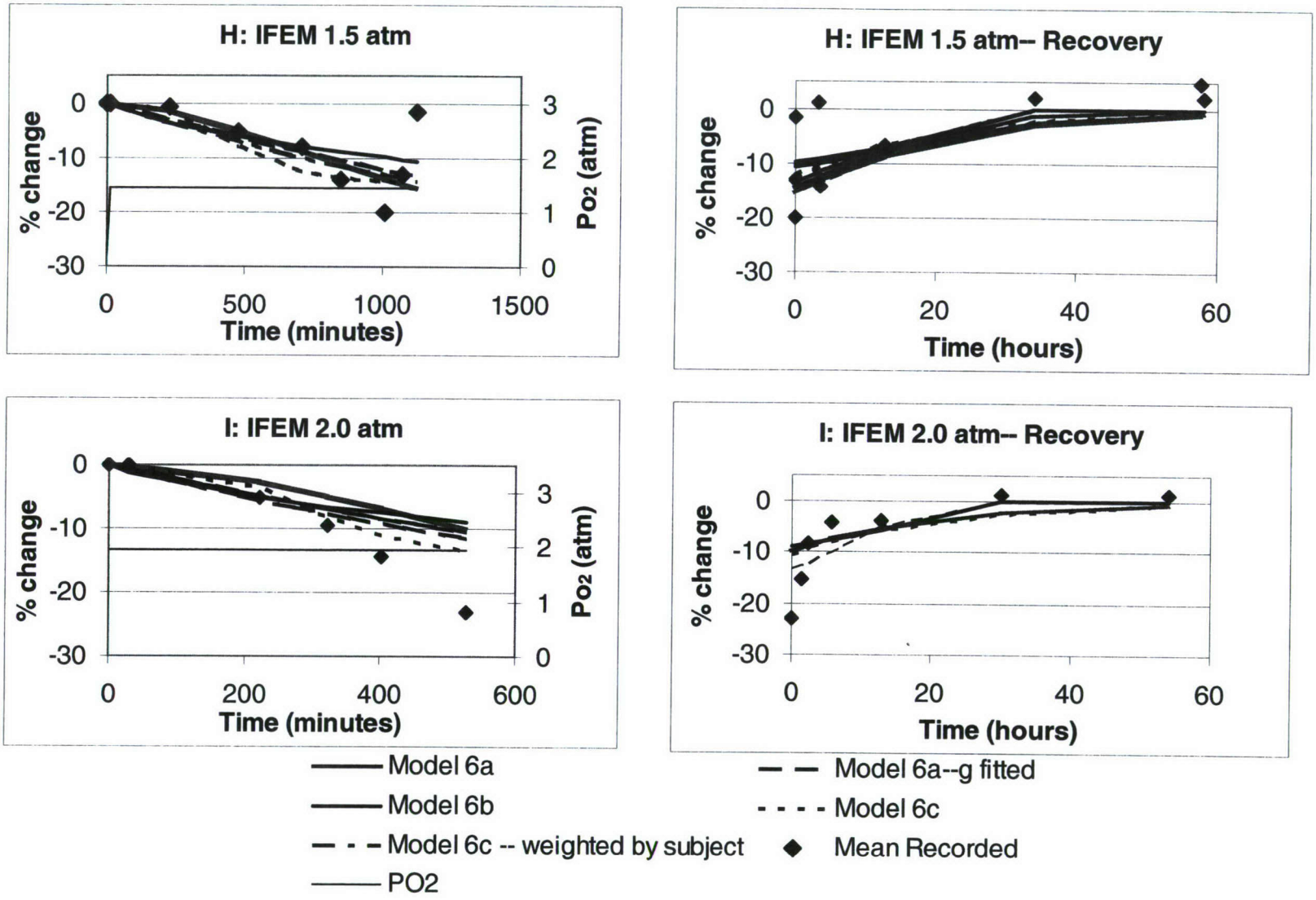

Figure 19 (continued). Sigmoidal Models 6a–6c. Recovery in room air. Correspondence to data, Experiments H and I.

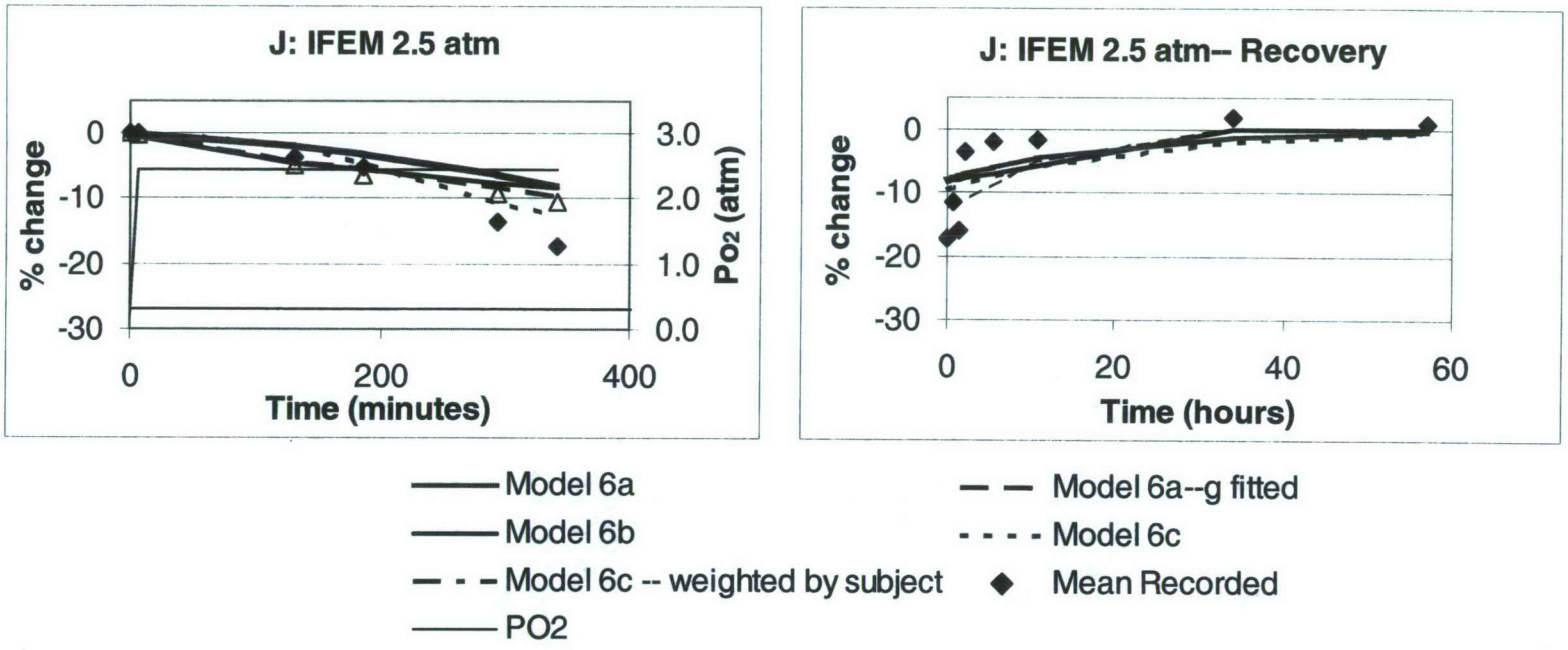

Figure 19 (continued). Sigmoidal Models 6a–6c. Recovery in room air. Correspondence to data, Experiment J.

Figure 19 shows fits with parameters for eight-hour recovery and Data Group 4 of Model 6a with fixed g (Table A17), Model 6a with fitted g (Table A18), Model 6b with fixed g (Table A19), and Model 6c with fixed g, weighted by both datum and subject (Table A20). The correlation coefficients between average responses for the intermittent DISSUB measurements N–O and the model predictions are Model 6a, 0.30; Model 6b, 0.23; and Model 6c, 0.29.

Model 7. Different Kinetics Model

$$\%\Delta VC = [\{a \cdot c \cdot (P_{O_2} - P_{th}) - b \cdot F_0\} / (f - b)] \cdot (e^{-bt} - e^{-gt}) + [a \cdot (P_{O_2} - P_{th}) / (b \cdot g)] \cdot (1 - e^{-gt}) + (\%\Delta VC)_0 \cdot e^{-gt}$$

The parameters of this model (Fig. 8) could not be determined with any confidence from the data. Although the model explained some of the experimental variation, confidence intervals around the individual parameter estimates spanned zero. The data are not sufficiently varied to distinguish among the closely related parameters.

Model 8. Injury-Memory Model

$$\%\Delta VC = a \cdot b^{-2} \cdot (P_{O_2} - P_{th}) \cdot [e^{-(b \cdot t)} - e^{-[b \cdot (t - t_{mem})]}] + a \cdot b^{-1} \cdot \text{memory} \cdot (P_{O_2} - P_{th}) + I_0 \cdot b^{-1} \cdot [e^{-(b \cdot t)} - e^{[b \cdot (t - t_{mem})]}].$$

Figure 20 illustrates the fit of the injury-memory Model 8 with a three-hour memory. It uses the parameters from Data Group 4, weighted by datum, with all recovery, and it uses those, weighted by subject, for eight hours of recovery from Data Groups 2 and 4 (Table A21). Of the three traces shown, that for Data Group 2, weighted by subject, has the largest exponent of recovery b.

This model, an integration of Model 3, corresponds better to the curvatures of the data than does Model 3 but does not curve sufficiently at $P_{O_2} \geq 1.5$ atm. In the intermittent DISSUB experiments N–O, the model tends to overestimate ΔVC, but the correlation coefficient between the model prediction and the average data is moderately high at 0.43.

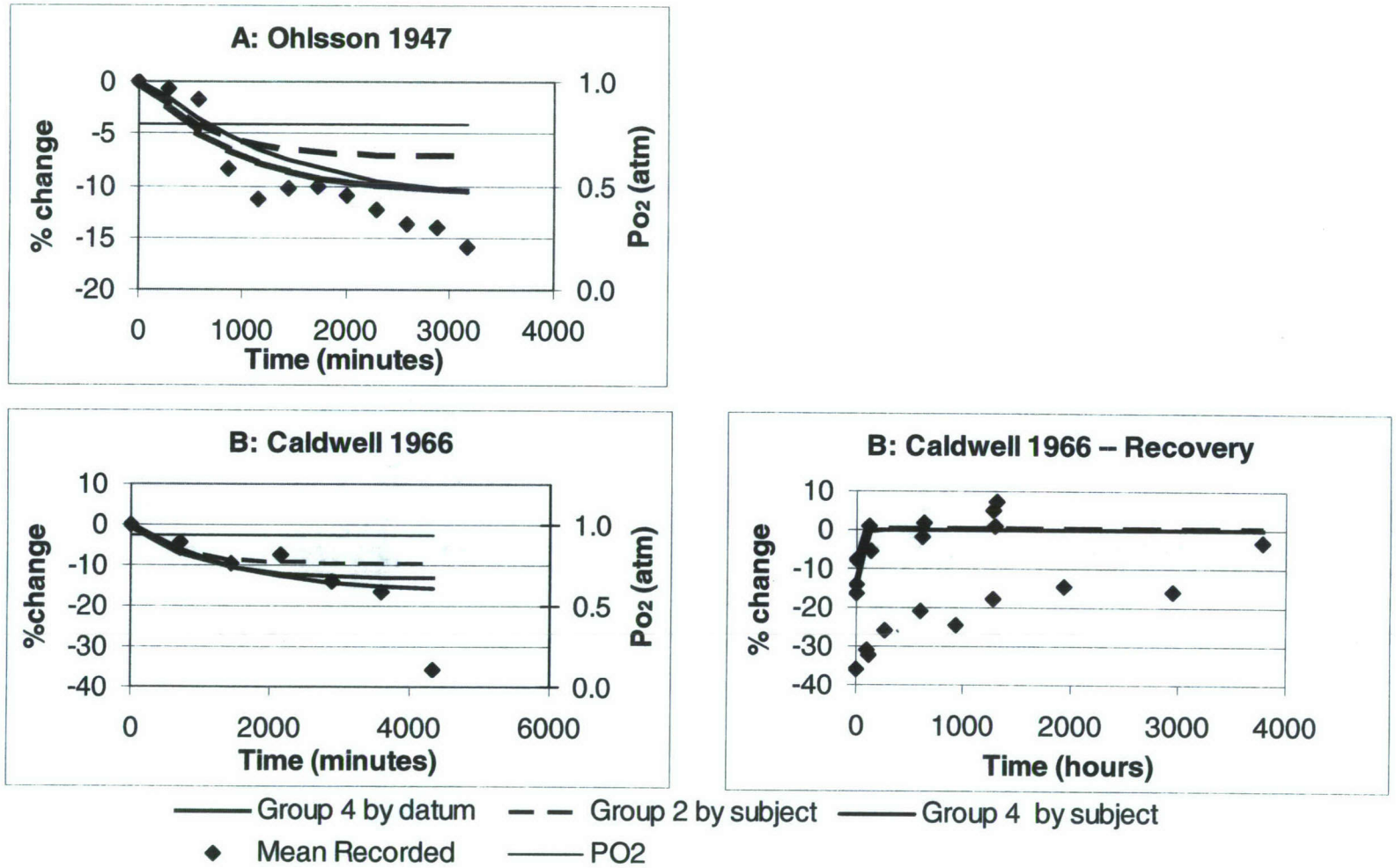

Figure 20. Injury-Memory Model 8, with three-hour memory. Recovery in room air. Correspondence to data, Experiments A and B.

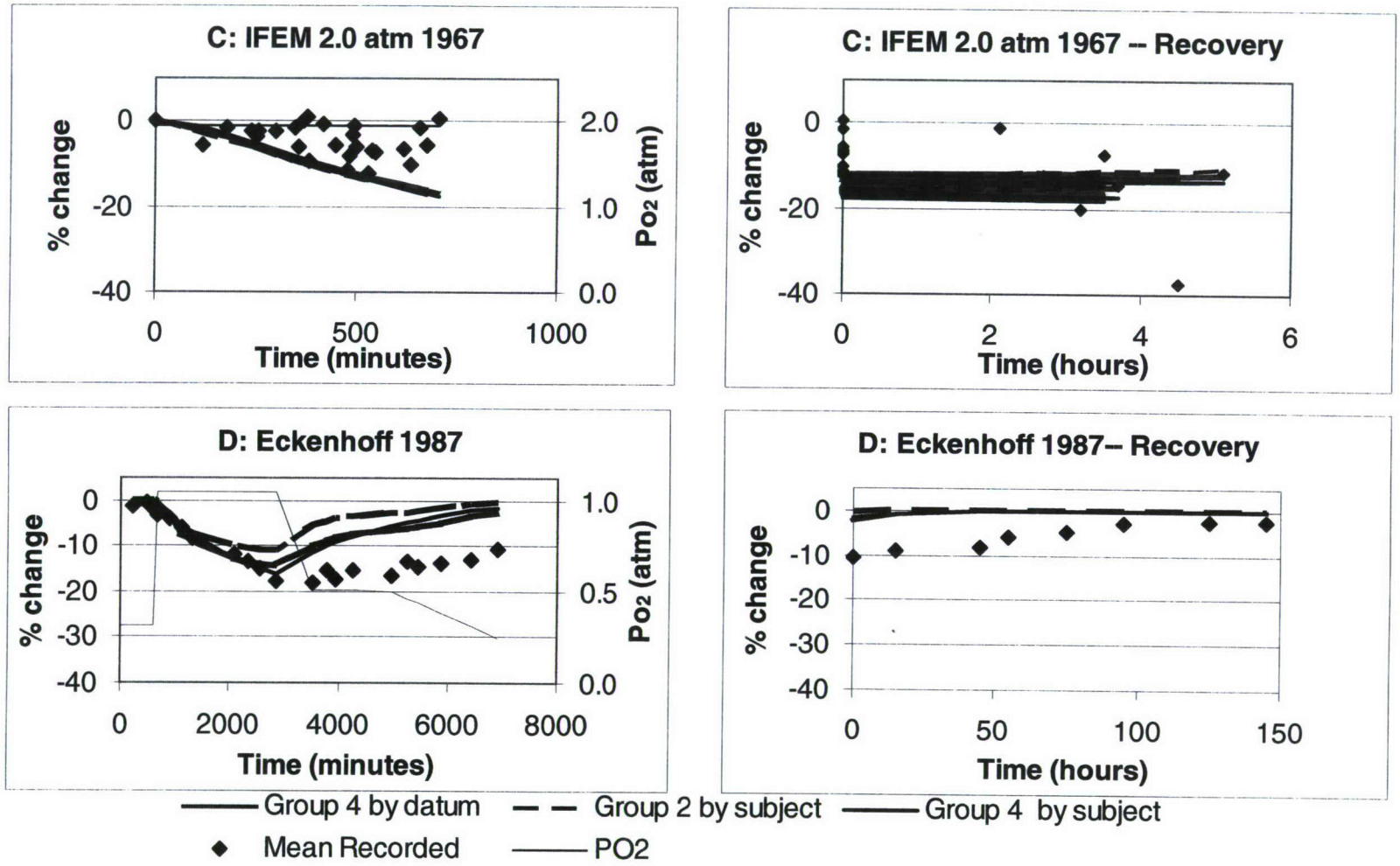

Figure 20 (continued). Injury-Memory Model 8, with three-hour memory. Recovery in room air. Correspondence to data, Experiments C and D.

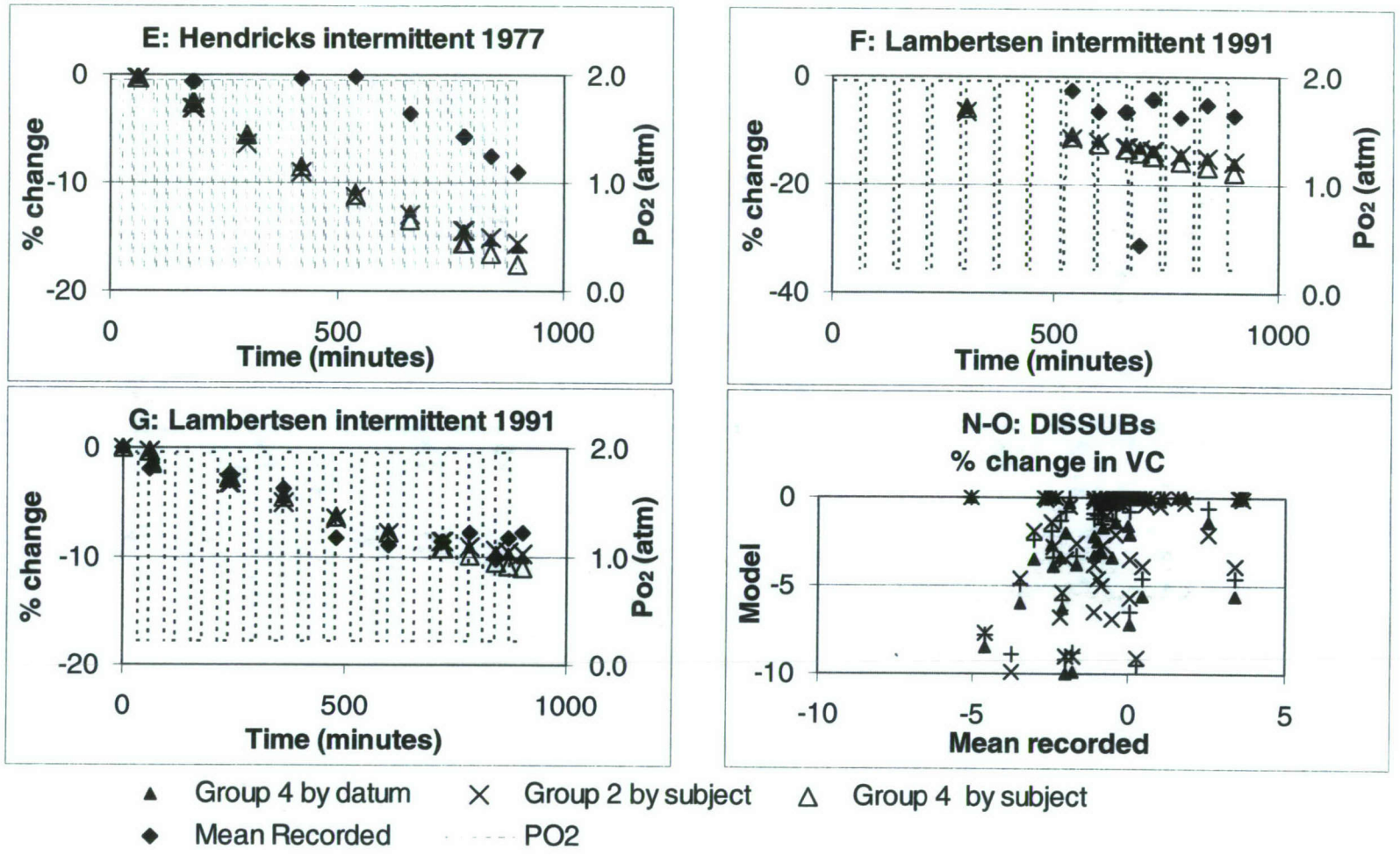

Figure 20 (continued). Injury-Memory Model 8, with three-hour memory.
Correspondence to data, intermittent Experiments E–G, N, and O. The complicated exposures N and O are shown as a correlation plot.

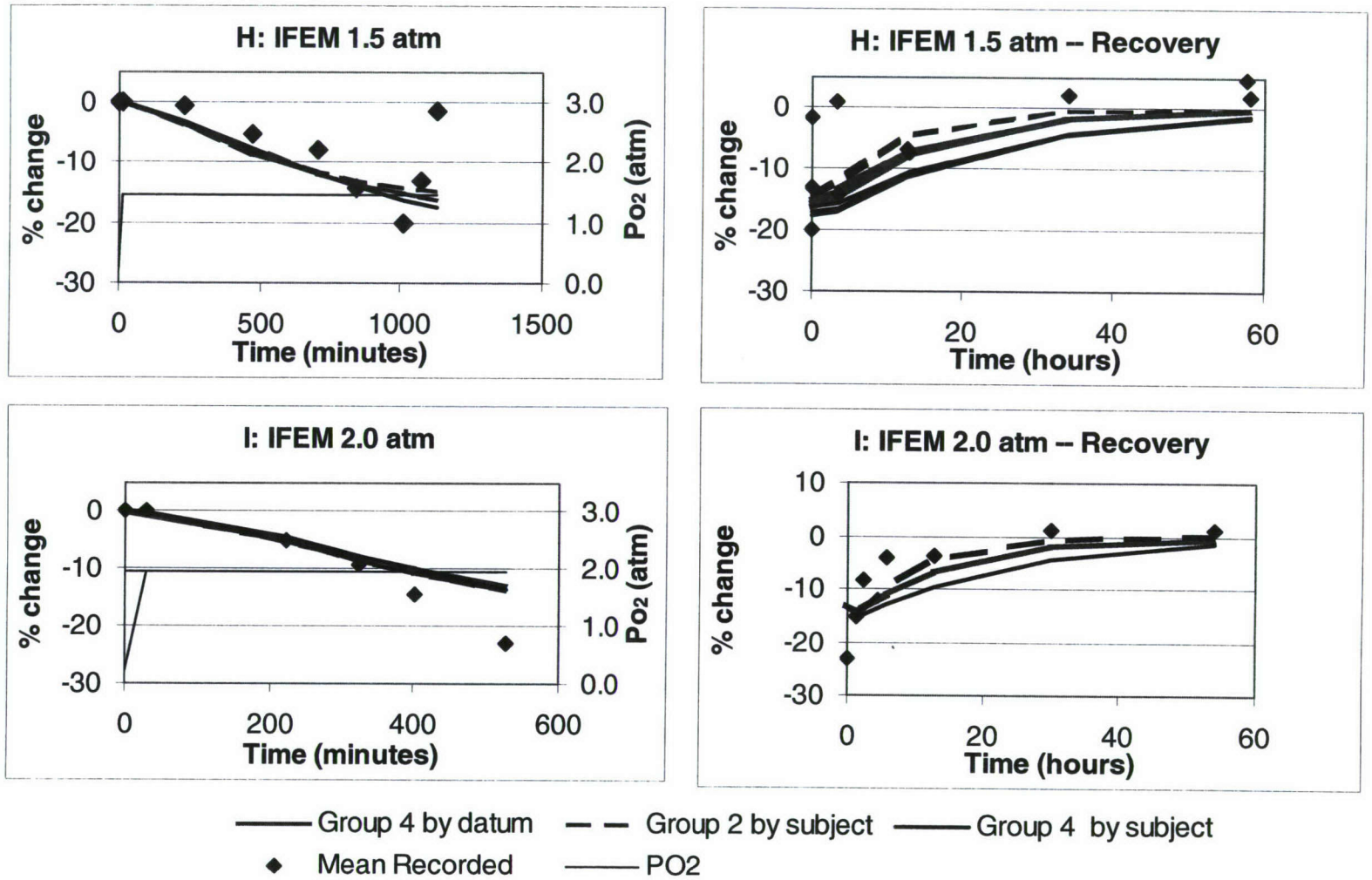

Figure 20 (continued). Injury-Memory Model 8, with three-hour memory. Recovery in room air. Correspondence to data, Experiments H and I.

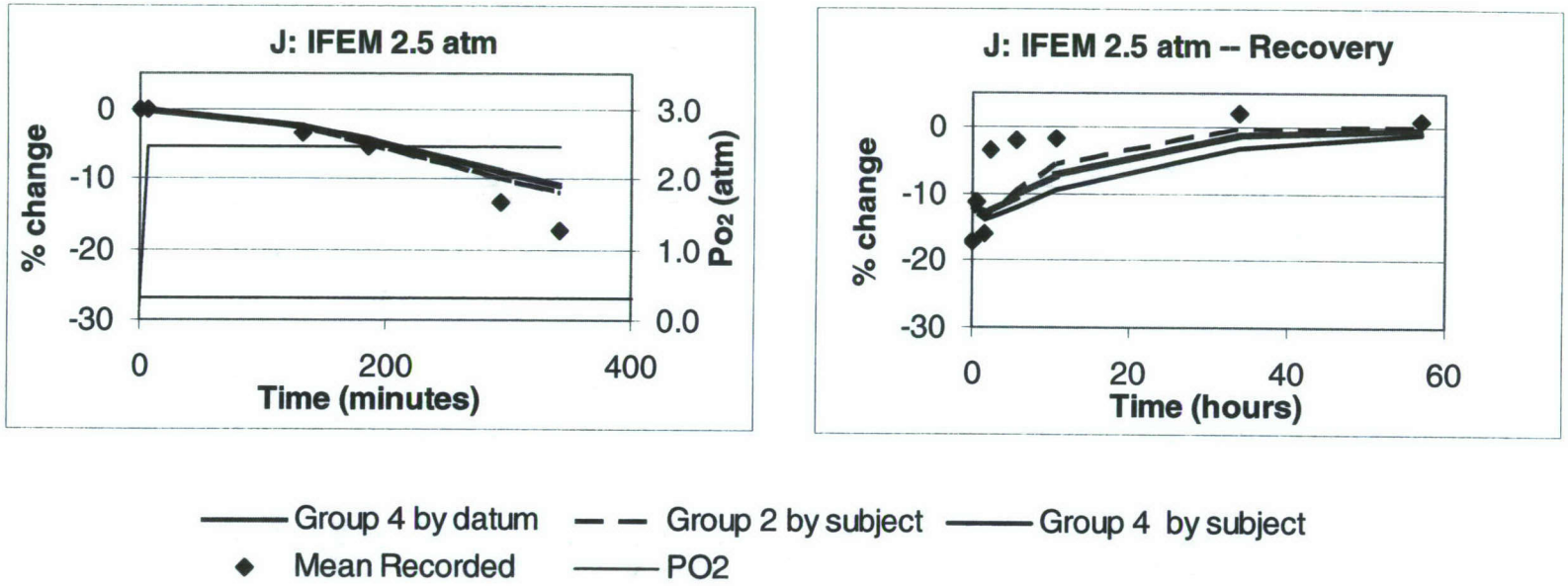

Figure 20 (continued). Injury-Memory Model 8, with three-hour memory. Recovery in room air. Correspondence to data, Experiment J.

Model 9. Delayed Inflammation Model

a. With instantaneous P_{O_2}
b. With average P_{O_2} for a time period
c. With average P_{O_2} but no inflammation

Let τ_{io} = time lag from acute injury to onset of inflammation, and τ_{id} = duration of inflammation.

$$\%\Delta VC = -\alpha \cdot F + K_{inflam} \cdot \Sigma\%\Delta VC\ (\theta),$$

where θ runs from $t - \tau_{io} + \tau_{id}$ to $t - \tau_{io}$ and $K_{inflam} > 0$.

Acute injury is modeled by the proportional rate of healing Model 3a:

$$-\alpha \cdot F = \begin{cases} (a/b) \cdot (P_{O_2} - P_{th}) \cdot [1 - e^{-(b \cdot t)}] + F_0 \cdot e^{-(b \cdot t)}, & P_{O_2} > P_{th} \\ F_0 \cdot e^{-(b \cdot t)}, & P_{O_2} \le P_{th}. \end{cases}$$

In Models 9b and 9c the moving average of P_{O_2} over an arbitrarily selected previous duration — here, the previous five hours (300 minutes) — is used instead of the instantaneous P_{O_2}.

The differences between Model 9 and Model 3a are small; Model 9 does not come significantly closer to the data than does Model 3. An inflammatory component that begins after 8 hours (480 minutes) and lasts for 36 hours (2160 minutes) slightly increases the coefficients of determination r^2 from those for Model 3a (Tables A22 and A23), but the "inflammation" makes only a small difference to the fitted curves (Figures 15 and 21). The inflammatory component does not improve the correlations between the average DISSUB data and the model predictions, correlations with coefficients 0.40 for Models 9a and 0.41 for Model 3a. Overall for Data Group 4 the major effect of the inflammatory component is to increase the magnitude of the exponent of healing b from that fitted to Model 3a (Tables A10 and A22).

Averaging P_{O_2} for 300 minutes has the most effect with short experiments, those for which the averaging time is a significant portion of the oxygen exposure. For the DISSUB data, averaging increases the correlation coefficient slightly, to 0.43 for both Models 9b and 9c.

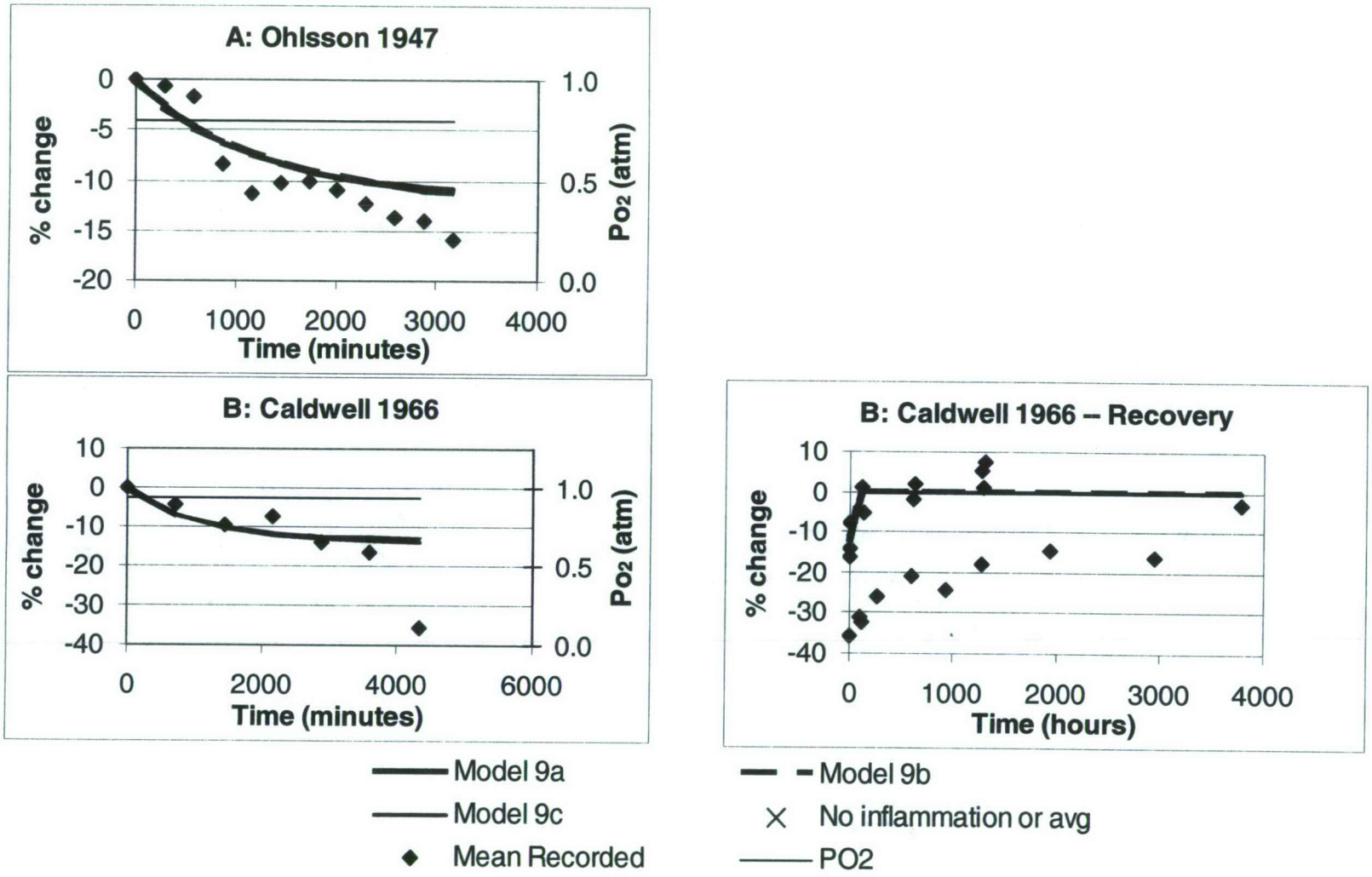

Figure 21. Models 9a–9c, proportional healing models with inflammation. Recovery in room air. Correspondence to data, Experiments A and B.

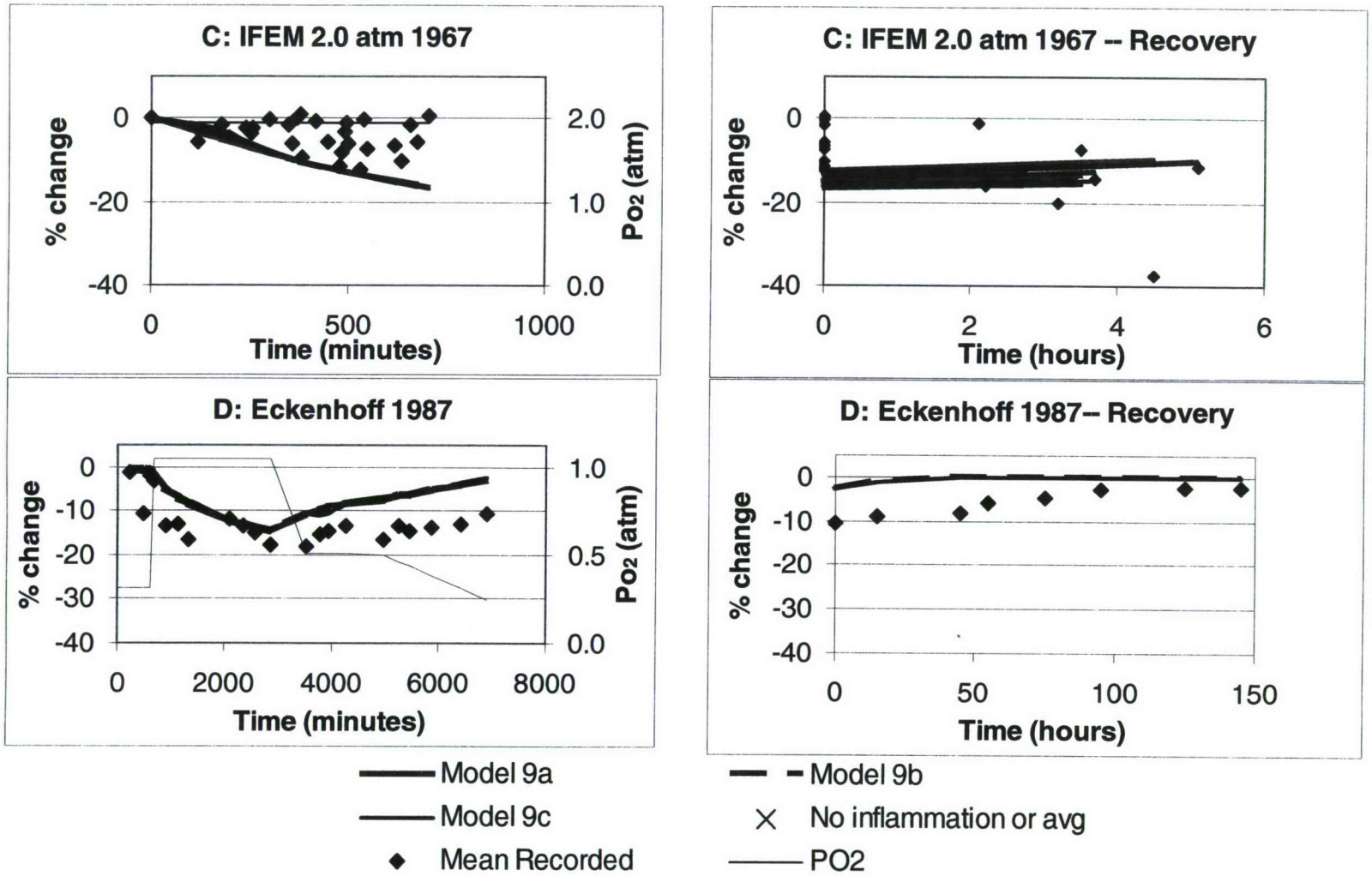

Figure 21 (continued). Models 9a–9c, proportional healing models with inflammation. Recovery in room air. Correspondence to data, Experiments C and D.

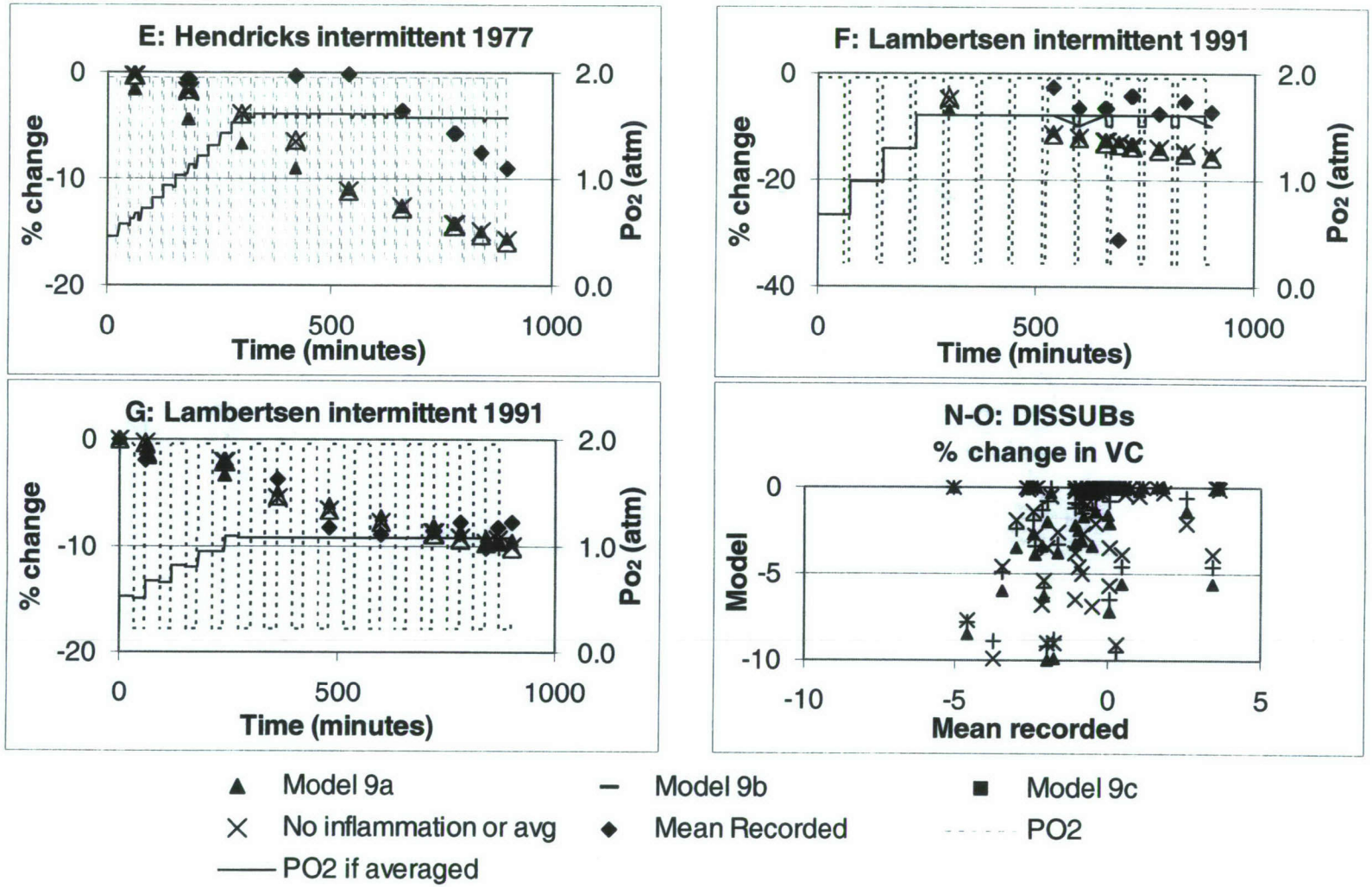

Figure 21 (continued). Models 9a–9c, proportional healing models with inflammation, averaging, or both. Correspondence to intermittent Experiments E–G, N, and O. Experiments N and O are shown as a correlation plot.

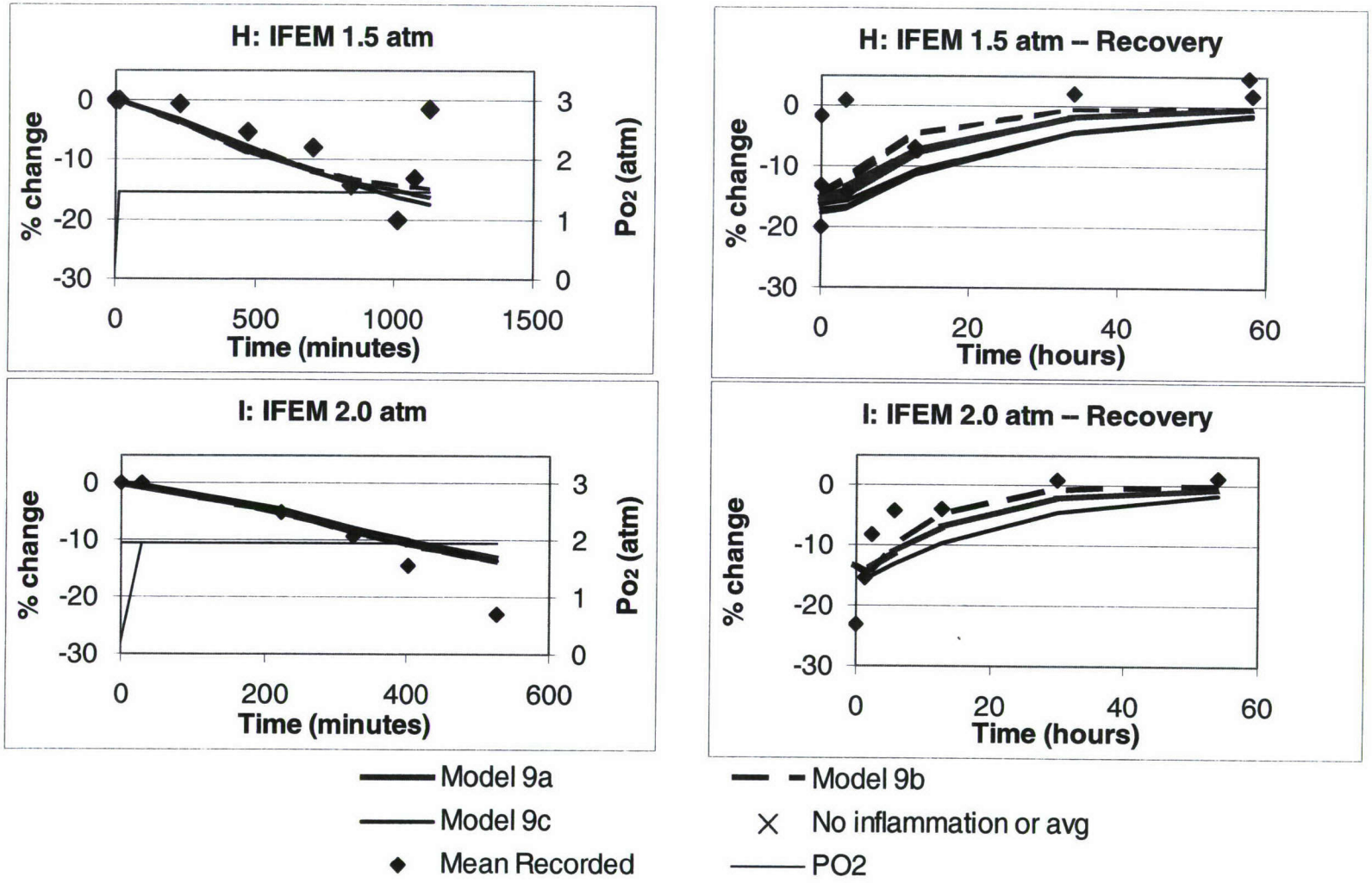

Figure 21 (continued). Models 9a–9c, proportional healing models with inflammation, averaging, or both. Recovery in room air. Correspondence to data, Experiments H and I.

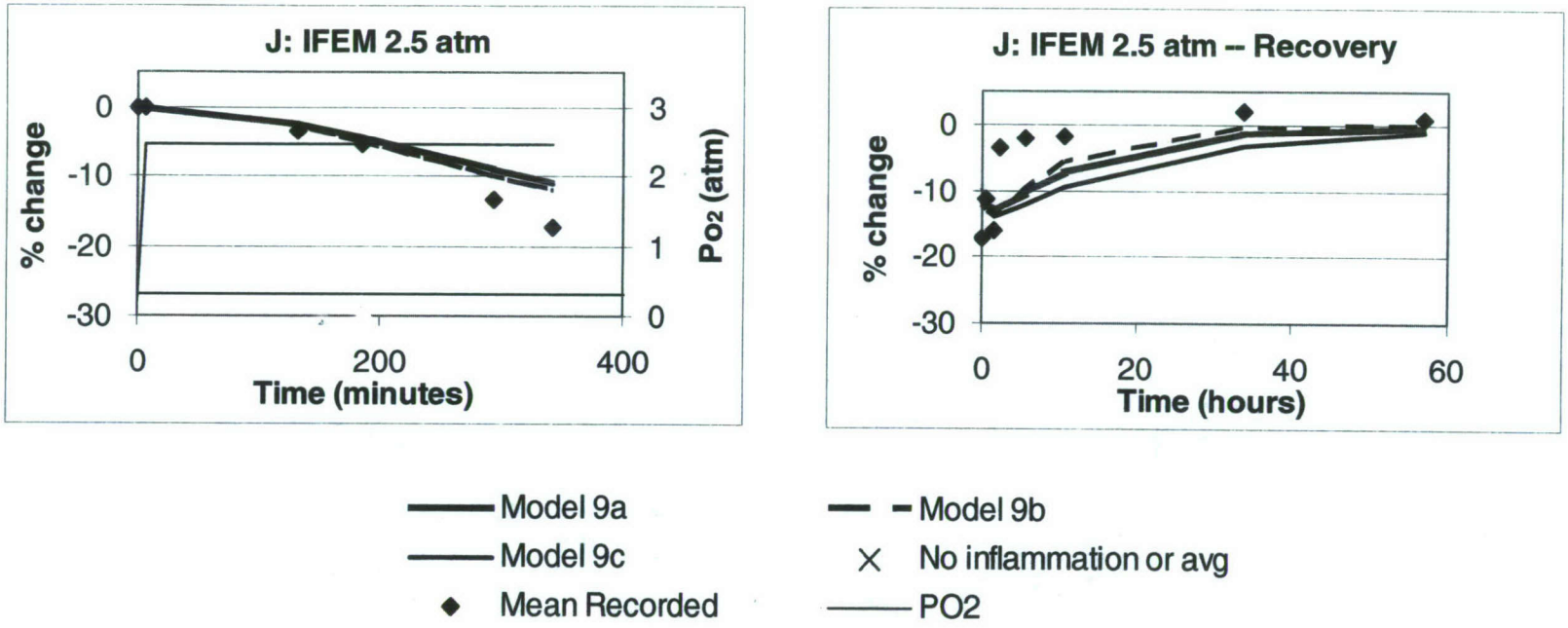

Figure 21 (continued). Models 9a–9c, proportional healing models with inflammation, averaging, or both. Recovery in room air. Correspondence to data, Experiment J.

The average P_{O_2} during the intermittent exposures increases at a rate that depends on the averaging period, and the steady-state P_{O_2} value attained depends on the cycling time of oxygen and air exposures. Models with and without averaging converge once the steady state value has been reached. P_{O_2} values averaged over 300 minutes are shown in panels E–G of Fig. 20 with the corresponding model fits. Although a longer averaging time (600–700 minutes; not shown) improves the fit of Model 9c to the data of Experiments E and F relative to the fits with the 300-minute average, it degrades its fit to all other data except those for Experiment C.

Comparison of Model Fits by Experiment

Tables 5 and 6 summarize goodness of fit by model and experiment — Table 5 for data collected only at elevated P_{O_2}, and Table 6 at elevated P_{O_2} and during early recovery. Parameter values are fitted to the entire data group, but fits are assessed on the basis of individual experiments within the group. Tabulated values are the coefficients of determination (r^2) of the fits for individual experiments expressed as a percentage of the r^2 of the intersubject averages for the same experiment. Values are <1 when the variance of the estimate exceeds that of the data. Note that models may provide good fits numerically but deviate from the data at one end of the curve, a deviation making any extrapolation risky.

We have not found a universal model. Although some models very successfully fit data from some experiments, none matches all data. Experiment C (P_{O_2} = 2 atm) is not described well by any of the proposed models, and the intermittent experiments E–G are described by very few.

When only the elevated P_{O_2} periods are considered (Table 5), the best matches to Experiment A (P_{O_2} = 0.8 atm) are Models 5d and 6a. The closest correspondence to Experiment B (P_{O_2} = 1 atm) is provided by Model 4d, and the best matches to Experiment D (5 atm air) are given by Models 1c and 5e. Experiments H and I (P_{O_2} = 1.5 or 2 atm) are best predicted by Model 4d. Experiment J (P_{O_2} = 2.5 atm) is best matched by Model 5e.

When elevated P_{O_2} periods and early recovery are included (Table 6), the best fit to Experiment B becomes Model 2. Experiment C with recovery, although poorly fitted by all models, is best fit by Model 2. Experiment D including early recovery is matched best by Model 5d. Intermittent exposure Experiment E is well described by Model 5b, which also describes the onset and early recovery data of Experiments H and J. Intermittent exposure Experiment F is poorly fitted by all models, with Model 2a performing least badly. Models 4a, 5a, 5b, and 6a describe Experiment H, including early recovery, equally well. Experiment I is best fitted by Model 4d. Experiment J is best described by Model 5b.

Table 5.
Selected models' goodness of fit for experiments, no recovery, and coefficients of determination as percentages of the coefficients of determination of the average. Fits to Data Group 3 (uninterrupted exposures) without recovery, weighted by data, were used. **Bold** highlights values ≥70%, and gray indicates <33% of the average variance explained.

Exp	Models with full fit No recovery data									
	1c	HL	2a	3b	4d	5a, b	5c	5d	5e	6a (*g*)
A	25%	<0	39%	54%	<0	<0	<0	**75%**	65%	**75%**
B	69%	57%	**71%**	58%	**75%**	<0	27%	68%	51%	27%
C	<0	<0	5%	<0	<0	<0	<0	<0	<0	<0
D	**94%**	58%	**77%**	**93%**	**88%**	59%	59%	**81%**	**94%**	<0
H	**73%**	54%	41%	**74%**	**77%**	**74%**	**75%**	56%	68%	66%
I	54%	<0	<0	53%	**75%**	30%	23%	21%	50%	**70%**
J	24%	23%	<0	**77%**	**91%**	**87%**	65%	**88%**	**98%**	**93%**

Experiment	Models with both fit and grid search No recovery data		
	8	9a	9b
A	50%	62%	62%
B	53%	31%	31%
C	<0	<0	<0
D	61%	31%	41%
H	**75%**	**71%**	**73%**
I	53%	58%	61%
J	66%	**81%**	**72%**

In Models 5a and 5b, accumulated time and averaged P_{O_2} were used.
Model 6a (*g*) is 6a with fitted parameter *g*.

Table 6.
Selected models' goodness of fit for individual experiments, including 8 hours' recovery data. Coefficients of determination are expressed as percentages of the coefficients of determination of the average. Parameters fit to Data Group 4 and weighted by data were used — except for Models 5a, b, and d, where the parameters fit to Data Group 3 without recovery and only those fits to recovery were used. **Bold** highlights values ≥70%, and gray indicates <33% of the average variance explained.

Exp	Models with full fit Recovery times up to 8 hours									
	HL	2a	3b	4a	4d	5a	5b	5d	5f	6a
B	57%	**70%**	58%	48%	52%	<0	<0	68%	50%	58%
C	8%	9%	<0	<0	<0	<0	<0	<0	<0	<0
D	58%	**77%**	**81%**	8%	**89%**	**90%**	60%	**95%**	51%	65%
E	<0	<0	<0	<0	<0	46%	**72%**	63%	<0	<0
F	5%	19%	<0	<0	<0	<0	10%	8%	<0	<0
H	48%	34%	67%	**70%**	69%	**70%**	**70%**	54%	67%	**70%**
I	<0%	<0	44%	44%	**77%**	<0	38%	0	57%	6%
J	26%	<0	37%	63%	56%	31%	**98%**	<0	54%	32%

Exp	Models with both fit and grid search		
	8	9a	9b
A	49%	62%	62%
B	54%	31%	31%
C	<0	<0	<0
D	55%	31%	41%
E	<0	<0	<0
F	<0	<0	<0
H	66%	66%	140%
I	29%	55%	54%
J	<0	60%	12%

In Models 5, accumulated time was used.
In Models 5a, 5b, and 5d, averaged P_{O_2} (120 min) was used.

For descriptions of experimental exposures, see Table 1. For coefficients of determination of the averages of the data, see Table 3.

Model HL refers to the Harabin Linear Vital Capacity Model.[13,21]

Models 8 and 9 include a grid search for one or more parameters; a better "best fit" may exist, but the data are too sparse to allow it to be determined.

Result Summary, by Model

Model 1, the UPTD model (Figs. 2 and 12, Tables A1–A3), fits an almost straight line after a latent period when P_{O_2} is constant and elevated, but many data are curvilinear in time. Although this model explains most of the average variance of Experiment D (Table 5) in which %ΔVC changes almost linearly with time, the fraction of variance explained is low in Experiments I and J where %ΔVC changes with time in a distinctly curvilinear pattern. Differences in performance are slight between the UPTD model with fixed threshold and exponent and the model with all three parameters fitted (Fig. 12), but the exponent varies considerably with the data set (Tables A1–A3). The UPTD model was developed to describe data only at steady, long exposures to one P_{O_2}, and healing is ignored; during intermittent exposures when P_{O_2} is below threshold, the model holds the last value for %ΔVC.

Proportional Model 2 (Figs. 3 and 14, Tables A8 and A9) produces a straight-line fit to injury at constant oxygen exposure and includes slow recovery at P_{O_2} below threshold: with atmospheric air, recovery is about 0.2% per hour with Harabin's linear model parameters[13,21] and about 0.01% per hour with the best fit from our complete data set. Like the UPTD model, the proportional model underestimates later injury when %ΔVC changes in a curvilinear pattern. Only in Experiments B and D is correspondence to data good (Tables 5, 6). Except for Experiment B, where recovery is very slow, the proportional model also fails on recovery; the best-fit parameters for this data set predict a much slower recovery than that seen in Experiments H–J. The proportional model seriously overestimates ΔVC in the complex, intermittent DISSUB experiments N and O. However, the best-fit parameters (Tables A8 and A9) are less sensitive to data set for this model than for Model 1.

Proportional rate of healing Model 3 (Figs. 4 and 15, Tables A10 and A11) is curvilinear in time (concave upward as injury develops; concave downward on recovery) for constant P_{O_2}, and the curvature is similar whether the fit is calculated with (Model 3b) or without (Model 3a) the logarithmic limit. Unfortunately, data during injury development at P_{O_2} of 2.0 and 2.5 atm curve in the opposite direction. Like the UPTD and proportional models, the proportional rate of healing model misses the extremes of %ΔVC in the experiments with P_{O_2} of 2.0 or 2.5 atm although the values of r^2 are high (Table 5) for some experiments without recovery. The proportional healing model overestimates the injury in intermittent exposures during Experiments E, F, and DISSUB Experiments N and O, but it fits well to the 30 min on, 30 min off intermittent exposure of Experiment G. Model 3 correlates with the DISSUB data, but the slope of the correlation line is different from 1 (Figure 15).

The Autocatalytic Models 4 at elevated P_{O_2} are concave upward or downward, depending on P_{O_2} (Figs. 5 and 16, Tables A12 and A13), and are concave downward during recovery. Models 4a and 4b have different autocatalytic thresholds and therefore give differing curvatures for some experiments. Models 4c and 4d allow the duration of exposure to affect the recovery rates. Despite the self-adjusting curvature, Model 4

does not curve as steeply as do the measured responses. During the intermittent exposures, the model overestimates ΔVC in Experiments E, F, and DISSUB N and O, but it underestimates ΔVC in Experiment G. Recovery corresponds better to the data when the function of exposure duration is introduced (4c, 4d) and when separate P_{O_2} thresholds are applied for onset of injury and for onset of healing (4d). Except for Experiments A and C (Table 5), Model 4d corresponds well to data at steady, elevated P_{O_2}. It does not fit as well when early recovery is included (Table 6); a different recovery function may be needed.

The Exponential Models 5 (Figs. 6, 17, and 18, Tables A14–A16) are of two classes at elevated P_{O_2}: those which are quadratic functions of time (Models 5a–5c), and those in which the exponent on time is a function of P_{O_2} (Models 5d–5f). The first group is concave downward with time both during injury development and during recovery, while the curvature in the second group changes with P_{O_2}. In those experiments where the response is nearly linear, Models 5a–5c underestimate ΔVC early in exposure and overestimate them later (Fig. 17, Table 5). The models are also of two types during recovery, with first-order kinetics in Models 5a–5c and 5f, and second-order kinetics in Models 5d and 5e. The first-order kinetics model with rate of recovery as a function of exposure duration or of both recovery P_{O_2} and exposure duration is successful for all the experimental data available. Model 5 describes intermittent exposures, but only when accumulated time at elevated P_{O_2} is used in conjunction with moving-average P_{O_2}.

The Sigmoidal Dose Response Models 6 (Figs. 7 and 19, Tables A17–A20) differ among themselves in part depending on the magnitude of *g*. Only when *g* is fitted does the inflection point of the sigmoid function of *dose* lie in the range of data, but an inflection in the curve as a function of *time* can fall within the measured time period if the dose becomes constant. Model 6a, where the dose in the sigmoidal equation is given by the proportional healing Model 3a, provides a good fit to Experiments B, C, and early H but to no others when parameter $g = 100$. Model 6a also provides a good fit to Experiments H and early I and J when *g* is fitted, but it does not provide a good fit to the intermittent data. Models 6b and 6c — where the dose is integrated P_{O_2} during periods of elevated P_{O_2}, but where healing is depicted as exponential decay of the injury in 6c, — underestimate ΔVC for Experiments A and B. Model 6b underestimates ΔVC in Experiment D in all phases while Model 6c corresponds well at elevated P_{O_2}. Both 6b and 6c underestimate the ΔVC at elevated P_{O_2} in Experiments H–J and recover more slowly than the data, and neither corresponds well to intermittent data. Both 6b and 6c overestimate the injury found in the DISSUB Experiment N and O data.

Model 7, while conceptually interesting, could not be fitted to the data because of the number of parameters.

The Injury-Memory Model 8 with a memory of three hours (Figs. 9 and 20, Table A21) shows continuing injury shortly after P_{O_2} is reduced in Experiments H, I, and J. This model, an integration of Model 3a, better reproduces the curvature at the start of

Experiment J but increasingly underestimates the rate of healing in Experiments H–J. Parameters of the fit were different for different data sets.

The Delayed Inflammation Model 9a (Figs. 10 and 21, Table A22) also is based on Model 3, a proportional rate of healing model. The inflammatory part of the model had little effect. Model 9b, the same model but with an averaged P_{O_2} as one of the independent variables, also produced results similar to those from the model without averaging, as did Model 9c, the proportional healing model with moving averaged P_{O_2}.

Stepwise Linear Regression Results

Stepwise regression analysis indicates that during injury development, the linear relations between %ΔVC and all of P_{O_2}, the previous P_{O_2} the time at the P_{O_2}, and the square of the time at the P_{O_2} are statistically significant, but that the linear relation with total pressure is not significant. During recovery, significant independent variables are P_{O_2}, elapsed time squared, and the duration of the previous exposure to elevated P_{O_2}, but not elapsed time, total pressure, or previous P_{O_2}. No other variables or combinations of variables were presented for inclusion in the possible linear models.

In-water Data — Correlations

Correlation coefficients and regression slopes of predicted ΔVC against measured values after in-water exposures (Table 1, entry P) are presented in Table 7. The models are not predictive for these low average ΔVC.

Table 7.
Correlation coefficients and regression slopes, model predictions vs. wet data

Model	Correlation Coefficient, average response	Correlation Coefficient, all data	Regression, all data	
			Slope	Intercept
Model 1c: UPTD	0.01	0.12	0.07	–3.7
Model 2a: Proportional	–0.10	0.14	0.05	–1.8
Model 3a: Proportional Healing	–0.31	0.08	0.05	–1.9
Model 3b: Proportional Healing with log limit	–0.07	0.07	0.0001	–0.0026
Model 4c: Autocatalytic	–0.20	0.13	0.06	–2.0
Model 5b: Exponential	0.59	0.37	0.11	–0.15
Model 5e: Exponential	0.36	0.23	0.19	–0.04
Model 6c: Sigmoidal	–0.31	0.07	0.03	–1.1
Model 8: Injury-Memory	–0.22	0.12	0.09	–1.7
Model 9a: Inflammation	–0.30	0.08	0.05	–1.8

Effects of Bias toward Experiments Where Each Subject Was Measured More Often

The number of times that VC was measured varied by experiment, a situation that causes those experiments with more frequent measurements in a time interval to have greater influence on the fits than those with less frequent measurements in the same time interval. This bias was removed by weighting the data by the numbers of subjects in each experiment rather than by the number of measurements. Although the fits may differ with the two weightings, weighting by subject does not improve the match to data.

DISCUSSION

Data and Modeling Issues

Data Set Characteristics

The experiments from which these data were gathered span about 53 years and were performed in multiple laboratories using different equipment and possibly different methodologies. Data Group 1 contains the oldest data, those that were available to Harabin *et al.*[13,21] and to Vann,[22] with many measurements having P_{O_2} at or less than 1 atm and only one experiment (Experiment C, Figure 1) at 2 atm. Few measures of acute healing (<8 hours) are included in these data. Data Group 3 experiments comprise the next largest group — containing, in addition to the data from the first group, those from noninterrupted exposures to 1.5, 2, and 2.5 atm of oxygen (Experiments H–J). These data include recovery measurements. Data Group 2 contains data that were available to Arieli et al.:[24–26] those from Data Group 3 plus intermittent exposures to 2 atm oxygen (Experiments E–G). Data Group 4 consists of Data Group 2 and the relatively recent intermittent multiple P_{O_2} DISSUB data, for which only recovery data are available. Data during exposures were generally collected at intervals of several hours, and those during recovery no more than once a day.

The P_{O_2} range of the data is from 0.21 atm to 2.5 atm for long, steady exposures and at levels decreasing from 2.8 atm for some of the intermittent exposures. In brief,

a) Seven experiments, grouped here as K–M, had $P_{O_2} \leq 0.55$ atm. Three of these were at elevated total pressure, one was at atmospheric pressure, and three were at subatmospheric total pressure. Except for a few outliers — notably, data from one subject breathing 0.55 atm P_{O_2} at a total pressure of 0.7 atm — ΔVC in these experiments was distributed equally on either side of zero. These data drove the threshold estimates.
b) Three experiments had P_{O_2} of about 1 atm: Experiments A and B with total pressure of 1 atm and almost 100% oxygen, and Experiment D with total pressure 5 atm and 21% oxygen, and ΔVC appears to be comparable among them (Figure 1).

c) Two experiments, C and I, involved steady exposure to 2 atm P_{O_2}, both with 2 atm total pressure, but Experiment I found much greater ΔVC than did Experiment C.
d) Experiment H was at 1.5 atm P_{O_2}.
e) Experiment J used 2.5 atm P_{O_2}.
f) Experiments N and O include short periods at P_{O_2} as high as 2.8 atm.

Only Experiments D, N, and O included measurements related to more than one elevated P_{O_2}. Experiments E–G, N, and O involved intermittent exposures: E–G to 2 atm P_{O_2} interrupted by normoxic periods, and N and O to oxygen-accelerated decompression profiles of decreasing total pressure with 100% oxygen interrupted by normoxic intervals.

Because none of the models except the UPTD with the classic parameters appears to fit Experiment C (Table 5), we reexamined those data. Final exposure values and some recovery data but not those during exposure have been published in one report.[4] Data collected during exposure are available from two sources: in the recent electronic transcription from Lambertsen et al.,[6] and in print from Harabin et al.[13] Unfortunately, numbers differ slightly among records. Perhaps slow VC is used in some records and forced VC in others; only the electronic record specifies, and it contains slow VC measurements. The report by Harabin et al.[13] includes more frequent measurements than does the electronic version, measurements transcribed by hand from paper records, and it includes two subjects for whom the oxygen exposure was interrupted briefly by diffusion capacity measurements and one subject for whom oxygen exposure was terminated at four hours after only one measurement. The electronic transmission has data for only ten subjects with steady exposure for eight or more hours, and it gives the values during the exposure only until eight hours had elapsed. After eight hours of exposure, the number of subjects decreased as individuals with large ΔVC were withdrawn, and the average ΔVC decreased as the exposure continued.

The Experiment C values used for parameter fitting were those from the electronic transmission[6] for ten subjects, those from the Harabin report[13] for the other two subjects with exposures longer than four hours, and then the recovery data.[4] The censoring of data for subject safety during the experiment makes the fits difficult to compare at the end of the exposure.

Recovery rates were clearly different across exposures and were not a function only of exposure P_{O_2}. Experiments B and D, both with exposures to P_{O_2} near 1 atm, differ in rate of recovery. From slowest to fastest, the order of recovery rates from steady P_{O_2} exposures were those of Experiment B (recovery from 83 hours near 1 atm), Experiment D (48 hours near 1 atm), Experiment H (18 hours at 1.5 atm), Experiment I (9 hours at 2 atm), and Experiment J (6 hours at 2.5 atm). Experiment C is not assessed, because its recovery data are complete for only for the subject who was the slowest to recover.

Modeling Considerations

For data collected during exposure to elevated P_{O_2}, stepwise linear regression indicated that both elapsed time t and t^2 should be included with P_{O_2} in any model. Models 1 and 2 are linear in time, Models 5a–5c use t^2, other Model 5s use exponents of time that are functions of P_{O_2}, and the exponent fit in the testing of proportionality yielded $t^{0.9}$. None of the models presented is binomial in time, and perhaps future attempts could include a model that is. However, Models 5d–5f include a range of time exponents, and Models 3, 4, 6a, 8, and 9 include a term with $(1-e^{-b \cdot t})$. Series expansion yields

$$(1-e^{-b \cdot t}) = b \cdot t - b^2 \cdot t^2/2 + b^3 \cdot t^3/6 + \ldots.$$

When $P_{O_2} > P_a$ in Model 4, the sign on the exponent changes, and the expression becomes

$$(1-e^{+b \cdot t}) = -b \cdot t - b^2 \cdot t^2/2 - b^3 \cdot t^3/6 - \ldots.$$

Neither the term $e^{-b \cdot t}$ nor any higher exponents on time were included as test variables in the stepwise regression.

For data collected during recovery, stepwise linear regression suggested that t^2 but not t itself is included; contributions of higher order terms were not tested. Model 1 has no recovery, Model 2 is linear in time for all P_{O_2}, and Model 6b recovers because the dose decreases. Recovery in Models 5d–5f includes t^{-1}, but all other recovery models include $e^{-b \cdot t}$. Attempts were made to include both a term linear in time and an exponential decay, but confidence on the separate first-order coefficient was low, and the linear term was dropped. However, if t is sufficiently large, the first-order term of the exponential expansion can become negligible as compared to the second-order term.

For data collected during recovery, stepwise regression also included duration of previous exposure, as included in some of the recovery models, but not previous P_{O_2}, a variable included in Model 5c. By chance, in Experiments D and H–J previous P_{O_2} is inversely related to the duration of the previous exposure.

Problems of the Approach

Data are serially correlated for any experiment where subjects are measured more than once and a change from baseline is used. Each subsequent value for a subject includes all preceding values: the more measurements that are made, the more influence the early changes have on the fit. Although serial correlation could be avoided by fitting stepwise ΔVC, that approach severely degrades the effective signal-to-noise ratio. Data also could be weighted progressively, with the weighting factor inversely related to the number of data at later times and for the same individual. We settled for being aware that the early measurements have more influence on the data fits than the late ones, while the late ones generally have more leverage because changes are greater.

With the same number of subjects, when each VC measurement is given the same weight, experiments with more measurement sessions for each subject count more heavily than those with fewer. The parameters presented in this report as "weighted by datum" are biased toward the experiments with more frequent measurements. Those reported as "weighted by subject" have been corrected for this effect, but not without introducing a different bias; the weighting is equal for experiments with the same number of measurements per subject independent of the length of the study. Parameters from fits with weighting by subject thus deemphasize longer exposures. However, fits with the different weightings were similar.

We assessed fits to exposure data alone, to exposure and 8-hours recovery, and to exposure and all recovery. Recovery by itself was assessed only for Exponential Model 5. The choice of eight hours duration for early recovery was entirely arbitrary.

Models

The temptation is strong to try to match a model to a putative mechanism, and many of the models described in this report have been explained in terms of chemical kinetics. However, the multiple biological factors of oxygen injury — briefly described in the next section — complicate any mechanistic approach. Any chemical kinetics suggested by a model is approximate at best.

Biological Factors in Pulmonary Oxygen Toxicity

Oxygen and Free Radicals

Free radical reactions are a normal part of oxygen metabolism. Since free radicals are defined as molecules with at least one unpaired electron in the outer shell, oxygen itself is a free radical. Each molecule of oxygen accepts four electrons before it is reduced to water during oxidative energy production, and highly reactive intermediate products, any of which can damage tissue, may be produced in the process. Antioxidant enzymes normally control the concentrations of ROS.

While high P_{O_2} generally means increased free radical concentration, not all the pathways of free-radical formation are sensitive to P_{O_2}.[30] Furthermore, multiple kinetic expressions relate the concentrations of different oxygen-related reactive species to P_{O_2}; after molecular oxygen traps an electron to form a superoxide ion, O_2^-, many other species may form. A superoxide ion may convert rapidly to hydrogen peroxide (H_2O_2) in the presence of superoxide dismutase (SOD), may react rapidly with the sparsely present free radical nitric oxide (NO), or may react with water to produce H_2O_2. Hydrogen peroxide can cross cell membranes and, in the presence of metallic ions such as iron, release very toxic hydroxyl ions, OH^-.

If the concentration of oxygen free radicals increases, reactive species can cause direct oxidative damage to lipids, proteins, deoxyribonucleic acid (DNA), or lung surfactant.

ROS also have other, more insidious effects. They can alter enzyme activity by changing the configuration of enzyme proteins, and they are normally involved in inter- and intracellular signaling.[32] For example, oxygen free radicals can block NO-dependent vasodilation; increase lung permeability; limit cell growth, proliferation, and transformation; initiate cellular self-destruction; or, under other circumstances, promote cell proliferation. Increased concentrations of oxygen radicals may limit the expression of genes for antioxidants,[32] but an increase in production of antioxidant enzymes has been observed in rats after three days of oxygen exposure.[29] Different ROS effects may even dominate under differing experimental conditions or for various individuals. Furthermore, indirect effects such as absorption atelectasis following surfactant depletion or an alteration of the sympathetic nervous system or of adrenal hormone control can result.[28]

Inflammatory Injury

ROS-induced injury may trigger inflammation through the response to cellular damage. Also, ROS signal the inflammatory response and contribute to it in multiple ways.[33] For example, superoxide ions interact with extracellular fluid to activate neutrophils, and hydrogen peroxide elicits the release of platelet activating factors from the endothelium and stimulates the synthesis and mobilization of leukocyte adhesion molecules.[33]

A few hours after an inflammatory stimulus has ended, leukocyte adhesion and migration usually stop. Leukocyte clearance from tissue has a half-time of about twelve hours but sometimes causes the release of more inflammatory mediators, prolonging the recovery.[34] Late effects are also known: for example, investigators injecting a bolus of vascular endothelial growth factor into tissue observed an increase in permeability to water that started half a minute later and lasted less than two minutes but recurred two days later with a duration of two days.[32]

Vital Capacity as an Index of Lung Injury

Because the dependent variable for these models is ΔVC, the kinetics of the models should not be expected to indicate the kinetics of ROS production. Decreases in VC, which can occur for a variety of reasons, reflect a summation of regional injury, inflammatory responses, and compensatory mechanisms.

VC decreases if potential alveolar air space is reduced by vascular engorgement, interstitial edema, or alveolar edema. Engorgement is generally transient, is likely eliminated by VC maneuvers, and is not evidence of injury. Interstitial edema can decrease VC by less than 50 mL (less than 2%), because interstitial membrane thickness can increase by no more than 15% to 20%.[35] Thus, repeated measurable ΔVC can be expected only from alveolar edema, airway closure, or atelectasis.

Alveolar edema occurs when lymphatic drainage is overwhelmed by the inflow from leaky capillaries. Because lymphatic drainage can increase ten- to fifteenfold in the face of increased membrane permeability,[35] early or small increases in permeability will not

reduce VC, and kinetics of increased ROS production are unlikely to be evident in the kinetics of ΔVC. The rate of VC recovery after alveolar edema is most likely to reflect the rate of reduction of inappropriate membrane permeability, with the maximum recovery rate equal to that of lymphatic drainage.

VC decreases also if airways or alveoli close. Alveolar atelectasis occurs if no non-absorbable gas is present and local absorption of oxygen into the blood exceeds local ventilation. If local ventilation is low only because of regional heterogeneity in ventilation, in the presence of adequate lung surfactant, maximal inspiratory efforts associated with VC measurement will inflate atelectic regions. However, if excessive secretions are present in small airways — for example, because ciliary action has been disrupted — small airways may remain closed. Even if airways are not plugged, VC may remain low if surfactant has been degraded. The rate of VC reduction because of small airway obstruction or collapse thus will be related to rates of degradation of mucociliary clearance and of surfactant production by ROS. The rate of recovery will depend on the rates of recovery of ciliary function and of surfactant production. Additionally, bronchoconstriction could occur during oxygen exposure because of bronchiolar smooth muscle reactivity to ROS or because of later C-fiber stimulation by inflammatory mediators. The rates of onset and recovery depend on the rates of generation and clearance of the causative agents.

Variability

Responses to oxygen stimuli show enormous biological variation,[28] and the average response, the target for the model, may differ widely from that of any individual. Some variability could be environmental. Although prior exposure to elevated P_{O_2} can be controlled by experimenters, individuals are always exposed to varying concentrations of ozone, carbon monoxide (CO), and other inspired oxidizing agents. After hyperbaric oxygenation, concentrations of antioxidant enzymes in animal lungs have been seen to increase[29,30] and, after exposure to high P_{O_2}, to remain elevated for 72 hours.[30] CO in breathing gas has been found to protect rats from hyperoxic lung injury.[31]

Whatever its sources, the variance of this data set is large but known. If one assumes that the scatter is normally distributed around the mean and is independent of P_{O_2} and other experimental conditions, a first estimate of prediction interval is given by the Student's t-statistic for the selected percentile multiplied by the square root of the residual variance. For example, for Data Group 3 at elevated P_{O_2}, the residual standard deviation around the intersubject average is 7.44, and that around Model 5e is 8.08. The 95% prediction limits are approximately ±14.6 around the intersubject mean and ±15.8% around the modeled value, and the decrement in VC that is expected for at most 10% of the population is the model value minus 10.3 (standard deviation multiplied by the one-sided Student's t-value for $\alpha = 0.1$, n large). For a better estimate of the prediction interval, the residual variance is supplemented by the model variance at the P_{O_2} and exposure duration of interest.

Week-to-week or even day-to-day variability of VC measurements is also moderately large. The lower 95% confidence interval around normal, as defined at NEDU,[17] was not reached on the average in the experimental exposures until about 500 min at P_{O_2} = 1 or 1.5 atm, until after 250 to 400 min at P_{O_2} = 2 atm, until after 200 min at P_{O_2} = 2.5 atm, and until 500 to 700 min during the intermittent exposures to P_{O_2} = 2 atm. The models of the average responses thus cannot be expected to provide information in those ranges. However, prediction intervals about those average responses can provide estimates of the maximum number of subjects expected to experience measurable decrements in VC.

Acute Injury Models: Development of Injury

Model 1: UPTD Model

The UPTD model simply seeks to describe exposure data. The initial analysis was done graphically on a logarithmic scale for exposures to P_{O_2} levels of 0.83, 0.98, and 2 atm (Experiments A, B, and C). For those data the model is descriptive, but its predictions deviate from the data of Experiments E–J (Fig. 12).

Clark and Lambertsen[3] found that for any chosen %ΔVC,

$$t^{-m} \cdot (P_{O_2} - P_{th}) = \text{constant}.$$

This describes a family of P_{O_2} curves graphed against time, one curve (different constant) for each %ΔVC. The authors defined the point on each curve at P_{O_2} = 1 atm to be a reference point and designated the time coordinate as t^*. To cancel the units of measurement before taking the logarithms, they divided by the equation

$$t^{*-m} \cdot (1 - \text{threshold}) = \text{constant}.$$

Thus,

$$(t / t^*)^{-m} \cdot (P_{O_2} - P_{th}) / (1\ \text{atm} - P_{th}) = 1,$$

and

$$-m \cdot \ln t + \ln(P_{O_2} - P_{th}) = -m \cdot \ln(t^*) + \ln(1\ \text{atm} - P_{th}),$$

where ln is the natural logarithm.

P_{th} was set at half an atmosphere, because multiple subjects previously had been exposed to P_{O_2} of half an atmosphere for long periods without experiencing pulmonary problems.[27] Fitting by eye, Clark and Lambertsen[3] determined that the exponent m was 1.2. However, the relationship is more complicated than can be determined fully by graphic analysis: if one examines his log–log plot, the data points for each VC isopleth

deviate from straight lines with the same pattern and show a slope more negative than –1.2 at low P_{O_2}.

Bardin and Lambertsen[19] and Wright[20] express the %ΔVC isopleths numerically, in terms of t^* above. When m is 1.2 (thus, m^{-1} is 0.833) and P_{th} is 0.5 atm, they named t^* the UPTD and expressed it in minutes. One UPTD is purported to cause the same average decrement in VC as one minute with P_{O_2} of 1 atm.

From the logarithmic equation immediately above,

$$\ln t^* = (-1 / m) \cdot \ln[(1 \text{ atm} - P_{th}) / (P_{O_2} - P_{th})] + \ln t,$$

and

$$t^* = t \cdot [(P_{O_2} \text{ atm} - P_{th}) / (1 \text{ atm} - P_{th})]^{1/m}$$

while

$$\text{UPTD} = t \cdot [(P_{O_2} - 0.5) / (0.5)]^{0.833}$$

$$= 1.78 \cdot t \cdot (P_{O_2} - 0.5)^{0.833},$$

with P_{O_2} expressed in atm and t in minutes.

The relation between UPTD and %ΔVC was given as tabular data.[13,18,20] By linear regression of these,

$$\%\Delta VC = -0.011 \cdot \text{UPTD} + 5.6, \quad r^2 = 0.9929$$

or

$$\%\Delta VC = -2 \cdot 10^{-6} \cdot \text{UPTD}^2 - 0.006 \cdot \text{UPTD} + 2.5, \quad r^2 = 0.9998.$$

We elected to use the first-order relation, $\%\Delta VC = a \cdot \text{UPTD} + c$.

With the definition of UPTD given above — that is, with the fixed exponent and threshold — we found a, depending on the data set, to be between –0.005 and –0.006 (Table A1) and c to be between –1.0 and –1.6. In no case was the intercept c greater than zero. When we fitted all parameters, we concurred with a threshold of 0.5 atm for all data sets (Table A3). However, we found that the exponent of P_{O_2} — that is, $1/m$ — differed from 0.833. The exponent had the value 0.5 with Data Group 1, in which many values at low P_{O_2} are included, and 1.1 to 1.2 with Data Groups 2 and 3, which include higher P_{O_2} exposures (Tables A2 and A3). The number from the smaller data set suggests a steeper log–log plot line than Clark found,[3] while those from the larger data sets predict plots less steep.

The disparities could have several causes:

(1) Clark weighted the data obtained at 2 atm more heavily than the others — clearly a correct decision to pull the exponent toward values found with larger numbers of high P_{O_2} data.
(2) Because he used a logarithmic transformation, Clark was forced to censor data at the lowest P_{O_2} values, where VC sometimes increases during exposures.
(3) From Experiment C we used electronically compiled data[6] rather than tabulated data used by Harabin et al.,[16] although we included the two subjects missing from the electronic record. The electronic record has fewer time points than the paper record, and we do not know exactly which data were included in the original fit.
(4) Both the use of a logarithmic transform and the fit of m instead of $1/m$ produce different minimization criteria from that which results from fitting $1/m$ without transforming the data.

However, as Harabin et al.[13,21] demonstrated, the effect of an exponent different from 1 is very slight in the range of most of these data (Fig. 2). For partial pressures near 1.5 atm, the estimate of %ΔVC is insensitive to the exact value of the exponent when a threshold of 0.5 atm is subtracted from P_{O_2}. At partial pressures higher than 1.5 atm, small differences in the exponent have increased effect.

The UPTD model remains one of those used frequently to estimate pulmonary effects of oxygen. Although it does provide an estimate of average ΔVC as a function of exposure duration for a single exposure to elevated P_{O_2} near 1 atm, it fails to match the curvature with time at higher P_{O_2}, and, as the original authors recognized, it overestimates ΔVC if oxygen exposure is intermittent.

Model 2: Proportional Model

Harabin et al.[13,21] began with Clark and Lambertsen's concept that, for a particular decrement in VC, the plot of P_{O_2} against exposure time is nearly a rectangular hyperbola.[3,13] They proposed that the exponent of time might differ from unity and that time might have an offset. This they expressed as

$$\%\Delta VC = a \cdot (P_{O_2} - P_{th}) \cdot (t - t_{th})^c.$$

This expression differs from that for the UPTD model given in the preceding paragraphs, where the exponent different from 1 is on the P_{O_2} term. (The variable c is used for the exponent for consistency with the discussion that follows.)

We began with the still more general case,

$$\%\Delta VC = a \cdot (P_{O_2} - P_{th})^b \cdot (t - t_{th})^c + (\%\Delta VC)_0, \qquad P_{O_2} > P_{th}.$$

This model, like that of Harabin et al.,[13,21] was equivalent to the proportional model when we used Data Set 1, the data that were available to those authors; b and c were within one standard error of unity, and t_{th} was set to zero (Table A4). However, when additional data (Data Set 3) at P_{O_2} higher than those available to Harabin et al. were included, the exponent b was two standard errors greater than unity.

When the model was fitted with fixed exponent $c = 1$, P_{th} increased, an increase causing fewer data to be used, and the exponent b decreased in magnitude to become similar to that for the UPTD models (Tables A3 and A5), more than two standard errors from 1 for Data Group1, and 1.25 standard errors greater than 1 for Data Set 3. When the model was fitted with fixed $b = 1$, as had been done by Harabin et al., exponent c was 1.5 standard errors less than 1 (Table A6). The differences in exponents from unity are real but have little effect in the range of data available (Figure 13).

The mechanistic interpretation of the differential form of the proportional model is that the rate of destruction for reactive species is constant, independent of P_{O_2}, while the rate of generation depends directly on P_{O_2}. Thus, the concentration of reactive species increases linearly with time once the rate of removal is swamped by the rate of generation, and it decreases linearly with time if the P_{O_2} is less than threshold. However, as indicated in the *Biological Factors in Pulmonary Oxygen Toxicity* subsection, the biochemistry of oxygen toxicity is much more complex than this interpretation allows.

Harabin et al.[13,21] found the best proportional model fit to their data with

$$a = -0.009 \text{ (atm} \cdot \text{min)}^{-1} = -1.2 \cdot 10^{-5} \text{ (Torr} \cdot \text{min)}^{-1},$$
inspired $P_{th} = 0.38$ atm or 289 Torr,

and a fit almost as good with

$$a = -0.011 \text{ (atm} \cdot \text{min)}^{-1} = -1.45 \cdot 10^{-5} \text{ (Torr} \cdot \text{min)}^{-1},$$
and a fixed inspired partial pressure threshold $P_{th} = 0.5$ atm = 380 Torr,

a widely used set of parameters to which we have referred (Fig. 13, Table A15) as the Harabin Linear VC Model.

Vann[22] fitted this proportional model with a larger data set than that used by Harabin and found that

$$a = -0.0024 \text{ (atm} \cdot \text{min)}^{-1} = -3.2 \cdot 10^{-6} \text{ (Torr} \cdot \text{min)}^{-1}$$

and inspired $P_{th} = 0.28$ atm = 213 Torr.

The values we fitted, intermediate between those of Harabin and those of Vann, are listed in Table A7; for Data Group 4 and up to eight hours' recovery, we found

$$a = -0.007 \text{ (atm} \cdot \text{min)}^{-1} = -9.2 \cdot 10^{-6} \text{ (Torr} \cdot \text{min)}^{-1},$$

and alveolar P_{th} = 0.16 atm = 121 Torr; that is, inspired P_{th} = 0.27 atm if $F_IO_2 = 1$.

Although the proportional model is still used to predict decrements in VC, it does not describe the data (Fig. 14), and we cannot recommend its use. Experiments conducted since the model was first proposed demonstrate strongly curvilinear responses with increasing time, while the proportional model is a straight-line model.

Vann also fitted the proportional model with an addition.[22] Because %ΔVC cannot decrease by more than 100%, he chose to limit the value with the function:

$$\%\Delta VC = -100\ (1 - base^{-F}).$$

In Model 2b, the parameter *base* was fixed at 1.005, as Vann had determined. He found

$$a = 0.021 \text{ (atm} \cdot \text{min)}^{-1} = 2.8 \cdot 10^{-5} \text{ (Torr} \cdot \text{min)}^{-1},$$

and inspired P_{th} = 0.41 atm = 312 Torr, where the values we found (Table A8) changed between Data Group 1 — where most data were obtained at $P_{O_2} \leq 1$ atm — and the data groups with data obtained at 1.2 to 2.5 atm. For Data Group 4 and all recovery data, we found

$$a = 2.1 \cdot 10^{-5} \text{ (Torr} \cdot \text{min)}^{-1} = 0.016 \text{ (atm} \cdot \text{min)}^{-1},$$

and alveolar P_{th} = 129 Torr = 0.17 atm , or inspired P_{th} = 0.28 atm if $F_IO_2 = 1$.

Model 3: Proportional Rate of Healing Model

If we assume reactive species are produced at a rate proportional to the elevation of P_{O_2} above a threshold and are eliminated at a rate proportional to their concentration, we have a proportional rate of healing model in differential form. No ROS are generated when P_{O_2} is below threshold. Concentrations of ROS, and thus ΔVC, approach steady state after long times (Fig. 4). Vann[22] proposed this formulation in part as a mechanistic model. Although the complexity of the biochemistry (see *Biological Factors in Pulmonary Oxygen Toxicity*) makes the explanation unlikely in general, the model is also descriptive in the ranges discussed below.

The parameters Vann[22] obtained were, for Model 3a (not log limited),

$$a = 0.009 \text{ (atm} \cdot \text{min)}^{-1} = 1.2 \cdot 10^{-5} \text{ (Torr} \cdot \text{min)}^{-1},$$
$$b = 3.1 \cdot 10^{-4}\ \text{min}^{-1}, \text{ and}$$

inspired P_{th} = 0.17 atm = 130 Torr.

For Model 3b (log limited), the parameters were

$a = 0.021$ (atm · min)$^{-1} = 2.7 \cdot 10^{-5}$ (Torr · min)$^{-1}$,
$b = -2.8 \cdot 10^{-7}$ min^{-1}, and
inspired P_{th} = 0.41 atm = 312 Torr.

Parameter *b* has different signs given here for the different versions of the model in Vann's report. Our values (Tables A10 and A11) are slightly higher than Vann's for parameters *a* and *b* and yield different P_{th} values depending on the range of P_{O_2} in the data group. We do not change sign on parameter *b*.

With Data Group 1 and no recovery, for Model 3a we found

$a = 1.5 \cdot 10^{-5}$ (Torr · min)$^{-1} = 0.011$ (atm · min)$^{-1}$,
$b = 2.0 \cdot 10^{-4}$ min^{-1}, and
alveolar P_{th} = 170 Torr = 0.22 atm; inspired P_{th} = 0.33 atm if $F_IO_2 = 1$.

And for Model 3b we found

$a = 3.2 \cdot 10^{-5}$ (Torr · min)$^{-1} = 0.024$ (atm · min)$^{-1}$,
$b = 2.0 \cdot 10^{-4}$ min^{-1}, and
alveolar P_{th} = 170 Torr = 0.22 atm ; inspired P_{th} = 0.33 atm if $F_IO_2 = 1$.

The proportional rate of healing model predicts a rapid initial ΔVC, which then attains a steady state. This is opposite to the direction of curvature seen in Experiments H–J (Fig. 15). However, because this model matches early data moderately well, it is one of the more successful at accounting for overall variance (Table 4). It also provides relatively high correlation coefficients with the DISSUB data, where each step of the exposure is short.

Model 4: Autocatalytic Models

To attempt to explain the increasingly rapid loss in VC with time at high P_{O_2} we employed an autocatalytic model similar to one proposed by Harabin et al. in another context.[23] A steady-state balance between increasing injury and repair can be attained relatively rapidly at low P_{O_2} and more slowly at an increased P_{O_2} until, for Model 4a fitted to the data, if alveolar P_{O_2} is greater than 1000 Torr, injury increases exponentially with time. This model has the appealing feature that both concave up and concave down patterns can be obtained (Figure 5). However, it does not correspond well to the data (Figure 16). In Model 4b we based our attempt to fix the autocatalytic threshold on curvature of the time traces of different experiments; in Model 4a the precision of the threshold estimate is not high (Table A12). However, improvements in fit were slight (Figure 16). We also tried some modifications in which duration of exposure was

included (Table A13) with some success (Table 6). The introduction of a "dead zone" between the threshold for injury development and that for recovery (Model 4d) improved the fit to Experiment D.

Model 5: Exponential Models

Plots of the data (Fig. 1) show that the decrease in VC with time at constant P_{O_2} ≥1.5 atm is curvilinear and concave down. The exponential Models 5 (Figure 17) match these characteristics by using a time term raised to an exponent.

Arieli[24–26] proposed that injury is proportional to the square of exposure time multiplied by normalized P_{O_2} raised to an exponent, where the exponent of P_{O_2} is a parameter and normalized P_{O_2} is numerically equivalent to P_{O_2} expressed in atmospheres.

$$\%\Delta VC = -a \cdot P_{O_2}{}^{b} \cdot t^2, \qquad P_{O_2} > P_{th}$$

The quadratic function of time was derived from data but was considered to correspond to the expression for the rate of production of hydrogen peroxide.[24,26] This proposed mechanism, like the others already discussed, is an oversimplification (see *Biological Factors in Pulmonary Oxygen Toxicity*), but the model does describe the data at P_{O_2} ≥1.5 atm.

For injury development, Arieli found a P_{O_2} exponent of 4.6, while in Model 5a we fitted values between 2.7 and 4.0, depending on the data group. The multiplier fitted by Arieli was $-2.3 \cdot 10^{-6}$ min^{-2}, as compared to our value of $-2.7 \cdot 10^{-6}$ min^{-2}. These differences may result from using slightly different data sets. More likely, they result from using different weighting and techniques of optimization: we used nonlinear regression, while the other authors transformed the data and used linear techniques.

Subtraction of a threshold in Model 5c caused the exponent on P_{O_2} to decrease to a range of 1.4 to 2.6, but it also slightly decreased the coefficient of determination r^2 (Tables A14 and A15).

Most of the available data are from P_{O_2} values near 1 atm and thus do not strongly steer the fit of the exponent. Because a small change in exponent causes a large change in predicted %ΔVC (Figure 6), extrapolating this model to P_{O_2} higher than 1 atm would be unwise; the difference in exponent from 4.3 to 4.6 represents a 13% difference in predicted %ΔVC if P_{O_2} = 1.5 atm and a 23% difference if P_{O_2} = 2 atm.

Figure 17 shows that the data of Experiments A, B, and D, where the P_{O_2} is approximately 1 atm, are more linear in time than is predicted by Model 5a or 5b. In response to this observation, we tested an alternative exponential model, Model 5d:

$$\%\Delta VC = -a \cdot P_{O_2}{}^{b} \cdot t^{P_{O_2}} + (\%\Delta VC)_0, \qquad P_{O_2} > 0.58 \text{ atm.}$$

P_{O_2} is normalized by 1 atm to be dimensionless, and t is considered to be normalized by 1 minute.

Model 5d (Figure 17) is descriptive, not mechanistic. At $P_{O_2} = 1$ atm it reduces to a proportional model. It is odd that b, the exponent of P_{O_2}, is negative (Table A13), a result meaning that the divisor of the time expression becomes greater as the time expression increases more rapidly with time.

Normalizing factors are arbitrary in Model 5d. To test the normalizing factor, a multiplier of P_{O_2} was included in Model 5e. The fitted factor on P_{O_2} was 0.55 (Table A13), to yield a model with approximately $t^{0.5}$ for Experiments A, B, and D; $t^{0.8}$ for experiment H; t^{1} for Experiments C and I; and $t^{1.4}$ for Experiment J. The exponent on P_{O_2} as a multiplier remains negative but is smaller in magnitude than for Model 5d (Table A14).

For the intermittent exposures, the exponential models become somewhat predictive when the accumulated times at elevated P_{O_2} are used instead of the time since last air break. Whatever recovery process is occurring during short air breaks is insufficient to restart the "injury clock." In light of the cascade of events necessary before increased P_{O_2} manifests as decreased VC (see *Vital Capacity as an Index of Lung Injury*), successive oxygen exposures probably have cumulative effects even before ΔVC is evident, and probably until P_{O_2} and VC have been back at baseline for multiple hours. It is also likely that multiple different recovery functions occur when P_{O_2} returns to normal: the rapid removal of ROS, and the relatively slow removal of liquid, restoration of surfactant, repair of the microvasculature, etc. Only the slow recovery functions are observable, and only in their integration throughout the lungs.

The exponential models used with the accumulative times at elevated P_{O_2} overestimate ΔVC relative to the data and curve more steeply than do the experimental records. Using the P_{O_2} averaged over the last 90 to 120 minutes rather than the instantaneous P_{O_2} improves the model's correspondence to data. Using it also eliminates the recovery phase from consideration, since the average P_{O_2} remains elevated. Perhaps the average P_{O_2} better approximates the value that propagates the cascade of events than the instantaneous P_{O_2} does. Still unknown are the most correct period over which to average and the length of air break needed for an intermittent exposure to become two successive exposures with recovery between them.

The use of accumulated time at elevated P_{O_2} approximates integration from the starting time onward. We attempted a less arbitrary approach by integrating a differential form of Model 5e, but with repair modeled as being continuous when VC has decreased,

$$d(\%\Delta VC) / dt_{dur} = -a \cdot (c \cdot P_{O_2})^{b-1} \cdot t^{c \cdot P_{O_2}} - g / t_{dur} \cdot (\%\Delta VC), \quad P_{O_2} > 0.58 \text{ atm}$$

$$= g / t_{dur} \cdot (\%\Delta VC), \quad P_{O_2} < 0.58 \text{ atm}$$

where t_{dur} is the time with $P_{O_2} > 0.58$ atm.

The rate of repair decreases as the duration of the exposure increases. The portion of healing that is independent of t_{dur} in the recovery portion of Model 5b has been omitted to allow for closed form integration during elevated P_{O_2}. After any period at constant elevated P_{O_2},

$$\%\Delta VC = -a \cdot [(c \cdot P_{O_2})^{b-1} / (c \cdot P_{O_2} + g)] \cdot [t_{dur2}{}^{c \cdot P_{O_2}} - t_{dur1}{}^{c \cdot P_{O_2}}] + (\%\Delta VC) \text{ at } t_{dur1}.$$

After time t at low P_{O_2},

$$\%\Delta VC = (\%\Delta VC)_0 \cdot e^{-g \cdot t / t_{dur}},$$

where t_{dur} is the duration of previously elevated P_{O_2} and $(\%\Delta VC)_0$ is $\%\Delta VC$ when P_{O_2} is first low.

Model 6: Sigmoidal Dose Response Curves

The sigmoidal model choice was driven by inspection of the data and the different curvatures of experiments. Although the curvature was in the correct direction, each of the sigmoidal models fitted moderately well to some experiments and poorly to others (Figure 19, Tables 5 and 6).

The shapes of the model responses are affected by the parameter values. Parameter *a* — often called P_{50}, the dose for 50% effect — sets the left-right position of the response relative to the dose. The Hill exponent determines how abrupt the response to an increasing dose will be: a small exponent causes a gradual onset of response. With an exponent equal to 1, 25% of the response is achieved when the dose is one-third of the P_{50} — while an exponent approaching infinity gives a square wave response: no effect until the dose reaches P_{50}, then a step to full response.

Sigmoidal dose response curves can arise from dynamic equilibria, among other mechanisms. However, we propose no functional model. Some different relationships of P_{O_2} to the doses driving the sigmoid are proposed. In Model 6a the dose is generated and cleared according to the proportional healing model. In Models 6b and 6c the integral of P_{O_2} difference from threshold represents the dose during exposure. In Model 6b when the P_{O_2} drops below threshold, the dose — and thus the $\%\Delta VC$ — decreases, while in Model 6c $\%\Delta VC$ recovers exponentially once P_{O_2} drops below the fitted threshold.

Model 7: Different Kinetics Model

This model introduces a possible explanation for a latent onset of $\%\Delta VC$: the concentration of reactive species may not have reached its final values when the first measurements were made. Although the first measurements were hours apart (many orders of magnitude longer than times for these chemical reactions), biological factors such as antioxidant enzymes being consumed faster than they can be generated could

gradually increase the concentration of reactive species over time. However, the number of model parameters cannot be justified by the data.

Acute Injury Models: Recovery from Injury

Recovery data are available from Experiments B–D, H–J, N, and O.

Model 1: UPTD Model—recovery

The UPTD model does not consider recovery. Thus, the use of cumulative pulmonary oxygen toxicity[19] based on this model will overestimate toxicity in any situation following an interval during which recovery occurred. The overestimation will result even if the UPTD model might otherwise provide an adequate match to data (i.e., P_{O_2} near 1.5 atm, steady exposure, as stated in "Acute Injury Models: Development of Injury").

Model 2: Proportional Model—recovery

Slow recovery, linear with time, is predicted by this model when P_{O_2} is below threshold. Fitting of recovery is integral to the fitting of injury development. Only for Experiment B does this prediction approximate the data; the other experiments indicate faster recovery (Figure 3).

Model 3: Proportional Rate of Healing Model—recovery

Fitting of recovery is integral to the fitting of injury development. The exponential form of recovery appears to be a reasonable form for the data, but the single time constant of this model does not match the experimental record in which recovery rate varies in ways depending on the prior exposure (Figure 4).

Model 4: Autocatalytic Models—recovery

The autocatalytic models represent a refinement of the proportional rate of healing models. Like them, the autocatalytic models include the recovery parameters during injury development and after the return to normoxia. As in the other models, a single time constant does not match the recovery records, but the inclusion of a time duration term improves the recovery fits.

Model 5: Exponential Models—recovery

The exponential model is the only one discussed here for which, except for the starting point, the recovery can be fitted independently of the injury onset. The recovery parameters reported for Models 5a–5e were fitted separately from the injury onset. We used nonlinear regression with grouped data from all experiments and, with F_0 defined as the last measured point before recovery began, a different value for each subject. Our approach differed from that used by Arieli for his fit to the model we call 5a: he fitted a separate exponential decay function to data from each of Experiments D and H–J, and then found the linear relation between the exponent of healing and the P_{O_2} that caused the injury.[26] The effective differences between his technique and ours are in weighting of data and in selecting error terms to minimize. His technique weights each experiment equally but minimizes the logarithmic transforms of the error terms, and our technique weights each measurement equally, a weighting thus emphasizing some experiments more than others but minimizing the raw error terms.

Arieli found

$$\text{Exponent coefficient} = -0.42\ \text{hour}^{-1} + 3.8 \cdot 10^{-3}\ (\text{kPa} \cdot \text{hour})^{-1} \cdot P_{O_2\,\text{is}}\ (\text{kPa})$$
$$= -0.007\ \text{min}^{-1} + 0.006\ (\text{min} \cdot \text{atm})^{-1} \cdot P_{O_2\,\text{is}}\ (\text{atm}).$$

This model provides a very good fit to recovery in Experiments H–J (Figure 18). However, the sign on the exponent reverses if $P_{O_2\,\text{is}} < 1.17$ atm, and the expression indicates that injury will continue rather than recovery occurring for subjects who have breathed P_{O_2} near 1 atm, as in Experiment D (Figure 18). The problem is in the expression, not in the fit; for the same functional relationship, the best fits that we found also fail in the range of the data.

Intriguingly, the P_{O_2} values in Experiments D and H–J are inversely proportional to the exposure durations. We thus proposed Model 5b, like Model 5a but with the inverse of prior exposure duration instead of $P_{O_2\,\text{is}}$. This formulation corresponds to the stepwise linear regression, is more intuitive (longer exposure, not lower P_{O_2}, means slower healing), and does not become unstable in the range of the data. In the limit as T_{dur} approaches zero, there is no injury to heal as healing apparently becomes infinitely fast. Only for very long exposures — outside the range of the data — will the exponent change sign and thereby indicate continued injury. Unfortunately, Model 5b accounts for marginally less variance for recovery data than does Model 5a (Table A16).

Model 5c introduced the idea that the recovery rate should be a function of both P_{O_2} and duration of exposure. This explained as much of the variance in recovery alone as did Model 5b — or slightly more than did 5b (Table A16).

Like Model 3, Models 5a–5c assume that the rate of recovery is proportional to the damage present, the first-order kinetic model where, if $\%\Delta VC = -a \cdot F$,

$$dF / dt = -k \cdot F, \text{ and therefore } F = F_0 \cdot e^{-k \cdot t}.$$

Models 5d and 5e propose second-order kinetics:

$$dF/dt = -k \cdot F^2, \text{ and therefore } F = F_0 / [1 - k \cdot t \cdot F_0].$$

If recovery follows first-order kinetics, $\ln(F/F_0)$ against time will be a straight line. If recovery follows second-order kinetics, however, F_0/F against time will be a straight line. When recovery data averaged across subjects are used and each recovery experiment is considered on its own, the F_0/F vs. time relation fits slightly better for more experiments than does the $\ln(F/F_0)$ vs. time relation, an observation that stimulated the introduction of second-order kinetics in Models 5d and 5e. However, when individual recovery data are used and values where $F/F_0 \leq 0$ are censored, first-order kinetics provides a better fit to recovery in all experiments except Experiment J.

Model 6: Sigmoidal Dose Response Curves

In sigmoidal Models 6a and 6b, dose reductions allow the corresponding dose response to generate healing. In Model 6c %ΔVC recovers exponentially once P_{O_2} is reduced below the fitted threshold. The single time constant used does not fit well, and adjustments to that expression, like those in the exponential model, would provide improvement.

Models with Inflammatory Injury

Model 8: Injury-Memory Model

The injury-memory model considers a cumulative "memory" effect of injury to be caused by elevated P_{O_2}: oxygen is assumed to cause immediate injury that takes hours to resolve, and this injury-memory model integrates the proportional healing model over a "memory" period. However, the integrated form does not appear to describe the inflammatory process well. In general, the goodness of fit is slightly reduced from that with Model 3 when the integration is included, and the model does not predict intermittent effects any better than the proportional healing model (Tables 4 and 5) does. Perhaps a similar integration of a model with the correct curvature could be more successful than this injury-memory model.

Model 9: Delayed Inflammation Models

The delayed inflammation models present a view of inflammation as a delayed secondary injury. Inflammatory injury is modeled as proportional to the primary injury and appearing at full severity until it disappears abruptly. Although the steplike nature of

the model is crude, it matches the general physiological situation in that a time lag occurs before the secondary injury becomes apparent.

Inflammatory injury was added to the proportional healing Model 3a. Other models of primary injury could have been used and might have been more successful than Model 3a if the curvature of the data had been matched. However, adding inflammation just slightly increased the overall variance for which Model 3a accounts. Inflammation as modeled here had little effect on the fits to individual data sets, but it delayed the start of recovery.

The initial curvature of responses might be explained if the body reacts to the average of P_{O_2} over a time rather than to the instantaneous P_{O_2}. However, the improvement in fit is slight when averaging is applied. Average periods long enough to improve the fits of intermittent data degrade the fit of steady exposure data. Thus, a response to the moving average of P_{O_2} rather than to instantaneous P_{O_2} is unlikely.

Fits to Data after In-water Exposure

The available data for in-water exposures to elevated P_{O_2} are from exposures that, on the average, resulted in little ΔVC despite a few large decrements and some moderate increases in VC. The average ΔVCs among the in-water data range from –2.9 to 3.8%, while changes of absolute value less than 7.7% are within the 95% confidence bands of normal fluctuation.[17] With values so close to zero, correlations of models to data are forced to be low; little can be concluded about the match of models and in-water data.

CONCLUSIONS

The variables P_{O_2} and accumulated exposure time may suffice to characterize average ΔVC. However, all proposed models of pulmonary oxygen toxicity remain descriptive and thus should be used only in the ranges of P_{O_2} and exposure duration that have been measured.

Changes in VC for exposures with $P_{O_2} \geq 1.5$ atm appear to be curvilinear in time with more rapid change as exposure continues, but for exposures with lower P_{O_2}, linear or curvilinear and stabilizing with time. Thus, models with curvature that differs depending on P_{O_2} can fit a wide range of data. Of the models tested here, Models 5e and 5f — exponential models with the exponent of time a function of P_{O_2} — perform best overall. Nevertheless, for constant P_{O_2} near 1 atm, the simpler linear models may be adequate for interpolation. The intermittent data seem to be better explained by the exponential models with accumulated time and moving average P_{O_2} than by the others. However, accumulated time was not tested in Models 3, 4, or 6, the other models with nonlinear time expressions. Recovery is moderately well characterized by first-order kinetics, with rate a function of prior exposure duration.

Even within the measurement periods, many models are unacceptable for some data ranges. Models 1 and 2, the UPTD and proportional models, should not be used except for steady exposures to P_{O_2} of approximately 1 atm and for times up to 1000 min. Model 3, proportional rate of healing, can be used for up to 1000 min at $P_{O_2} \leq 1.5$ atm and for up to 250 min at $1.5 < P_{O_2} \leq 2.5$ atm, but it overestimates injury from intermittent exposures and does not model recovery adequately. The autocatalytic Model 4s are problematic because their thresholds must be chosen carefully, but the range of usability for Model 4d is similar to that for Model 3: up to 1000 min at $P_{O_2} \leq 1.5$ atm and up to 250 min at $P_{O_2} \leq 2.5$ atm, but not recovery. The thresholds of Model 5, the exponential models, that are quadratic in time should not be used for $P_{O_2} < 1.5$ atm, but they are acceptable for up to 800 min at $P_{O_2} = 1.5$ atm, up to 400 min at $P_{O_2} = 2$ atm and up to 350 min at $P_{O_2} = 2.5$ atm. Those of Model 5s with the exponent of time a function of P_{O_2} appear valid for up to 3000 min at $P_{O_2} \leq 1.5$ atm and up to 400 min for $1.5 < P_{O_2} \leq 2.5$ atm. Of the sigmoidal Model 6s, only Model 6a with fitted *g* gave useful predictions — acceptable for up to 3000 min at P_{O_2} near 1 atm and up to 250 min for $1.5 \leq P_{O_2} \leq 2.5$ atm — but the additional complication added to Model 3, the source of the "dose" term, may not be justified. Model 7 could not be fitted. Models 8 and 9, the injury-memory and the delayed inflammation models, are both derived from Model 3 and do not offer substantial improvements over it.

Regression models can predict only average responses. The high variability among subjects in response to oxygen exposure makes individual prediction nearly impossible. However, the probability of a serious VC decrement is predictable. Even lacking a universal model of ΔVC after oxygen exposure, a model that fits a particular P_{O_2} profile — a curve-fit, if you will — can be used to predict the average response to a similar profile. The population standard deviation estimate from this large data set — namely, ΔVC of approximately 7.5% to 8% — can then be multiplied by the appropriate t-statistics to construct the prediction bands.

REFERENCES

1. W. T. L. Ohlsson, "A Study on Oxygen Toxicity at Atmospheric Pressure," *Acta Med. Scand.*, Vol. 128 (supplement 190, 1947), pp. 1–93.

2. P. R. B. Caldwell, W. L. Lee Jr., H. S. Schildkraut, and E. R. Archibald, "Changes in Lung Volume, Diffusing Capacity, and Blood Gases in Men Breathing Oxygen," *J. Appl. Physiol.*, Vol. 21 (1966), pp. 1477–1483.

3. J. M. Clark and C. J. Lambertsen, *Pulmonary Oxygen Tolerance in Man and Derivation of Pulmonary Oxygen Tolerance Curves*, Institute for Environmental Medicine Report No. 1-70, University of Pennsylvania Medical Center, 1970.

4. J. M. Clark and C. J. Lambertsen, "Rate of Development of Pulmonary O_2 Toxicity in Man During O_2 Breathing at 2.0 Ata," *J. Appl. Physiol.*, Vol. 30, No. 5 (1971), pp. 739–752.

5. J. M. Clark, "Pulmonary Limits of Oxygen Tolerance in Man," *Experimental Lung Research*, Vol. 14 (1988), pp. 897–910.

6. C. J. Lambertsen, J. M. Clark, R. Gelfand, and E. Hopkin, "Transfer of Selected Pulmonary O_2 Poisoning Data to the U.S. Navy Experimental Diving Unit," Institute for Environmental Medicine, Environmental Biomedical Stress Data Center Report No. 4-1-2003, May 2003.

7. A. B. Fisher, R. W. Hyde, R. J. M. Puy, J. M. Clark, and C. J. Lambertsen, "Effect of Oxygen at 2 Atmospheres on the Pulmonary Mechanics of Normal Man," *J. Appl. Physiol.*, Vol. 24, No. 4 (1968), pp. 529–536.

8. R. G. Eckenhoff, J. H. Dougherty Jr., A. A. Messier, S. F. Osborne, and J. W. Parker, "Progression of and Recovery from Pulmonary Oxygen Toxicity in Humans Exposed to 5 ATA Air," *Aviat. Space Environ. Med.*, Vol. 58 (1987), pp. 658–667.

9. P. L. Hendricks, D. A. Hall, W. L. Hunter Jr., and P. J. Haley, "Extension of Pulmonary O_2 Tolerance in Man at 2 ATA by Intermittent O_2 Exposure," *J. Appl. Physiol.*, Vol. 42, No. 4 (1977), pp. 593–599.

10. C. J. Lambertsen and J. M. Clark, *Extension of Oxygen Tolerance in Man (Predictive Studies VI)*, Institute for Environmental Medicine, University of Pennsylvania Medical Center, Dec 1991.

11. C. J. Lambertsen, J. M. Clark, and R. Gelfand, *The Oxygen Research Program, University of Pennsylvania, Physiologic Interactions of Oxygen and Carbon Dioxide Effects and Relations for Hyperoxic Toxicity, Therapy, and Decompression, Summation: 1940 to 1999*, Institute for Environmental Medicine Report 3-1-2000, Mar 2000.

12. J. M. Clark, C. J. Lambertsen, R. Gelfand, N. D. Flores, J. B. Pisarello, M. D. Rossman, and J. A. Elias, "Effects of Prolonged Oxygen Exposure at 1.5, 2.0, or 2.5 ATA on Pulmonary Function in Men (Predictive Studies V)," *J. Appl. Physiol.*, Vol. 86, No. 1 (1999), pp. 243–259.

13. A. L. Harabin, L. D. Homer, P. K. Weathersby, and E. T. Flynn, *Predicting Pulmonary O_2 Toxicity: A New Look at the Unit Pulmonary Toxicity Dose*, Report NMRI 86-52, Naval Medical Research Institute, Dec 1986.

14. G. Latson, E. Flynn, W. Gerth, E. Thalmann, J. Maurer, and M. Lowe, *Accelerated Decompression Using Oxygen for Submarine Rescue — Summary Report and Operational Guidance*, NEDU TR 11-00, Navy Experimental Diving Unit, Dec 2000.

15. B. E. Shykoff, *Pulmonary Function after Oxygen-Accelerated Decompressions from Repetitive Sub-Saturation Air Dives*, NEDU TR 05-05, Navy Experimental Diving Unit, Apr 2005.

16. K. J. Marienau and J. Maurer, *The Pulmonary Effects of Exposure to High PO_2 During Prolonged Lar V / MK 25 Dives*, NEDU TM 97-14, Navy Experimental Diving Unit, Nov 1997.

17. B. E. Shykoff, *Pulmonary Effects of Submerged Breathing of Air or Oxygen*, NEDU TR 02-14, Navy Experimental Diving Unit, Nov 2002.

18. J. M. Clark and C. J. Lambertsen, "Pulmonary Oxygen Tolerance and the Rate of Development of Pulmonary Oxygen Toxicity in Man at Two Atmospheres Inspired Oxygen Tension," in C. J. Lambertsen, ed., *Underwater Physiology* (Baltimore, MD: Williams and Wilkins, 1967), pp. 439–451.

19. H. Bardin and C. J. Lambertsen, *A Quantitative Method for Calculating Cumulative Pulmonary Oxygen Toxicity: Use of the Unit Pulmonary Toxicity Dose (UPTD)*, Institute for Environmental Medicine Report No 4-1970, University of Pennsylvania Medical Center, 1970.

20. W. B. Wright, *Use of the University of Pennsylvania, Institute for Environmental Medicine Procedure for Calculation of Cumulative Pulmonary Oxygen Toxicity*, NEDU TR 2-72, Navy Experimental Diving Unit, 1972.

21. A. L. Harabin, L. D. Homer, P. K. Weathersby, and E. T. Flynn, "An Analysis of Decrements in Vital Capacity as an Index of Pulmonary Oxygen Toxicity," *J. Appl. Physiol.*, Vol. 63, No. 3 (1987), pp. 1130–1135.

22. R. D. Vann, "Oxygen Toxicity Risk Assessment," Final Report on ONR Contract N00014-87-C-0283, May 1988.

23. L. Harabin, S. S. Survanshi, P. K. Weathersby, J. R. Hays, and L. D. Homer, "The Modulation of Oxygen Toxicity by Intermittent Exposure," *Toxicology and Applied Pharmacology*, Vol. 93 (1988), pp. 298–311.

24. R. Arieli, "Oxygen Toxicity as a Function of Time and P_{O_2}," *J. Basic and Clin. Physiol. and Pharmacol.*, Vol. 5, No. 1 (1994), pp. 67–87.

25. R. Arieli, "Power Equation for All-or-None Effects of Oxygen Toxicity and Cumulative Oxygen Toxicity," *J. Basic and Clin. Physiol. and Pharmacol.*, Vol. 5, No. 3–4 (1994), pp. 207–225.

26. R. Arieli, A. Yalov, and A. Goldenshluger, "Modeling Pulmonary and CNS O_2 Toxicity and Estimation of Parameters for Humans," *J. Appl. Physiol.*, Vol. 92 (2002), pp. 248–256.

27. J. M. Clark and S. R. Thom, "Oxygen Under Pressure," in A. O. Brubakk and T. S. Neuman, eds., *Bennett and Elliott's Physiology and Medicine of Diving*, fifth edition (Edinburg, U.K., and New York, NY: Saunders, 2003), pp. 358–418.

28. J. M. Clark and C. J. Lambertsen, "Pulmonary Oxygen Toxicity: A Review," *Pharmacological Reviews*, Vol. 23, No. 2 (1971), pp. 37–133.

29. A. L. Harabin, J. C. Braisted, and E. T. Flynn, "Response of Antioxidant Enzymes to Intermittent and Continuous Hyperbaric Oxygen," *J. Appl. Physiol.*, Vol. 69, No. 1 (1990), pp. 328–335.

30. J. D. Crapo and D. F. Tierney, "Superoxide Dismutase and Pulmonary Oxygen Toxicity," *American J. of Physiol.*, Vol. 226, No. 6 (June 1974), pp. 1401–1407.

31. L. E. Otterbein, L. L. Mantell, and A. M. K. Choi, "Carbon Monoxide Provides Protection Against Hyperoxic Lung Injury," *Am. J. Physiol.*, Vol. 276 (Lung Cell Mol. Physiol., Vol 20) (1999), pp. L688–L694.

32. V. J. Thannickal and B. L. Fanburg, "Reactive Oxygen Species in Call Signaling," *Am. J. Physiol. Lung Cell Mol. Physiol.*, Vol. 279 (2002), pp. L1005–L1028.

33. N. R. Harris and D. N. Granger, "Oxygen Radicals in Inflammation," in K. Levy, ed., *Physiology of Inflammation* (New York: Oxford University Press, 2001), pp. 437–446.

34. J. Savill and C. Haslett, "Resolution of Inflammation," in K. Levy, ed., *Physiology of Inflammation* (New York: Oxford University Press, 2001), pp. 496–525.

35. A. E. Taylor, K. Rehder, R. E. Hyatt, and J. C. Parker, *Clinical Respiratory Physiology* (Philadelphia, PA: W. B. Saunders, 1989), pp. 179–189.

APPENDIX
Fitted Parameters of Models

Model 1. UPTD (No recovery data used in fitting)

$$\%\Delta VC = a \cdot t \cdot [(P_{O_2} - P_{th}) / (1\ atm - P_{th})]^b + c + \%\Delta VC_0,$$

where $\%\Delta VC_0$ is the change caused by a previous elevation in P_{O_2}, if such a change has occurred.

Table A1.
Fitted parameters *a*, *c* — two-parameter UPTD model 1a.
$b = 1/1.2 = 0.833$ and $P_{th} = 0.5$ atm. Standard errors of estimates are in parentheses; *italics* indicate low confidence in parameter value. Units are *a*: $\%\cdot min^{-1}$ and *c*: %.

Data Group	Parameter	All elevated P_{O_2}, No recovery data	
		weighted by datum	weighted by subject
Clark[3,18]	*a*	$-5.6 \cdot 10^{-3}$ $(8 \cdot 10^{-4})$	$-5 \cdot 10^{-3}$ $(2 \cdot 10^{-3})$
	c	*–1 (1)*	*–0 (3)*
	r^2	0.26	0.20
1	*a*	$-5.4 \cdot 10^{-3}$ $(2 \cdot 10^{-4})$	$-5.2 \cdot 10^{-3}$ $(6 \cdot 10^{-4})$
	c	–1.4 (0.3)	–1.2 (0.3)
	r^2	0.48	0.20
2	*a*	$-5.8 \cdot 10^{-3}$ $(3 \cdot 10^{-4})$	$-6.4 \cdot 10^{-3}$ $(7 \cdot 10^{-4})$
	c	–1.4 (0.4)	–1.2 (0.4)
	r^2	0.30	0.21
3	*a*	$-5.9 \cdot 10^{-3}$ $(3 \cdot 10^{-4})$	$-6.9 \cdot 10^{-3}$ $(7 \cdot 10^{-4})$
	c	–1.6 (0.4)	–1.2 (0.4)
	r^2	0.31	0.22

Table A2.
Fitted parameters *a, b, c* — three-parameter UPTD model 1b.

P_{th} = 0.5 atm. Standard error (SE) of estimates are in parentheses; *italics* indicate low confidence in parameter value. Units are *a*: % · min^{-1}, *b*: dimensionless, and *c*: %.

Data Group	Parameters	All elevated PO_2, No recovery data	
		weighted by datum	weighted by subject
1	*a*	$-5.6 \cdot 10^{-3}$ $(2 \cdot 10^{-4})$	$-5.9 \cdot 10^{-3}$ $(7 \cdot 10^{-4})$
	b	0.4 (0.1)	*0.2 (0.3)*
	c	−1.5 (0.3)	−1.3 (0.3)
	r^2	0.49	0.21
2	*a*	$-4.5 \cdot 10^{-3}$ $(2 \cdot 10^{-4})$	*$-9 \cdot 10^{-4}$ $(2 \cdot 10^{-4})$*
	b	1.40 (0.07)	4.0 (0.3)
	c	−1.3 (0.4)	−1.9 (0.4)
	r^2	0.29	0.11
3	*a*	$-5.4 \cdot 10^{-3}$ $(3 \cdot 10^{-4})$	$-5.4 \cdot 10^{-3}$ $(7 \cdot 10^{-3})$
	b	1.26 (0.07)	1.2 (0.2)
	c	−1.2 (0.4)	−1.2 (0.2)
	r^2	0.34	0.23

Table A3.
Fitted parameters *a*, *b*, *c*, and P_{th} — four-parameter UPTD model 1c.

Standard errors of estimates are in parentheses; *italics* indicate low confidence in parameter value. Units are *a*: % · min^{-1}, *b*: dimensionless, P_{th}: atm, and *c*: %.

Data Group	Parameter	All elevated PO_2, No recovery data	
		weighted by datum	weighted by subject
1	*a*	$-5.6 \cdot 10^{-3}$ $(2 \cdot 10^{-4})$	$-5.9 \cdot 10^{-3}$ $(7 \cdot 10^{-4})$
	b	0.4 (0.1)	*0.2* *(0.3)*
	c	−1.5 (0.3)	−1.2 (0.3)
	P_{th}	0.487 (0.001)	0.487 $(3 \cdot 10^{-7})$
	r^2	0.49	0.21
2	*a*	$-4.5 \cdot 10^{-3}$ $(3 \cdot 10^{-4})$	$-2.3 \cdot 10^{-3}$ $(4 \cdot 10^{-4})$
	b	1.3 (0.2)	*0.8* *(0.5)*
	c	−1.3 (0.4)	−1.4 (0.4)
	P_{th}	0.53 (0.09)	0.9 (0.2)
	r^2	0.29	0.18
3	*a*	$-5.4 \cdot 10^{-3}$ $(3 \cdot 10^{-4})$	*$-6 \cdot 10^{-3}$* *$(6 \cdot 10^{-3})$*
	b	1.2 (0.4)	1.1 (0.3)
	c	−1.3 (0.4)	*0* *(3)*
	P_{th}	0.53 (0.08)	*0.5* *(0.4)*
	r^2	0.34	0.21 * simplex

Model 2. Proportional and Related Models

a. Testing proportionality

$$\%\Delta VC = a \cdot (P_{O_2} - P_{th})^b \cdot (t - t_{th})^c + \%\Delta VC_0, \qquad t > t_{th},\ P_{O_2} > P_{th}$$

Table A4.
Four-parameter model, considering only nonintermittent data without recovery.

Standard errors of estimates in parentheses; *italics* indicate low confidence in parameter value; units are *a*, *b*, and *c*: dimensionless; P_{th}: atm.

$P_{O_2} > P_{th}$	Data Group 1	Data Group 3
a	– 0.7 (0.2)	– 0.8 (0.3)
P_{th}	0.31 (0.01)	0. 39 (0.00)
b	1.0 (0.1)	1.4 (0.2)
c	0.9 (0.1)	1.0 (0.1)
r^2	0.44	0.23
n	534	543

Table A5.
Three-parameter model linear in time, without recovery.

Standard errors of estimates in parentheses. Units are *a, b*: dimensionless; P_{th}: atm. Exponent $c = 1$.

$P_{O_2} > P_{th}$	Data Group 1	Data Group 3
a	–0.58 (0.05)	– 0.92 (0.04)
P_{th}	0.486 (0.004)	0.525 (0.00)
b	0.6 (0.1)	1.10 (0.08)
r^2	0.36	0.24
n	301	447

Table A6.
Three-parameter model linear in P_{O_2}, without recovery.

Standard errors of estimates are in parentheses. Units are *a*, *c*: dimensionless, and P_{th}: atm. $b = 1$.

$P_{O_2} > P_{th}$	Data Group 1	Data Group 3
a	–0.7 (0.2)	–1.0 (0.2)
P_{th}	0.31 (0.01)	0.532 (0.00)
c	0.91 (0.06)	0.90 (0.06)
r^2	0.44	0.20
n	534	436

Table A7.
Proportional model without recovery.

Standard error estimates are in parentheses. Units are *a*: dimensionless; P_{th}: atm.

$P_{O_2} > P_{th}$	Data Group 1	Data Group 3
a	–0.67 (0.05)	–0.91 (0.04)
P_{th}	0.44 (0.03)	0.532 (0.00)
r^2	0.31	0.22
n	325	436

b. Proportional model

If we consider *F* instead of %ΔVC directly, the proportional model equation can be written

$$F = a_1 \cdot (P_{O_2} - P_{th}) \cdot t + F_0.$$

This is the integration of the differential equation

$$dF / dt = a_1 \cdot (P_{O_2} - P_{th}), \qquad F \geq 0.$$

If we remove the restriction on P_{O_2}, when $P_{O_2} < P_{th}$ the free radical concentration *F* decreases, and healing occurs.

We considered two forms of this model, both previously published:[13,21]

a) $\%\Delta VC = -\alpha \cdot F$ and the parameter *a* in Table A7 is $a = -\alpha \cdot a_1$, and
b) $\%\Delta VC = -100\,[1 - 1.005^{-F}]$.

Table A8.
Fitted parameters for proportional Model 2a, without log limit.

Standard errors of estimates in parentheses. Units are a: $(\text{Torr} \cdot \text{min})^{-1}$, P_{th}: Torr.

Data Group	Param	No recovery data	Recovery to 8 hr		All recovery
		Weighted by datum	Weighted by datum	Weighted by subject	Weighted by datum
1	$a = \alpha \cdot a_1$	$9.1 \cdot 10^{-6}$ $(5 \cdot 10^{-6})$	$9.1 \cdot 10^{-6}$ $(5 \cdot 10^{-7})$	$3.5 \cdot 10^{-6}$ $(8 \cdot 10^{-6})$	$9.3 \cdot 10^{-6}$ $(5 \cdot 10^{-7})$
	P_{th}	119 (2)	119 (3)	*117 (6)*	121 (2)
	r^2	0.37	0.36	0.01	0.21
2	$a = \alpha \cdot a_1$	$9.4 \cdot 10^{-6}$ $(5 \cdot 10^{-7})$	$9.4 \cdot 10^{-6}$ $(5 \cdot 10^{-7})$	$4.6 \cdot 10^{-6}$ $(9 \cdot 10^{-7})$	$9.4 \cdot 10^{-6}$ $(5 \cdot 10^{-7})$
	P_{th}	121 (3)	121 (3)	*118 (6)*	123 (2)
	r^2	0.16	0.14	–0.01	0.07
3	$a = \alpha \cdot a_1$	$9.4 \cdot 10^{-6}$ $(5 \cdot 10^{-7})$	$9.4 \cdot 10^{-6}$ $(6 \cdot 10^{-7})$	$5 \cdot 10^{-6}$ $(1 \cdot 10^{-6})$	$9.3 \cdot 10^{-6}$ $(5 \cdot 10^{-7})$
	P_{th}	121 (3)	121 (3)	*118 (6)*	123 (2)
	r^2	0.16	0.14	0.00	0.07
4	$a = \alpha \cdot a_1$	$9.2 \cdot 10^{-6}$ $(5 \cdot 10^{-7})$	$9.2 \cdot 10^{-6}$ $(5 \cdot 10^{-7})$	$4.6 \cdot 10^{-6}$ $(8 \cdot 10^{-7})$	$9.8 \cdot 10^{-6}$ $(5 \cdot 10^{-7})$
	P_{th}	121 (3)	121 (3)	*118 (6)*	133 (2)
	r^2	0.17	0.15	–0.01	0.12

Table A9.
Fitted parameters for proportional Model 2b, with log limit.

Weighted by datum.
Standard errors of estimates in parentheses. Units are a_1: $(\text{Torr} \cdot \text{min})^{-1}$, P_{th}: Torr.

Data Group	Parameter	No recovery	Recovery to 8 hr	All recovery
1	a_1	$1.9 \cdot 10^{-5}$ $(1 \cdot 10^{-6})$	$1.9 \cdot 10^{-5}$ $(1 \cdot 10^{-6})$	$1.9 \cdot 10^{-5}$ $(1 \cdot 10^{-6})$
	P_{th}	118 (2)	118 (2)	120 (2)
	r^2	0.37	0.36	0.22
2	a_1	$2.0 \cdot 10^{-5}$ $(1 \cdot 10^{-6})$	$2.0 \cdot 10^{-5}$ $(1 \cdot 10^{-6})$	$2.0 \cdot 10^{-5}$ $(1 \cdot 10^{-6})$
	P_{th}	120 (3)	120 (3)	122 (2)
	r^2	0.16	0.14	0.08
3	a_1	$2.0 \cdot 10^{-5}$ $(1 \cdot 10^{-6})$	$2.0 \cdot 10^{-5}$ $(1 \cdot 10^{-6})$	$2.0 \cdot 10^{-5}$ $(1 \cdot 10^{-6})$
	P_{th}	120 (3)	120 (3)	121 (2)
	r^2	0.16	0.15	0.07
4	a_1	$2.0 \cdot 10^{-5}$ $(1 \cdot 10^{-6})$	$2.0 \cdot 10^{-5}$ $(1 \cdot 10^{-6})$	$2.1 \cdot 10^{-5}$ $(1 \cdot 10^{-6})$
	P_{th}	120 (3)	120 (3)	129 (2)
	r^2	0.17	0.15	–0.18

Model 3. Proportional Rate of Healing Models

$$\text{If } dF/dt = \begin{cases} a_1 \cdot (PO_2 - P_{th}) - b \cdot F, & PO_2 > \text{threshold} \\ -b \cdot F, & PO_2 \le \text{threshold}, \end{cases}$$

a. $\%\Delta VC = -\alpha \cdot F$ b. $\%\Delta VC = -100\,[1 - 1.005^{-F}]$

Table A10.
Fitted parameters for proportional healing Model 3a, without log limit.
Standard errors of parameters are in parentheses; *italics* indicate low confidence in parameter value. Units are a: $(\text{Torr} \cdot \text{min})^{-1}$, b: min^{-1}, P_{th}: Torr. ** indicates that a Simplex fit is given, because the Marquardt fit for general starting values reduces to the proportional Model 2a.

Data Group	Param	No recovery Weighted by datum	Recovery to 8 hr		All recovery Weighted by datum
			Weighted by datum	Weighted by subject	
1	$a = \alpha \cdot a_1$	$1.5 \cdot 10^{-5}$ $(7 \cdot 10^{-6})$	$1.6 \cdot 10^{-5}$ $(1 \cdot 10^{-6})$	$1.2 \cdot 10^{-5}$ $(3 \cdot 10^{-6})$	$1.5 \cdot 10^{-5}$ $(1 \cdot 10^{-6})$
	B	$2.0 \cdot 10^{-4}$ $(9 \cdot 10^{-5})$**	*$7.0 \cdot 10^{-5}$* *$(8 \cdot 10^{-5})$*	$3.0 \cdot 10^{-4}$ $(2 \cdot 10^{-5})$	$2.0 \cdot 10^{-4}$ $(3 \cdot 10^{-5})$
	P_{th}	170 (10)	250 (30)	160 (20)	170 (10)
	r^2	0.46	0.45	0.19	0.39
2	$a = \alpha \cdot a_1$	$2.4 \cdot 10^{-5}$ $(2 \cdot 10^{-6})$	$2.4 \cdot 10^{-5}$ $(2 \cdot 10^{-6})$	$2.7 \cdot 10^{-5}$ $(4 \cdot 10^{-6})$	$2.5 \cdot 10^{-5}$ $(2 \cdot 10^{-6})$
	b	$1.8 \cdot 10^{-4}$ $(8 \cdot 10^{-5})$	$2.6 \cdot 10^{-4}$ $(9 \cdot 10^{-5})$	$8 \cdot 10^{-4}$ $(3 \cdot 10^{-4})$	$6.2 \cdot 10^{-4}$ $(9 \cdot 10^{-5})$
	P_{th}	340 (20)	320 (20)	250 (60)	230 (40)
	r^2	0.30	0.26	0.20	0.22
3	$a = \alpha \cdot a_1$	$2.4 \cdot 10^{-5}$ $(2 \cdot 10^{-6})$	$2.3 \cdot 10^{-5}$ $(2 \cdot 10^{-6})$	$2.6 \cdot 10^{-5}$ $(4 \cdot 10^{-6})$	$2.5 \cdot 10^{-5}$ $(2 \cdot 10^{-6})$
	b	$1.8 \cdot 10^{-4}$ $(8 \cdot 10^{-5})$	$6 \cdot 10^{-4}$ $(1 \cdot 10^{-4})$	$7 \cdot 10^{-4}$ $(3 \cdot 10^{-4})$	$6.2 \cdot 10^{-4}$ $(9 \cdot 10^{-5})$
	P_{th}	340 (20)	180 (20)	250 (60)	230 (40)
	r^2	0.34	0.29	0.21	0.25
4	$a = \alpha \cdot a_1$	$2.3 \cdot 10^{-5}$ $(1 \cdot 10^{-6})$	$2.4 \cdot 10^{-5}$ $(4 \cdot 10^{-6})$	$2.4 \cdot 10^{-5}$ $(3 \cdot 10^{-6})$	$2.5 \cdot 10^{-5}$ $(2 \cdot 10^{-6})$
	b	$1.6 \cdot 10^{-4}$ $(2 \cdot 10^{-5})$**	$2.4 \cdot 10^{-4}$ $(6 \cdot 10^{-5})$**	*$4 \cdot 10^{-4}$* *$(3 \cdot 10^{-4})$*	$9.8 \cdot 10^{-4}$ $(9 \cdot 10^{-5})$
	P_{th}	340 (20)	320 (20)	290 (30)	*110* *(20)*
	r^2	0.31	0.24	0.23	0.22

Table A11.
Fitted parameters for proportional healing Model 3b, with log limit.

Weighted by datum. Standard errors of parameters are in parentheses. Units are *a*: $(\text{Torr} \cdot \text{min})^{-1}$, *b*: min^{-1}, P_{th}: Torr. * indicates that a Simplex estimate was needed to start the Marquardt fit; ** indicates that a Simplex fit is given. The Marquardt fit for other starts reduced to the proportional Model 2b.

Data Group	Parameter	No recovery	Recovery to 8 hr	All recovery
1	*a*	$3.2 \cdot 10^{-5}$ $(3 \cdot 10^{-6})$	$3.2 \cdot 10^{-5}$ $(1 \cdot 10^{-6})$	$3.3 \cdot 10^{-5}$ $(2 \cdot 10^{-6})$
	b	$2 \cdot 10^{-4}$ $(1 \cdot 10^{-4})$**	$2 \cdot 10^{-4}$ $(3 \cdot 10^{-5})$**	$2.0 \cdot 10^{-4}$ $(3 \cdot 10^{-5})$
	P_{th}	170 (10)	170 (10)	170 (10)
	r^2	0.46	0.45	0.39
2	*a*	$4.6 \cdot 10^{-5}$ $(4 \cdot 10^{-6})$	$5.2 \cdot 10^{-5}$ $(4 \cdot 10^{-6})$	$5.5 \cdot 10^{-5}$ $(4 \cdot 10^{-6})$
	b	$2.4 \cdot 10^{-4}$ $(1 \cdot 10^{-4})$	$2.3 \cdot 10^{-4}$ $(9 \cdot 10^{-5})$*	$6.2 \cdot 10^{-4}$ $(9 \cdot 10^{-5})$
	P_{th}	270 (50)	330 (20)	240 (30)
	r^2	0.30	0.26	0.21
3	*a*	$4.7 \cdot 10^{-5}$ $(4 \cdot 10^{-6})$	$5.3 \cdot 10^{-5}$ $(4 \cdot 10^{-6})$	$5.5 \cdot 10^{-5}$ $(4 \cdot 10^{-6})$
	b	$2.4 \cdot 10^{-4}$ $(1 \cdot 10^{-4})$*	$2.4 \cdot 10^{-4}$ $(9 \cdot 10^{-4})$*	$6.2 \cdot 10^{-4}$ $(9 \cdot 10^{-5})$
	P_{th}	270 (50)	330 (20)	250 (30)
	r^2	0.33	0.30	0.25
4	*a*	$5.0 \cdot 10^{-5}$ $(5 \cdot 10^{-6})$	$5.1 \cdot 10^{-5}$ $(4 \cdot 10^{-6})$	$5.3 \cdot 10^{-5}$ $(3 \cdot 10^{-6})$
	b	$1.4 \cdot 10^{-4}$ $(8 \cdot 10^{-5})$**	$2.2 \cdot 10^{-4}$ $(1 \cdot 10^{-5})$**	$1.01 \cdot 10^{-3}$ $(9 \cdot 10^{-5})$
	P_{th}	340 (20)	330 (20)	120 (20)
	r^2	0.31	0.24	0.22

Model 4. Autocatalytic Models

$$dF/dt = a_1 \cdot (PO_2 - P_{th}) + b \cdot F \cdot (PO_2 - P_a)$$

$$\%\Delta VC = -\alpha \cdot F \qquad \text{Let } a = -\alpha \cdot a_1.$$

Model 4a: P_{th} set to 110 Torr. Model 4b: P_a set to 760 Torr.

Note that the time constant of recovery is $1 / [b \cdot (PO_2 - P_a)]$, not $1 / b$.

Model 4c:

$$dF/dt = a_1 \cdot (PO_2 - P_{th}) + (b + c/T_{dur}) \cdot F \cdot (PO_2 - P_a), \quad P_a = 760 \text{ Torr},$$

where T_{dur} is the duration of exposure to elevated PO_2.

Model 4c1:

$$dF/dt = \begin{cases} a_1 \cdot (P_{O_2} - P_{th}) + [b + c \cdot (P_{O_2} - P_a) / T_{dur}] \cdot F, & P_{O_2} > P_{th} \\ 0, & 200 \text{ Torr} < P_{O_2} < P_{th} \\ [b + c \cdot (P_{O_2} - P_a) / T_{dur}] \cdot F, & P_{O_2} < 200 \text{ Torr}, \end{cases}$$

where P_{th} = 330 Torr , P_a = 760 Torr,

and T_{dur} = duration of exposure to elevated P_{O_2}.

Table A12.
Fitted parameters for autocatalytic Model 4a.
Standard errors of parameters are in parentheses; *italics* indicate low confidence in parameter value. Units are *a*, *b*: $(\text{Torr} \cdot \text{min})^{-1}$, P_a: Torr. * on r^2 value indicates a Simplex fit that yielded a much greater value of r^2 and different parameters than did the Marquardt fit.

Data Group	Param	No Recovery	Recovery to 8 hr		*All recovery*
		Weighted by datum	**Weighted by datum**	**Weighted by subject**	*Weighted by datum*
1	Model increases variance.				
2	$a = \alpha \cdot a_1$	$1.6 \cdot 10^{-5}$ $(2 \cdot 10^{-6})$	$1.7 \cdot 10^{-5}$ $(2 \cdot 10^{-6})$	$1.6 \cdot 10^{-5}$ $(5 \cdot 10^{-6})$	$1.7 \cdot 10^{-5}$ $(2 \cdot 10^{-6})$
	b	$1.0 \cdot 10^{-6}$ $(4 \cdot 10^{-7})$	$1.0 \cdot 10^{-6}$ $(4 \cdot 10^{-7})$	*$1.4 \cdot 10^{-6}$ $(8 \cdot 10^{-7})$*	$1.0 \cdot 10^{-6}$ $(3 \cdot 10^{-7})$
	P_a	1000 (300)	1000 (300)	*1000 (500)*	1000 (300)
	r^2	0.29*	0.26*	0.21*	0.24*
3	$a = \alpha \cdot a_1$	$1.6 \cdot 10^{-5}$ $(2 \cdot 10^{-6})$	$1.6 \cdot 10^{-5}$ $(2 \cdot 10^{-6})$	$1.6 \cdot 10^{-5}$ $(4 \cdot 10^{-6})$	$1.6 \cdot 10^{-5}$ $(2 \cdot 10^{-6})$
	b	$1.0 \cdot 10^{-6}$ $(4 \cdot 10^{-7})$	$1.1 \cdot 10^{-6}$ $(4 \cdot 10^{-7})$	*$1.4 \cdot 10^{-6}$ $(8 \cdot 10^{-7})$*	$1.1 \cdot 10^{-6}$ $(3 \cdot 10^{-7})$
	P_a	1000 (300)	1000 (200)	1000 (400)	1000 (200)
	r^2	0.31*	0.29	0.21	0.26
4	$a = \alpha \cdot a_1$	$1.6 \cdot 10^{-5}$ $(2 \cdot 10^{-6})$	$1.6 \cdot 10^{-5}$ $(2 \cdot 10^{-6})$	$1.6 \cdot 10^{-5}$ $(4 \cdot 10^{-7})$	Does not converge
	b	$1.0 \cdot 10^{-6}$ $(4 \cdot 10^{-7})$	$1.1 \cdot 10^{-6}$ $(4 \cdot 10^{-7})$	*$1.4 \cdot 10^{-6}$ $(8 \cdot 10^{-7})$*	
	P_a	1000 (200)	1000 (200)	1000 (400)	
	r^2	0.30*	0.24	0.23	

Table A13.
Fitted parameters for autocatalytic Models 4b, 4c.

Standard errors of parameters are in parentheses; *italics* indicate low confidence in parameter value. Units are a, b: $(\text{Torr} \cdot \text{min})^{-1}$, P_a: Torr.

Data Group	Parameter	4b All recovery	4c All recovery	4c1 All recovery
		Weighted by datum	Weighted by datum	Weighted by datum
1	$a = \alpha \cdot a_1$	$1.4 \cdot 10^{-5}$ $(2 \cdot 10^{-6})$	Does not converge	$2.9 \cdot 10^{-5}$ $(4 \cdot 10^{-6})$
	b	$1.0 \cdot 10^{-6}$ $(2 \cdot 10^{-7})$		$-5 \cdot 10^{-4}$ $(2 \cdot 10^{-4})$
	c			*$-1 \cdot 10^{-5}$ $(4 \cdot 10^{-4})$*
	P_{th}	230 (70)		200, 330
	P_a			760
	r^2	0.33		0.30
2	$a = \alpha \cdot a_1$	$1.4 \cdot 10^{-5}$ $(1 \cdot 10^{-6})$	$1.7 \cdot 10^{-5}$ $(1 \cdot 10^{-6})$	$1.35 \cdot 10^{-5}$ $(8 \cdot 10^{-7})$
	b	$1.4 \cdot 10^{-6}$ $(2 \cdot 10^{-7})$	$-2.8 \cdot 10^{-7}$ $(3 \cdot 10^{-8})$	$2.3 \cdot 10^{-4}$ $(2 \cdot 10^{-5})$
	c		$1.2 \cdot 10^{-3}$ $(1 \cdot 10^{-4})$	$1.5 \cdot 10^{-3}$ $(1 \cdot 10^{-4})$
	P_{th}	150 (40)	340 (10)	200, 330
	P_a		760	760
	r^2	0.24	0.17	0.30
3	$a = \alpha \cdot a_1$	$1.4 \cdot 10^{-5}$ $(1 \cdot 10^{-6})$	$1.68 \cdot 10^{-5}$ $(9 \cdot 10^{-7})$	$1.35 \cdot 10^{-5}$ $(9 \cdot 10^{-7})$
	b	$1.4 \cdot 10^{-6}$ $(2 \cdot 10^{-7})$	$-3.0 \cdot 10^{-7}$ $(3 \cdot 10^{-8})$	$2.3 \cdot 10^{-4}$ $(2 \cdot 10^{-5})$
	c		$1.3 \cdot 10^{-3}$ $(1 \cdot 10^{-4})$	$1.6 \cdot 10^{-3}$ $(1 \cdot 10^{-4})$
	P_{th}	150 (40)	340 (10)	200, 330
	P_a		760	760
	r^2	0.26	0.31	0.31
4	$a = \alpha \cdot a_1$	$1.32 \cdot 10^{-5}$ $(9 \cdot 10^{-7})$	$1.25 \cdot 10^{-5}$ $(9 \cdot 10^{-7})$	$2.1 \cdot 10^{-5}$ $(2 \cdot 10^{-6})$
	b	$1.7 \cdot 10^{-6}$ $(2 \cdot 10^{-7})$	$1.2 \cdot 10^{-6}$ $(2 \cdot 10^{-7})$	$-3.0 \cdot 10^{-4}$ $(8 \cdot 10^{-5})$
	c		$6 \cdot 10^{-4}$ $(2 \cdot 10^{-4})$	$9 \cdot 10^{-4}$ $(2 \cdot 10^{-4})$
	P_{th}	*110 (40)*	120 (36)	200, 330
	P_a		760	760
	r^2	0.27	0.23	0.28

Model 5.
Exponential Models

$$\%\Delta VC = -\alpha \cdot F, \text{ where}$$

a. $$F = \begin{cases} a_1 \cdot PO_2^{\,b} \cdot t^2 + F_0, & PO_2 > 0.58 \text{ atm} \\ F_0 \cdot e^{-[c + g \cdot PO_{2is}] \cdot t}, & PO_2 \le 0.58 \text{ atm.} \end{cases}$$

b. $$F = \begin{cases} a_1 \cdot PO_2^{\,b} \cdot t^2 + F_0, & PO_2 > 0.58 \text{ atm} \\ F_0 \cdot e^{-[c + g / T_{dur}] \cdot t}, & PO_2 \le 0.58 \text{ atm.} \end{cases}$$

c. $$F = \begin{cases} a_1 \cdot (PO_2 - 0.5)^b \cdot t^2 + F_0, & PO_2 > 0.58 \text{ atm} \\ F_0 \cdot e^{-[c - g \cdot (PO_2 - 0.5) / T_{dur}] \cdot t}, & PO_2 \le 0.58 \text{ atm.} \end{cases}$$

d. $$F = \begin{cases} a_1 \cdot PO_2^{\,b} \cdot t^{PO_2} + F_0 & PO_2 < 0.58 \text{ atm} \\ F_0 / [1 - c + g / T_{dur}) \cdot t \cdot F_0] & PO_2 \le 0.58 \text{ atm.} \end{cases}$$

e. $$F = \begin{cases} a_1 \cdot (c \cdot PO_2)^b \cdot t^{c \cdot PO_2} + F_0, & PO_2 < 0.58 \text{ atm} \\ F_0 / [1 - (c + g / T_{dur}) \cdot t \cdot F_0], & PO_2 \le 0.58 \text{ atm.} \end{cases}$$

f. $$F = \begin{cases} a_1 \cdot [(c \cdot PO_2)^{b-1} / (c \cdot PO_2 + g)] \cdot [T_{dur2}^{\,c \cdot PO_2} - T_{dur1}^{\,c \cdot PO_2}] + F \text{ at } T_{dur1}, & PO_2 < 0.58 \text{ atm} \\ F_0 \cdot e^{-g \cdot t / T_{dur}}, & PO_2 \le 0.58 \text{ atm.} \end{cases}$$

Table A14.
Parameters for Exponential Models 5a–e, no recovery, weighted by datum.

Standard errors of parameters are in parentheses.
Model 5a, 5b, 5c: Units are a: $(\text{min})^{-2}$, b: dimensionless. *Models 5d, 5e*: Parameters are dimensionless.

Data Group	Parameter No Recovery	5a, 5b:	5c:	5d:	5e:
1	$a = \alpha \cdot a_1$	$-2.7 \cdot 10^{-6}$ $(1 \cdot 10^{-7})$	$-7.3 \cdot 10^{-6}$ $(9 \cdot 10^{-7})$	$-5.3 \cdot 10^{-3}$ $(2 \cdot 10^{-4})$	–0.011 (0.003)
	b	2.7 (0.2)	1.4 (0.2)	–7.7 (0.1)	–4.6 (0.6)
	c				0.56 (0.08)
	r^2	0.41	0.39	0.43	0.46
3	$a = \alpha \cdot a_1$	$-2.7 \cdot 10^{-6}$ $(2 \cdot 10^{-7})$	$-1.50 \cdot 10^{-5}$ $(7 \cdot 10^{-7})$	$-6.0 \cdot 10^{-3}$ $(3 \cdot 10^{-4})$	–0.018 (0.006)
	b	4.0 (0.1)	2.55 (0.09)	–7.25 (0.09)	–4.0 (0.5)
	c				0.55 (0.07)
	r^2	0.29	0.25	0.22	0.29

Table A15.
Parameters for integrated Exponential Model 5f, all data.

Standard errors of parameters are in parentheses. All parameters are dimensionless.

Data Group	Parameter	All recovery Weighted by datum	
1	$a = \alpha \cdot a_1$	$-9.7 \cdot 10^{-3}$ $(3 \cdot 10^{-3})$	
	b	–4.4	(0.7)
	c	0.66	(0.09)
	g	0.13	(0.03)
	r^2	0.38	
2	$a = \alpha \cdot a_1$	–0.03	(0.01)
	b	–3.2	(0.05)
	c	0.52	(0.07)
	g	0.6	(0.1)
	r^2	0.22	
3	$a = \alpha \cdot a_1$	–0.03	(0.01)
	b	–3.4	(0.05)
	c	0.54	(0.08)
	g	0.6	(0.1)
	r^2	0.23	
4	$a = \alpha \cdot a_1$	–0.21	(0.07)
	b	–3.9	(0.05)
	c	0.54	(0.07)
	g	10.2	(0.8)
	r^2	0.38	

Table A16.
Parameters for Exponential Models 5a–5e, recovery only, weighted by datum.

Standard errors of parameters are in parentheses. *Italics* indicate low confidence in parameter value. *Model 5a*: Units are c: $(\text{min})^{-1}$, g: $(\text{min} \cdot \text{atm})^{-1}$. *Model 5b*: Units are c: $(\text{min})^{-1}$, g: dimensionless. *Model 5c*: Units are c: $(\text{min})^{-1}$, g: $(\text{atm})^{-1}$. *Models 5d, 5e*: Second-order recovery. Units are c: $(\text{min})^{-1}$, g: dimensionless.

Data Group	Parameter	Model 5a	Model 5b	Model 5c	Models 5d, 5e
1	Not enough recovery data				
2	c	$-2.6 \cdot 10^{-3}$ $(32 \cdot 10^{-4})$	$-3.8 \cdot 10^{-4}$ $(4 \cdot 10^{-5})$	$-4.6 \cdot 10^{-4}$ $(4 \cdot 10^{-5})$	$-2.2 \cdot 10^{-5}$ $(3 \cdot 10^{-6})$
	g	$2.6 \cdot 10^{-3}$ $(3 \cdot 10^{-4})$	1.7 (0.2)	5.5 (0.5)	0.09 (0.01)
	r^2	0.42	0.41	0.57	0.46
3	c	$-4.3 \cdot 10^{-3}$ $(5 \cdot 10^{-4})$	$-3.8 \cdot 10^{-4}$ $(4 \cdot 10^{-5})$	$-4.6 \cdot 10^{-4}$ $(4 \cdot 10^{-5})$	$-2.2 \cdot 10^{-5}$ $(3 \cdot 10^{-6})$
	g	$4.0 \cdot 10^{-3}$ $(5 \cdot 10^{-4})$	1.7 (0.2)	5.5 (0.5)	0.09 (0.01)
	r^2	0.49	0.41	0.57	0.46
4	c	$-4.0 \cdot 10^{-3}$ $(4 \cdot 10^{-4})$	$-3.7 \cdot 10^{-4}$ $(3 \cdot 10^{-5})$	*$-7 \cdot 10^{-5}$ $(6 \cdot 10^{-5})$*	$-7.2 \cdot 10^{-5}$ $(3 \cdot 10^{-5})$
	g	$3.7 \cdot 10^{-3}$ $(3 \cdot 10^{-4})$	1.7 (0.1)	5.2 (0.5)	0.264 (0.009)
	r^2	0.57	0.50	0.50	0.36

Model 6. Sigmoidal Dose Response Models.

a. The Hill equation, scaled by parameter *g*, with *F* from Model 3 as the dose:

$$\%\Delta VC = -g \cdot [F^b / (F^b + a^b)],$$

where $F = (P_{O_2} / c) \cdot (1 - e^{-(c \cdot t)}) + F_0 \cdot e^{-(c \cdot t)}$.

b. The scaled Hill equation here has its dose given as the integral of the difference of P_{O_2} from a threshold, the cumulative dose model:

$$IntO_2 = \int (P_{O_2} - P_{th})\, dt, \text{ integrating from time} = 0 \text{ to time} = t$$

$$\text{Dose} = \begin{cases} IntO_2, & IntO_2 \geq 0 \\ 0, & IntO_2 < 0 \end{cases}$$

$$\%\Delta VC = -g \cdot [\text{dose}^b / (\text{dose}^b + a^b)]$$

$$\%\Delta VC = -g \cdot [\text{dose}^b / (\text{dose}^b + a^b)]$$

c. The scaled Hill equation here has the dose given as the integral of the difference of P_{O_2} from a P_{O_2} threshold greater than threshold, but only exponential healing applies when P_{O_2} is less than threshold:

$$\%\Delta VC = \begin{cases} -g \cdot [\text{dose}^b / (\text{dose}^b + a^b)], & P_{O_2} \geq P_{th} \\ (\%\Delta VC)_0 \cdot e^{-(c \cdot t)}, & P_{O_2} < P_{th}. \end{cases}$$

Table A17.
Fitted parameters for Sigmoidal Model 6a with $g = 100$, weighted by datum.

Standard errors of parameters are in parentheses. Units are a: Torr · min, b: dimensionless, c: $(\text{min})^{-1}$.

Data Group	Parameter	No recovery	Recovery to 8 hr	All recovery
1	a	$2.7 \cdot 10^6$ $(3 \cdot 10^5)$		$4.2 \cdot 10^6$ $(5 \cdot 10^5)$
	b	1.4 (0.1)		1.3 (0.1)
	c	$4.8 \cdot 10^{-4}$ $(6 \cdot 10^{-5})$		$2.5 \cdot 10^{-4}$ $(4 \cdot 10^{-5})$
	r^2	0.45		0.38
2	a	$2.1 \cdot 10^6$ $(3 \cdot 10^5)$	$2.3 \cdot 10^6$ $(3 \cdot 10^5)$	$2.2 \cdot 10^6$ $(3 \cdot 10^5)$
	b	1.5 (0.1)	1.5 (0.1)	1.5 (0.1)
	c	$6.6 \cdot 10^{-4}$ $(8 \cdot 10^{-5})$	$6.3 \cdot 10^{-4}$ $(7 \cdot 10^{-5})$	$6.5 \cdot 10^{-4}$ $(7 \cdot 10^{-5})$
	r^2	0.29	0.26	0.24
3	a	$1.9 \cdot 10^6$ $(3 \cdot 10^5)$	$1.9 \cdot 10^6$ $(3 \cdot 10^5)$	$2.0 \cdot 10^6$ $(3 \cdot 10^5)$
	b	1.4 (0.1)	1.4 (0.1)	1.3 (0.1)
	c	$1.0 \cdot 10^{-3}$ $(1 \cdot 10^{-4})$	$9 \cdot 10^{-4}$ $(1 \cdot 10^{-4})$	$1 \cdot 10^{-3}$ $(1 \cdot 10^{-4})$
	r^2	0.30	0.28	0.24
4	a	$2.2 \cdot 10^6$ $(3 \cdot 10^5)$	$2.1 \cdot 10^6$ $(2 \cdot 10^5)$	$1.8 \cdot 10^6$ $(1 \cdot 10^5)$
	b	1.5 (0.1)	1.8 (0.1)	1.9 (0.1)
	c	$6.4 \cdot 10^{-4}$ $(7 \cdot 10^{-5})$	$4.8 \cdot 10^{-4}$ $(5 \cdot 10^{-5})$	$6.0 \cdot 10^{-4}$ $(4 \cdot 10^{-5})$
	r^2	0.30	0.26	0.27

Table A18.
Fitted parameters for Sigmoidal Model 6a with *g* fitted.

Standard errors of parameters are in parentheses. *Italics* indicate low confidence in parameter values. Units are *a*: Torr · min, *b*: dimensionless, *c*: $(\text{min})^{-1}$, *g*: dimensionless.

Data Group	Parameter	No recovery weighted by datum	Recovery to 8 hr		All recovery weighted by datum
			Weighted by datum	Weighted by subject	
1	Did not fit — scaling parameter *g* reached upper limit.				
2	*a*	$3.7 \cdot 10^5$ $(3 \cdot 10^4)$	$3.8 \cdot 10^5$ $(3 \cdot 10^4)$	$3.1 \cdot 10^5$ $(4 \cdot 10^4)$	$3.7 \cdot 10^5$ $(3 \cdot 10^4)$
	b	5 (1)	4 (1)	6 (3)	3.9 (0.9)
	c	$7.8 \cdot 10^{-4}$ $(9 \cdot 10^{-5})$	$7.6 \cdot 10^{-4}$ $(9 \cdot 10^{-5})$	$1.1 \cdot 10^{-3}$ $(3 \cdot 10^{-4})$	$8.0 \cdot 10^{-4}$ $(9 \cdot 10^{-5})$
	g	15 (1)	16 (2)	14 (2)	16 (2)
	r^2	0.29	0.26	0.21	0.23
3	*a*	$3.1 \cdot 10^5$ $(2 \cdot 10^4)$	$3.1 \cdot 10^5$ $(2 \cdot 10^4)$	$3.1 \cdot 10^5$ $(4 \cdot 10^4)$	$3.0 \cdot 10^5$ $(2 \cdot 10^4)$
	b	6 (1)	6 (1)	*7 (4)*	4 (1)
	c	$1.0 \cdot 10^{-3}$ $(1 \cdot 10^{-4})$	$1.0 \cdot 10^{-3}$ $(1 \cdot 10^{-4})$	$1.1 \cdot 10^{-3}$ $(3 \cdot 10^{-4})$	$1.0 \cdot 10^{-3}$ $(1 \cdot 10^{-4})$
	g	15.0 (0.9)	15 (1)	14 (2)	15 (1)
	r^2	0.32	0.29	0.21	0.25
4	*a*	$3.8 \cdot 10^5$ $(3 \cdot 10^4)$	No confidence in parameters *a* or *g*. Fitted *g* equals its upper limit.	$3.2 \cdot 10^5$ $(4 \cdot 10^4)$	$6.0 \cdot 10^5$ $(8 \cdot 10^4)$
	b	4 (1)		5 (3)	3.1 (0.5)
	c	$7.6 \cdot 10^{-4}$ $(9 \cdot 10^{-5})$		$9 \cdot 10^{-4}$ $(3 \cdot 10^{-4})$	$5.8 \cdot 10^{-4}$ $(5 \cdot 10^{-5})$
	g	16 (27)		14 (2)	22 (5)
	r^2	0.30		0.23	0.28

Table A19.
Fitted parameters for Sigmoidal Model 6b, $g = 100$.

Standard errors of parameters are in parentheses. *Italics* indicate low confidence in parameter values. Units are a, b: dimensionless, P_{th}: Torr.

Data Group	Parameter	No recovery weighted by datum	8 hr recovery weighted by datum	All recovery	
				weighted by datum	weighted by subject
1	a	$7 \cdot 10^6$ ($2 \cdot 10^6$)	$8 \cdot 10^6$ ($2 \cdot 10^6$)	$8 \cdot 10^6$ ($2 \cdot 10^6$)	*$8 \cdot 10^6$ ($5 \cdot 10^6$)*
	b	0.9 (0.1)	0.85 (0.09)	0.9 (0.1)	0.9 (0.2)
	P_{th}	270 (20)	280 (20)	270 (10)	290 (20)
	r^2	0.46	0.46	0.39	0.25
2	a	$1.6 \cdot 10^7$ ($8 \cdot 10^6$)	$1.6 \cdot 10^7$ ($5 \cdot 10^6$)	$6 \cdot 10^6$ ($1 \cdot 10^6$)	$3 \cdot 10^6$ ($1 \cdot 10^7$)
	b	0.70 (0.07)	0.71 (0.08)	0.93 (0.09)	1.2 (0.3)
	P_{th}	110 (60)	184 (3)	330 (10)	410 (50)
	r^2	0.11	0.22	0.26	0.21
3	a	$1.2 \cdot 10^7$ ($4 \cdot 10^6$)	$1.3 \cdot 10^7$ ($4 \cdot 10^6$)	$7 \cdot 10^6$ ($1 \cdot 10^6$)	$3 \cdot 10^6$ ($1 \cdot 10^6$)
	b	0.70 (0.08)	0.70 (0.08)	0.86 (0.09)	1.2 (0.3)
	P_{th}	230 (50)	220 (50)	320 (20)	410 (50)
	r^2	0.28	0.24	0.27	0.22
4	a	$6 \cdot 10^6$ ($1 \cdot 10^6$)	$4.2 \cdot 10^6$ ($6 \cdot 10^5$)	$1.6 \cdot 10^7$ ($4 \cdot 10^6$)	*$4.5 \cdot 10^6$ ($2 \cdot 10^6$)*
	b	0.87 (0.09)	1.11 (0.08)	0.68 (0.05)	0.9 (0.2)
	P_{th}	340 (30)	320 (10)	330 (10)	390 (50)
	r^2	0.32	0.28	0.25	0.24

Table A20.
Fitted parameters for Sigmoidal Model 6c, $g = 100$.

Units are a: Torr · min, b: dimensionless, c: $(\text{min})^{-1}$, P_{th}: Torr. Standard errors of parameters are in parentheses. *Italics* indicate low confidence in parameter values.

Data Group	Parameter	Recovery to 8 hr weighted by datum	All recovery	
			weighted by datum	weighted by subject
1	a	Too few recovery data	$8 \cdot 10^6$ $(2 \cdot 10^6)$	*$7 \cdot 10^6$ $(4 \cdot 10^6)$*
	b		0.8 (0.1)	0.9 (0.2)
	c		$2.2 \cdot 10^{-4}$ $(3 \cdot 10^{-5})$	$1.3 \cdot 10^{-4}$ $(6 \cdot 10^{-5})$
	P_{th}		270 (20)	290 (20)
	r^2		0.39	0.25
2	a	$5 \cdot 10^6$ $(1 \cdot 10^6)$	$5.1 \cdot 10^6$ $(9 \cdot 10^5)$	*$4 \cdot 10^6$ $(2 \cdot 10^6)$*
	b	0.92 (0.09)	0.94 (0.09)	1.0 (0.2)
	c	$6 \cdot 10^{-4}$ $(3 \cdot 10^{-4})$	$8 \cdot 10^{-4}$ $(1 \cdot 10^{-4})$	$1.3 \cdot 10^{-3}$ $(4 \cdot 10^{-4})$
	P_{th}	332 (0)	332 (0)	390 (60)
	r^2	0.28	0.26	0.22
3	a	$5.8 \cdot 10^6$ $(1 \cdot 10^6)$	$5 \cdot 10^6$ $(1 \cdot 10^6)$	$3 \cdot 10^6$ $(2 \cdot 10^6)$
	b	0.85 (0.09)	0.88 (0.09)	1.0 (0.2)
	c	$8 \cdot 10^{-4}$ $(3 \cdot 10^{-4})$	$9 \cdot 10^{-4}$ $(1 \cdot 10^{-4})$	$1.3 \cdot 10^{-3}$ $(4 \cdot 10^{-4})$
	P_{th}	332 (0)	332 (0)	400 (60)
	r^2	0.31	0.28	0.24
4	a	$3.8 \cdot 10^6$ $(5 \cdot 10^5)$	$3.6 \cdot 10^6$ $(4 \cdot 10^5)$	$5 \cdot 10^6$ $(2 \cdot 10^6)$
	b	1.15 (0.08)	1.18 (0.07)	0.9 (0.2)
	c	$7.9 \cdot 10^{-3}$ $(3 \cdot 10^{-4})$	$1.1 \cdot 10^{-3}$ $(1 \cdot 10^{-4})$	$1.1 \cdot 10^{-3}$ $(4 \cdot 10^{-4})$
	P_{th}	320 (10)	320 (10)	332 (0)
	r^2	0.28	0.30	0.25

Model 8. Injury-Memory Model.

$$\%\Delta VC = a \cdot b^{-2} \cdot (PO_2 - P_{th}) \cdot [e^{-(b \cdot t)} - e^{-[b \cdot (t - t_{mem})]}] + a \cdot b^{-1} \cdot \text{memory} \cdot (PO_2 - P_{th}) + I_0 \cdot b^{-1} \cdot [e^{-(b \cdot t)} - e^{[b \cdot (t - t_{mem})]}].$$

Table A21.
Fitted parameters for Injury-Memory Model 8.

Standard errors of parameters are in parentheses. *Italics* indicate low confidence in parameter value. Units are a: $(\text{Torr} \cdot \text{min})^{-1}$, b: $(\text{min})^{-1}$, P_{th}: Torr, t_{mem}: hours.

Data Group	Param	No recovery > 0.5 hr weighted by datum	Recovery to 8 hr		All recovery weighted by datum
			Weighted by datum	Weighted by subject	
1	a	$-1.7 \cdot 10^{-5}$ $(1 \cdot 10^{-6})$	$-1.7 \cdot 10^{-5}$ $(1 \cdot 10^{-6})$	$-1.5 \cdot 10^{-5}$ $(3 \cdot 10^{-6})$	$-1.7 \cdot 10^{-5}$ $(1 \cdot 10^{-6})$
	b	$3.0 \cdot 10^{-4}$ $(9 \cdot 10^{-5})$	$2.9 \cdot 10^{-4}$ $(9 \cdot 10^{-5})$	*$4 \cdot 10^{-4}$ $(2 \cdot 10^{-4})$*	$2.3 \cdot 10^{-4}$ $(3 \cdot 10^{-5})$
	P_{th}	170 (10)	170 (10)	160 (20)	170 (10)
	t_{mem}	3	3	3	3
	r^2	0.47	0.46	0.21	0.39
2	a	$-2.8 \cdot 10^{-5}$ $(2 \cdot 10^{-6})$	$-2.9 \cdot 10^{-5}$ $(2 \cdot 10^{-6})$	$-3.7 \cdot 10^{-5}$ $(6 \cdot 10^{-5})$	$-3.0 \cdot 10^{-5}$ $(2 \cdot 10^{-6})$
	b	$7.9 \cdot 10^{-4}$ $(1 \cdot 10^{-4})$	$9.1 \cdot 10^{-4}$ $(1 \cdot 10^{-4})$	$1.8 \cdot 10^{-3}$ $(4 \cdot 10^{-4})$	$1.0 \cdot 10^{-3}$ $(1 \cdot 10^{-4})$
	P_{th}	170 (20)	160 (20)	200 (100)	140 (30)
	t_{mem}	3	3	3	3
	r^2	0.28	0.24	0.20	0.20
3	a	$-3.0 \cdot 10^{-5}$ $(2 \cdot 10^{-6})$	$-2.9 \cdot 10^{-5}$ $(2 \cdot 10^{-6})$	$-3.4 \cdot 10^{-5}$ $(5 \cdot 10^{-6})$	$-3.0 \cdot 10^{-5}$ $(2 \cdot 10^{-6})$
	b	$3.6 \cdot 10^{-4}$ $(1 \cdot 10^{-4})$	$9.2 \cdot 10^{-4}$ $(1 \cdot 10^{-4})$	$1.7 \cdot 10^{-3}$ $(4 \cdot 10^{-4})$	$1.1 \cdot 10^{-3}$ $(1 \cdot 10^{-4})$
	P_{th}	340 (20)	160 (20)	140 (30)	140 (30)
	t_{mem}	3	3	83	3
	r^2	0.33	0.27	0.21	0.23
4	a	$-2.9 \cdot 10^{-5}$ $(2 \cdot 10^{-6})$	$-2.8 \cdot 10^{-5}$ $(2 \cdot 10^{-6})$	$-3.1 \cdot 10^{-5}$ $(5 \cdot 10^{-6})$	$-2.9 \cdot 10^{-5}$ $(2 \cdot 10^{-6})$
	b	$3.3 \cdot 10^{-4}$ $(9 \cdot 10^{-5})$	$3.9 \cdot 10^{-4}$ $(1 \cdot 10^{-4})$	*$7.4 \cdot 10^{-4}$ $(4 \cdot 10^{-4})$*	$1.2 \cdot 10^{-3}$ $(1 \cdot 10^{-4})$
	P_{th}	340 (20)	320 (20)	270 (50)	110 (20)
	t_{mem}	3	3	3	3
	r^2	0.30	0.23	0.22	0.22

Model 9. Delayed Inflammation Model

a. With instantaneous P_{O_2}.
b. With average P_{O_2} for a time period.
c. With average P_{O_2} but no inflammation.

Table A22.
Fitted parameters for two-step models, Models 9a and 9b, and for 9c, the averaged P_{O_2} model. (See the simple proportional healing Model 3a for comparison.) All recovery data used, weighted by datum.

Standard errors of parameters are in parentheses. *Italics* indicate low confidence in parameter value. Units are a: $(\text{Torr} \cdot \text{min})^{-1}$; b: min^{-1}; P_{th}: Torr; K (inflammatory gain): dimensionless; τ_{io}, τ_{id}: hr; t_{avg}: min.

Data Group	Param	Inflammation (Model 9a) Weighted by datum	Inflammation and Averaging (Model 9b) Weighted by datum	Averaging, No inflammation (Model 9c) Weighted by datum
1	r^2 is not increased by inflammatory component or by averaging. Model 9 reduces to Model 3a. $r^2 = 0.39$			
2 (Model 3a: r^2 = 0.21)	a	$2.52 \cdot 10^{-5}$ $(2 \cdot 10^{-7})$	$2.54 \cdot 10^{-5}$ $(2 \cdot 10^{-7})$	$2.6 \cdot 10^{-5}$ $(2 \cdot 10^{-6})$
	b	$7.7 \cdot 10^{-4}$ $(1 \cdot 10^{-5})$	$9.5 \cdot 10^{-4}$ $(2 \cdot 10^{-5})$	$6.2 \cdot 10^{-4}$ $(9 \cdot 10^{-5})$
	P_{th}	197 (5)	146 (3)	250 (30)
	K	$1.7 \cdot 10^{-2}$ $(8 \cdot 10^{-3})$	$2.1 \cdot 10^{-2}$ $(8 \cdot 10^{-3})$	None
	τ_{io}	8	8	
	τ_{id}	36	36	
	t_{avg}	None	300	300
	r^2	0.21	0.22	0.22
3 (Model 3a: r^2 = 0.24)	a	$2.47 \cdot 10^{-5}$ $(2 \cdot 10^{-7})$	$2.56 \cdot 10^{-5}$ $(2 \cdot 10^{-7})$	$2.6 \cdot 10^{-5}$ $(2 \cdot 10^{-6})$
	b	$8.9 \cdot 10^{-4}$ $(1 \cdot 10^{-5})$	$9.6 \cdot 10^{-4}$ $(2 \cdot 10^{-5})$	$6.2 \cdot 10^{-4}$ $(1 \cdot 10^{-4})$
	P_{th}	148 (3)	144 (3)	250 (40)
	K	$2.1 \cdot 10^{-2}$ $(8 \cdot 10^{-3})$	$2.1 \cdot 10^{-2}$ $(8 \cdot 10^{-3})$	None
	τ_{io}	8	8	
	τ_{id}	36	36	
	t_{avg}	None	300	300
	r^2	0.25	0.23	0.23
4 (Model 3a: r^2 = 0.22)	a	$2.54 \cdot 10^{-5}$ $(2 \cdot 10^{-7})$	$2.61 \cdot 10^{-5}$ $(2 \cdot 10^{-7})$	$2.5 \cdot 10^{-5}$ $(1 \cdot 10^{-6})$
	b	$1.15 \cdot 10^{-3}$ $(2 \cdot 10^{-5})$	$1.16 \cdot 10^{-3}$ $(2 \cdot 10^{-5})$	$9.6 \cdot 10^{-4}$ $(9 \cdot 10^{-5})$
	P_{th}	110 (4)	117 (3)	120 (20)
	K	$2.7 \cdot 10^{-2}$ $(7 \cdot 10^{-3})$	$2.7 \cdot 10^{-2}$ $(7 \cdot 10^{-3})$	None
	τ_{io}	8	8	
	τ_{id}	36	36	
	t_{avg}	None	300	300
	r^2	0.24	0.26	0.25

Table A23.
Fitted parameters for two-step models, Models 9a and 9b, and for 9c, the averaged P_{O_2} model. (See the simple proportional healing Model 3a for comparison.) Up to 8 hours' recovery, weighted by datum.

Standard errors of parameters are in parentheses. *Italics* indicate low confidence in parameter value. Units are a: $(\text{Torr} \cdot \text{min})^{-1}$; b: min^{-1}; P_{th}: Torr; K (inflammatory gain): dimensionless; τ_{io}, τ_{id}: hr ; t_{avg}: min.

Data Group	Param	Inflammation 8 hr (Model 9a) Weighted by datum	Inflammation and Averaging (Model 9b) Weighted by datum	Averaging, No inflammation (Model 9c) Weighted by datum
1	r^2 is not increased by inflammatory component or by averaging. Model 9 reduces to Model 3a. $r^2 = 0.45$			
2 (Model 3a: $r^2 = 0.26$)	a	$2.45 \cdot 10^{-5}$ $(2 \cdot 10^{-7})$	$2.51 \cdot 10^{-5}$ $(2 \cdot 10^{-7})$	$2.5 \cdot 10^{-5}$ $(2 \cdot 10^{-6})$
	b	$2.7 \cdot 10^{-4}$ $(1 \cdot 10^{-5})$	$3.0 \cdot 10^{-4}$ $(1 \cdot 10^{-5})$	$2.7 \cdot 10^{-4}$ $(1 \cdot 10^{-5})$
	P_{th}	324 (2)	325 (3)	330 (20)
	K	*$2 \cdot 10^{-3}$ $(9 \cdot 10^{-3})$*	*$5 \cdot 10^{-3}$ $(9 \cdot 10^{-3})$*	None
	τ_{io}	8	8	
	τ_{id}	36	36	
	t_{avg}	None	300	300
	r^2	0.25	0.26	0.26
3 (Model 3a: $r^2 = 0.29$)	a	$2.49 \cdot 10^{-5}$ $(2 \cdot 10^{-7})$	$2.52 \cdot 10^{-5}$ $(2 \cdot 10^{-7})$	$2.5 \cdot 10^{-5}$ $(2 \cdot 10^{-6})$
	b	$2.9 \cdot 10^{-4}$ $(1 \cdot 10^{-5})$	$3.0 \cdot 10^{-4}$ $(1 \cdot 10^{-5})$	$2.7 \cdot 10^{-4}$ $(1 \cdot 10^{-4})$
	P_{th}	323 (3)	325 (3)	330 (20)
	K	*$6 \cdot 10^{-3}$ $(9 \cdot 10^{-3})$*	*$4 \cdot 10^{-3}$ $(9 \cdot 10^{-3})$*	None
	τ_{io}	8	8	
	τ_{id}	36	36	
	t_{avg}	None	300	300
	r^2	0.29	0.27	0.27
4 (Model 3a: $r^2 = 0.24$)	a	$2.40 \cdot 10^{-5}$ $(2 \cdot 10^{-7})$	$2.46 \cdot 10^{-5}$ $(2 \cdot 10^{-7})$	$2.4 \cdot 10^{-5}$ $(2 \cdot 10^{-6})$
	b	$2.5 \cdot 10^{-4}$ $(1 \cdot 10^{-5})$	$2.8 \cdot 10^{-4}$ $(1 \cdot 10^{-5})$	$2.5 \cdot 10^{-4}$ $(9 \cdot 10^{-5})$
	P_{th}	323 (3)	323 (3)	330 (20)
	K	*$1 \cdot 10^{-3}$ $(9 \cdot 10^{-3})$*	*$5 \cdot 10^{-3}$ $(9 \cdot 10^{-3})$*	None
	τ_{io}	8	8	
	τ_{id}	36	36	
	t_{avg}	None	300	300
	r^2	0.24	0.27	0.27